

South Dakota State University

Open PRAIRIE: Open Public Research Access Institutional Repository and Information Exchange

Electronic Theses and Dissertations

2017

Lignin Transformation and Characterization of Pyrolytic Products

Eric Amo Boakye

South Dakota State University

Follow this and additional works at: <https://openprairie.sdstate.edu/etd>



Part of the [Chemistry Commons](#)

Recommended Citation

Boakye, Eric Amo, "Lignin Transformation and Characterization of Pyrolytic Products" (2017). *Electronic Theses and Dissertations*. 1185.

<https://openprairie.sdstate.edu/etd/1185>

This Dissertation - Open Access is brought to you for free and open access by Open PRAIRIE: Open Public Research Access Institutional Repository and Information Exchange. It has been accepted for inclusion in Electronic Theses and Dissertations by an authorized administrator of Open PRAIRIE: Open Public Research Access Institutional Repository and Information Exchange. For more information, please contact michael.biondo@sdstate.edu.

LIGNIN TRANSFORMATION AND CHARACTERIZATION OF PYROLYTIC
PRODUCTS

BY
ERIC AMO BOAKYE

A dissertation submitted in partial fulfilment of the requirement for the

Doctor of Philosophy

Major in Chemistry

South Dakota State University

2017

LIGNIN TRANSFORMATION AND CHARACTERIZATION OF PYROLYTIC
PRODUCTS

This dissertation is approved as a creditable and independent investigation by a candidate for the Doctor of Philosophy degree in chemistry and is acceptable for meeting the dissertation requirements for this degree. Acceptance of this dissertation does not imply that the conclusions reached by the candidate are necessarily the conclusion of the major department.

Douglas E. Raynie, Ph.D.

Date

Dissertation Advisor

Douglas E. Raynie, Ph.D.

Date

Head, Department of Chemistry & Biochemistry

Dean, Graduate School

Date

ACKNOWLEDGEMENTS

My sincere gratitude to my advisor, Dr. Douglas Raynie for his continuous encouragement, support, and selfless and faithful guidance offered to me throughout my entire time in graduate school. Many thanks also go to my committee members for their uncommon guidance and directions. To my green chemistry lab members, my friends, and all the people at SDSU who made my stay here a very memorable one. Thank you to all of you for your constant support. Thank you to Doctors Wei, Zhang, Gu and all your students for opening your labs to me all the time.

I want to thank my wife, Attorney Doris Amo Boakye, my son, Bishop Kwaku Amo Boakye, and my daughter Joi Gyamfuah Amo Boakye as well as my in-laws - Pastors David and Grace Ntiamoah, Priscilla Ntiamoah, and Linda Ntiamoah for all the kindness and love shown to me, you have been my source of strength and encouragement. I want to especially thank my late father, Mr. Joseph Kwadwo Amo Boakye and my mother, Joyce Adwoa Gyamfuah, as well as my siblings - Mavis Amo Boakye, Patience Amo Boakye, Sandra Amo Boakye, Yaa Babe, and Frank Adusei for their unflinching support and belief in me all these years, for all the sacrifices that you have made on my behalf; You are all my heroes. Thank you all my nephews and nieces.

Last, but certainly not the least, I am grateful to God Almighty for his protection and guidance for me throughout this great journey. I also give thanks to my church family, Holy Life Tabernacle and the entire leadership, Pastors Dave and Jeanne Kaufman, Kevin and Cindy Suiter, and Frank and Lanita Vanderbush for all your prayers and support. The authors gratefully thank and acknowledge the financial support of this research work from DakotaBioCon project 1330842.

TABLE OF CONTENTS

LIST OF ABBREVIATIONS.....	vii
LIST OF FIGURES.....	ix
LIST OF TABLES.....	xii
LIST OF EQUATIONS.....	xiv
ABSTRACT.....	xv
CHAPTER 1: INTRODUCTION AND BACKGRROUND.....	1
1.1. Introduction.....	1
1.2. Lignocellulosic materials and pretreatment methods used to separate them.	4
1.2.1. Intrapolymer crosslinkages of lignocellulosic materials.....	8
1.2.2. Interpolymer crosslinkages of lignocellulosic materials.....	10
1.2.3. Physical pretreatment.....	11
1.2.4. Biological pretreatment.....	12
1.2.5. Chemical pretreatment.....	12
1.2.6. Physicochemical pretreatment.....	15

1.2.7. Explosion pretreatment.....	17
1.2.8. Liquid hot water pretreatment.....	18
1.3. Depolymerization of lignin for high-value biochemicals.....	18
1.3.1. Monomers of lignin.....	18
1.3.2. Hydrotreatment or hydrothermal liquefaction of lignin.....	21
1.3.3. Catalysts.....	23
1.3.4. Effect of hydrogen source in hydrothermal liquefaction.....	24
1.4. The purpose of this study.....	25
CHAPTER 2: HYDROTREATMENT OF KRAFT LIGNIN INTO PHENOLIC MONOMERS USING SUBCRITICAL WATER AND SUPPORTED-ZEOLITE METAL OXIDES.....	27
2.1. Introduction.....	27
2.2. Experimental.....	32
2.2.1. Materials and reagents.....	32
2.2.2. Methods.....	32
2.3. Results and discussions.....	40
2.3.1. Catalyst characterization.....	40
2.3.2. Lignin characterization.....	41
2.3.3. Catalytic hydrotreatment of lignin.....	49
2.4. Conclusion.....	59

CHAPTER 3: AROMATIC MONOMERS GENERATED FROM TORREFACTION AND PYROLYSIS OF PRAIRIE CORDGRASS.....	59
3.1. Introduction.....	59
3.2. Experimental.....	63
3.2.1. Materials and Reagents.....	63
3.2.2. Methods.....	64
3.3. Results and discussion.....	76
3.3.1. Yield of pyrolysis products.....	76
3.3.2. Lignin content and recovery in prairie cordgrass bio-chars.....	77
3.3.3. Characterization of bio-oil and lignin from prairie cordgrass bio-chars....	79
3.4. Conclusion.....	90
CHAPTER 4: CONCLUSIONS AND FUTURE WORK.	91
REFERENCES.....	95

LIST OF ABBREVIATIONS

AFEX.....	Ammonia fiber explosion
AIL.....	Acid-insoluble lignin
ASAP.....	Accelerated surface area and porosimetry
ASE.....	Accelerated solvent extraction
ASL.....	Acid-soluble lignin
BET.....	Bounauer- Emmett-Teller
CDS.....	Chemical Data Systems
DAD.....	Diode array detector
DFT.....	Density functional theory
DOE.....	Department of Energy
DSC.....	Differential scanning calorimetry
DTG.....	Differential thermal gravimetric
FDW.....	Furnace-dried weight
FTIR.....	Fourier transform infrared spectrometry
GC-MS.....	Gas chromatography-mass spectrometry
HHV.....	High heating value
HTL.....	Hydrothermal liquefaction
IS.....	Internal standard
MIBK.....	Methyl isobutyl ketone
NCG.....	Non-condensable gases
NIST.....	National Institute of Standards and Technology
NREL.....	National Renewable Energy Laboratory

ODW.....	Oven-dry weight
OSSP.....	Organic-solvent soluble products
PCG.....	Prairie cordgrass
Py-GC-MS.....	Pyrolysis-gas chromatography-mass spectrometry
TGA.....	Thermal gravimetric analysis
UHPLC.....	Ultra-high-performance liquid chromatography
UV-Vis.....	Ultraviolet visible
WDP.....	Weight of desired product
WIS.....	Weight of initial sample

LIST OF FIGURES

Figure	
1. Bioenergy cycle of ethanol production from lignocellulosic biomass.....	4
2. The distribution of the three major lignocellulosic materials.....	6
3. The impact of pretreatment of lignocellulosic biomass.....	7
4. Hydrogen bonds that give the cellulose polymer chains its parallel arrangement...	9
5. A model structure of lignin from softwood.....	19
6. Structures of three basic phenolic monomers that form lignin.....	20
7. Changes in properties of water under different temperatures and pressures.....	23
8. Lignin depolymerization reaction mechanism involving metal catalysts in hydrothermal liquefaction process.....	25
9. Schematic structure of a model compound bearing typical lignin linkages from hardwood.....	29
10. Outline of kraft lignin characterization and analysis of depolymerization processes.....	33
11. Helix SFE systems used for hydrothermal depolymerization of Kraft lignin.....	37
12. GC-MS total ion chromatogram showing phenolic moieties produced from oxidation of Kraft lignin using cupric oxide.....	42
13. Chromatogram of phenolic compounds produced during Py-GC-MS analysis of Kraft lignin.....	45
14. TG and DTG analysis curves of Kraft lignin performed at 900 °C under nitrogen atmosphere at constant heating rate of 15 °C/min.....	47
15. Heating curve of differential scanning calorimetry analysis of Kraft lignin	

from 20 to 400 °C at a constant heating rate of 10 °C/min.....	48
16. FTIR analysis spectra of Kraft lignin (blue), unreacted lignin (purple) from the hydrotreatment and organic-solvent soluble products (red) showing similarities and differences in peak absorption intensity.....	51
17. GC-MS total-ion chromatogram of vanillin, 4-propylguaiacol, acetovanillone, and homovanillic acid obtained from Kraft lignin at 200 °C	54
18. GC-MS total-ion chromatogram of guaiacol, 3-methoxyacetophenone, vanillin, 4-propylguaiacol, acetovanillone, and homovanillic acid obtained from Kraft lignin at 250 °C	55
19. Yields of phenolic monomers - vanillin (purple), 4-propylguaiacol (dark blue), acetovanillone (orange) from hydrothermal liquefaction of Kraft lignin at 200 °C using CoO, LaO, and MoO catalysts.....	56
20. Yields of phenolic monomers - guaiacol (red), 3-methoxyacetophenone (green), vanillin (purple), 4-propylguaiacol (dark blue), acetovanillone (orange), and homovanillic acid (light blue) from hydrothermal liquefaction of Kraft lignin at 240 °C using CoO, LaO, and MoO catalysts.....	57
21. HPLC analysis of phenolic monomers in the ethyl acetate extract of depolymerized Kraft lignin using MoO catalysts.....	58
22. Outline for pyrolysis of prairie cordgrass and separation and analysis of pyrolytic products.....	63
23. Pyrolysis-reactor system for torrefaction and pyrolysis of prairie cordgrass.....	66
24. FTIR spectra of bio-oil extracts from Pyro900 (blue), Tor250 (red),	

Tor300 (purple), Pyro600 (green), and Tor350 (pink) of prairie cordgrass.....	81
25. GC-MS chromatograms of bio-oil extracts from Pyro900, Pyro600, Tor250, Tor300, and Tor350 of prairie cordgrass.....	83
26. FTIR spectra for extracted lignin from Tor250 (blue), Tor300 (red), Tor350 (green), and PCG (violet).....	87
27. Thermogravimetric analysis curves obtained for organosolv lignin extracted from Tor250, Tor300, PCG and Tor350 (from bottom to top) with a temperature range from 25 to 500 °C.....	89

LIST OF TABLES

Table

1. The different crosslinkages formed between the monomers of cellulose, hemicellulose, and lignin.....	11
2. Characterization of the three different catalysts by their textural properties; BET surface area, molecular cross-sectional areas, and total pore volume.....	41
3. Structure of phenolic monomers in Kraft lignin produced during cupric oxide oxidation.....	42
4. Phenolic monomers, groups, molecular weights, and formula identified using Py-GC-MS analysis of Kraft lignin.....	44
5. Functional group assignment of FTIR analysis of Kraft lignin, unreacted lignin and organic solvent-soluble products.....	52
6. Yield of products obtained from torrefaction and pyrolysis of prairie cordgrass at different temperatures.....	77
7. Amount of total solids, moisture, extractives, ash, and total lignin with % RSD determined for torrefaction biochar samples at 250 °C (Tor250), 300 °C (Tor300), 350 °C (Tor350) and pyrolysis biochar samples at 600°C (Pyro 600) and 900°C (Pyro 900).....	78
8. Physicochemical properties of pyrolysis of prairie cordgrass at different temperatures.....	80
9. Assignments of FTIR absorption bands of lignin from Tor250, Tor300, Tor350, and PCG.....	82
10. GC-MS aromatic composition of bio-oils obtained from torrefaction	

and pyrolysis of prairie cordgrass at different temperatures.....	84
11. Elemental compositions and High Heating Values (HHV) of lignin extracted from PCG, Tor250, Tor300, and Tor350.....	86
12. Thermogravimetric analysis of extracted lignins from PCG, Tor250, Tor300, and Tor350 showing mass losses at different degradation stages....	90

LIST OF EQUATIONS

1. Determination of pyrolysis products yields.....	66
2. Determination of non-condensable gases.....	66
3. Determination of amount of total solids.....	68
4. Moisture content determination.....	68
5. Determination of amount of extractives.....	69
6. Ash content determination.....	70
7. Determination of acid-insoluble lignin.....	71
8. Determination of acid soluble lignin.....	72
9. Lignin recovery determination.....	72

ABSTRACT

LIGNIN TRANSFORMATION AND CHARACTERIZATION OF PYROLYTIC
PRODUCTS

ERIC AMO BOAKYE

2017

Lignocellulosic materials derived from plants have the ability to serve as feedstocks in place of depleting petroleum and coal for production of fuels and chemicals. Lignin forms about 30% of lignocellulosic material, and is the second most abundant non-fossil organic carbon source in the biosphere. However, it is often treated as waste or, in some instances, burned to supply energy. Developing an efficient and environmentally benign method to convert lignin to high value-added aromatic monomers (e.g., guaiacol, vanillin, acetovanillone, and eugenol) for synthesis of polymers is of interest. Mineral bases, such as NaOH and CsOH, or supported-metal catalysts (Pt, Ru, Pd, and Ni on C) have been used to form aromatic monomers, but associated drawbacks are corrosion, catalyst recovery, sintering of metals, and loss of activity. Lignin conversion into useful aromatic compounds is highly desired but often hindered by recondensation and accompanied undesired products.

Zeolite-supported metal oxide catalysts (CoO, LaO, and MoO) with subcritical water at 200°C and 240°C were used to convert lignin to value-added aromatic monomers. Separation of the resulting organic and aqueous phases was done by liquid-liquid extraction using ethyl acetate. Our results indicate the formation of guaiacol, homovanillic acid, isoeugenol, 3-methoxyacetophenone, acetovanillone, and vanillin as the main products. GC-MS analysis of the organic extract shows 2-4.8 wt% and 3-15

wt% formation of phenolic compounds at 200 °C and 240 °C, respectively, at 12 MPa and 15 minutes. MoO catalyst gave the highest yield of phenolic monomers at both temperatures. The presence of the aromatic products was confirmed by FTIR, GC-MS, and UHPLC analysis.

Extracted lignin from torrefied prairie cordgrass at 250 °C (Tor250), 300 °C (Tor300), and 350 °C (Tor350) yielded 23.5 ± 1.6 wt%, 5.4 ± 6.8 wt%, and 4.1 ± 7.3 wt% of lignin respectively with 92-93.1 wt% recovered lignin relative to the organosolvent method. Torrefaction at 350 °C provided higher lignin purity (93.1 ± 3.2 wt%) than lignin extracted from PCG (89.2 ± 2.5 wt%). Thermogravimetric analysis shows breakdown of β -O-4 linkages in the lignin by mass loss between 250 to 350°C. Pyrolytic bio-oil obtained ranged between 13 and 37 wt% of prairie cordgrass at temperatures of 250°C, 300 °C, 350 °C, 600 °C, and 900 °C. The bio-oil contains the useful aromatic compounds - phenol, guaiacol, m-cresol, xyleneol, ethyl-phenol, ethyl-guaiacol, catechol, syringol, furan-2-one, vanillin, and 3-furancarboxaldehyde.

CHAPTER 1

INTRODUCTION AND BACKGROUND

1.1. Introduction

The reliance on petroleum for the production of energy and materials has increased in demand. This is causing a rapid depletion of crude oil reserves¹, which has raised legitimate concern among the global community. Presently, about 80 wt% by weight of the chemicals generated by the petrochemical industry is used in producing polymers for different applications.² These polymers include vinyl polymers, polyesters, polyamides, and polyurethanes etc.² These materials can be produced from biomass instead of petroleum products, and thus help grow the economic base of bio-based products. Continuous dependence on petroleum for the production of energy and materials is not sustainable. Therefore, a renewable source is needed as a replacement. Plant products are seen as an inexhaustible source for energy and materials production. However, most of the chemicals produced today are of first generation, which is from sugar and starch-based agricultural crops that compete with global food production. Therefore, this represents a limited supply.

The use of lignocellulosic biomass for production of biofuel and materials is a promising plant-derived option. The U.S. Department of Energy (DOE) has identified the following as sources of lignocellulosic biomass³:

- Municipal solid waste, such as household garbage and paper products,
- Waste from food processing and other industries, such as black liquor from ethanol production and paper manufacturing,

- Grasses such as switchgrass, prairie cordgrass, miscanthus grass, and big bluestem grass and fast growing trees, which are grown purposely for utilization as lignocellulosic biomass because of their low mineral content, low nutrient content, and efficient utilization of water,⁴
- Forestry waste such as dead trees, wood chips, sawdust, and cut tree branches,
- Agriculture residue such as wheat straw, sugar cane bagasse, and corn stover.

These raw materials are abundant and renewable, and form the basis of the second-generation technologies for producing biofuels and bio-chemicals. The use of suitable methods to depolymerize the components of lignocellulosic biomass will help reduce greenhouse gas emissions and increase the revenue for biofuel and biochemical industries.

Finding a perfect solution to solve the challenges in energy production is very difficult because every process for energy production requires some amount of energy utilization. The use of energy crops, such as grasses and fast-growing trees, for the production of ethanol requires fossil fuel, herbicide, fertilizer, and other chemicals for cultivation and production. However, production of biochemicals from lignocellulosic materials is an improvement over fossil fuel use that may lead to sustainable energy production in the near future. A study by Farrell et al.⁵ compared the production of ethanol and gasoline indicate that producing 1 MJ of ethanol uses far less petroleum than is required to produce 1 MJ of gasoline, not taking into account the coproducts that have been developed in recent times. Greenhouse gas emissions from ethanol produced by the first-generation technology can be slightly different than that obtained from gasoline per unit of energy⁵. However, studies have shown that there is a substantial reduction in

greenhouse gas emission and petroleum utilization by ethanol produced from second-generation technology (i.e., lignocellulosic materials).⁵⁻⁶ Lignocellulosic ethanol production uses fewer petroleum products mainly because they are perennial crops, which require less nutrients, herbicides, and other agricultural-maintenance practices often required by annual crops such as corn, sugar cane, and cassava. There are limitations, though, posed by the use of aboveground agricultural crop biomass residue for lignocellulosic ethanol. Lignocellulosic materials such wheat straw, corn stover, and corn husks are needed to maintain soil carbon to produce good properties leading to enhanced soil nutrients, and also prevent erosion by wind or rain.⁷⁻⁹ However, the perennial energy crops, especially grasses, have extensive root systems that help improve the soil quality, leading to an increase in soil nutrients and carbon dioxide capture, thereby aiding carbon sequestration and preventing erosion, even after harvesting. Figure 1¹⁰ shows the bioenergy cycle of ethanol production from lignocellulosic biomass. The available data suggest that only lignocellulosic biochemicals production can offer a large reduction in greenhouse gas emissions.⁵

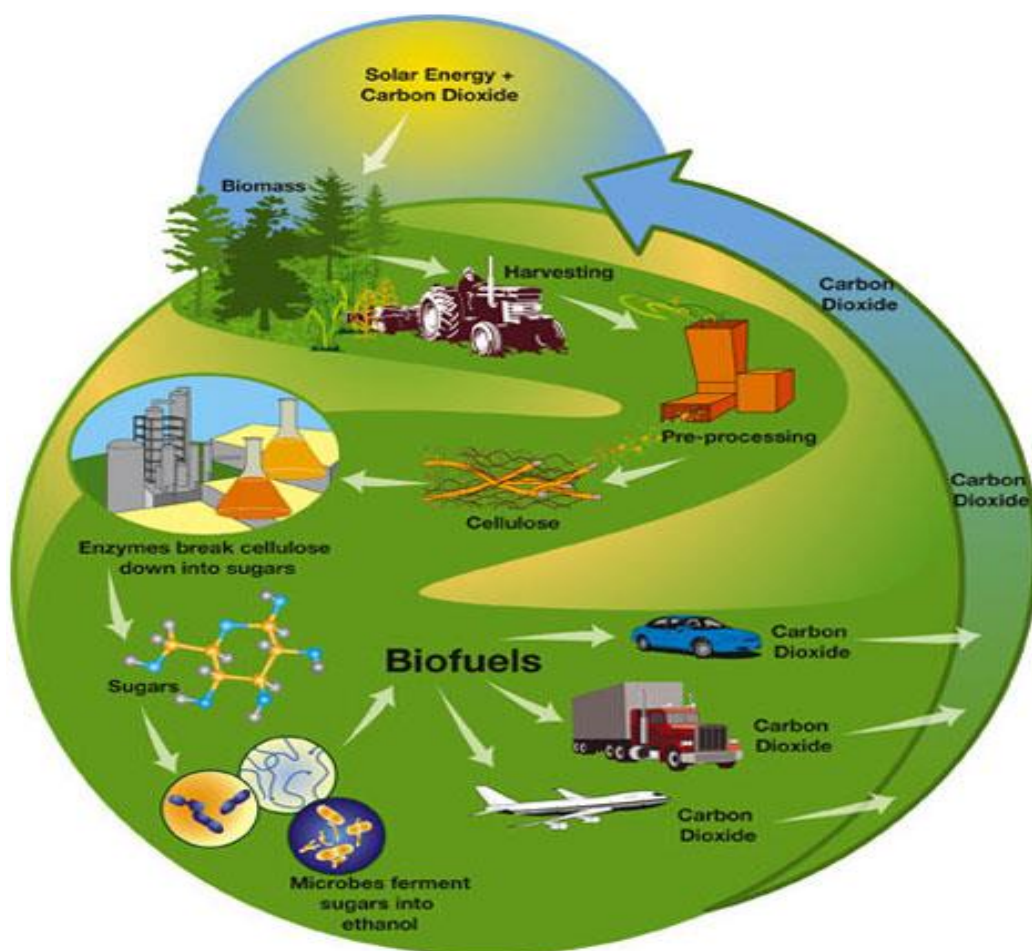


Figure 1. Bioenergy cycle of ethanol production from lignocellulosic biomass.¹⁰

1.2. Lignocellulosic materials and pretreatment methods used to separate them

The cell of the plant is composed of cellulose, hemicellulose, and lignin with small portions of pectin, minerals, salts, fat and fatty acids, proteoglycans, etc. The different components of the plant cell protect it from mechanical, physical, biological, and chemical damage from the environment. Figure 2 shows the three main components of lignocellulosic materials, cellulose, hemicellulose, and lignin.¹¹ Cellulose and hemicellulose occupy about two-thirds of the total dry biomass. The cellulose and hemicellulose are made up of polymers of sugars, and thereby represent a potential

source of fermentable sugars. After pretreatment, these fermentable sugars are treated to produce biofuels and chemicals. The amount of polysaccharide present in the plant dry matter and the methods of treatment affect the yield of the biofuel greatly. Lignin, which is the phenolic-rich component of the dry matter of lignocellulosic materials, makes up to about one-quarter of plant biomass. Lignin serves as a crosslinkage between hemicellulose and cellulose, therefore providing support within the cell wall and the plant as a whole. The majority of the lignin is located in the interfibrous area of cellulosic biomass, whereas smaller portions cover the cell surface¹². Lignin is able to resist biological and moisture attacks from the environment because it is insoluble in water and interferes with enzymatic activities of microbes. Lignin is not used during fermentation of polysaccharides present in lignocellulosic biomass to ethanol or in the processing of paper from wood. The separated lignin is burned in order to provide heat for these processes. Therefore, lignin is underutilized. Efficient utilization of lignin to produce value-added chemicals is necessary to reduce the overall cost of biofuel production.

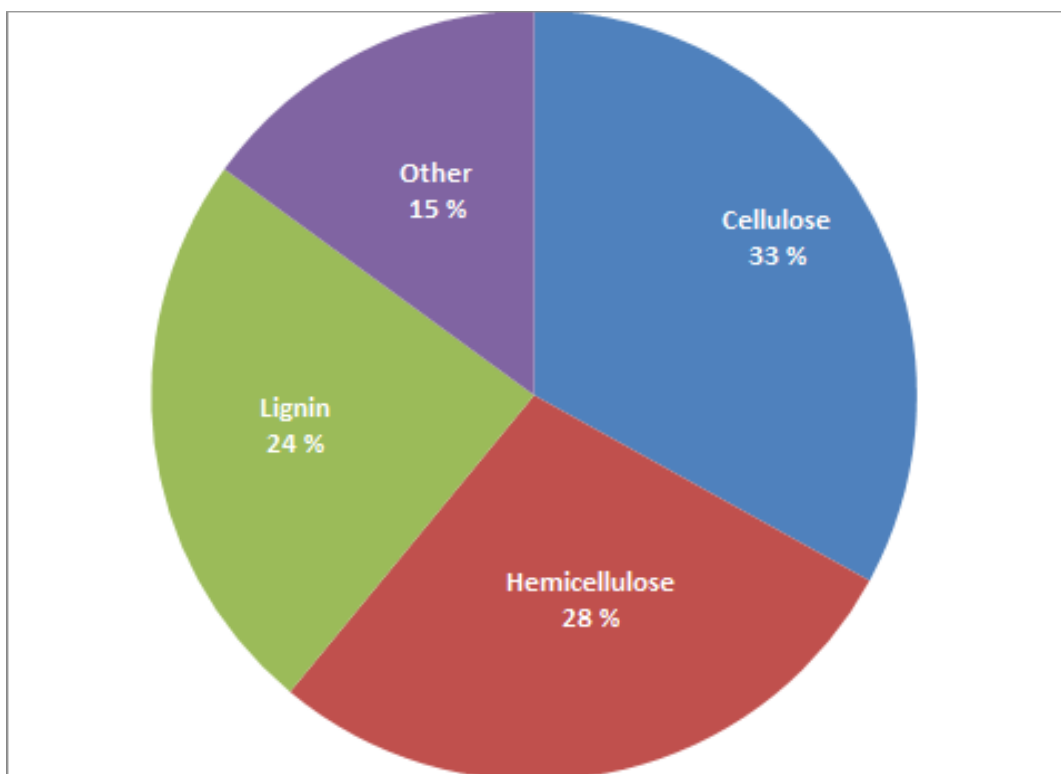


Figure 2. The distribution of the three major lignocellulosic materials.¹¹

A wide range of pretreatment methods such as biological, chemical, mechanical, physical, and thermochemical have been designed to break the crosslinkages between lignocellulosic materials to release the carbohydrates and lignin-rich materials for conversion to chemicals.¹³ About 90 % of the dry weight of most plant matter is stored in the form of cellulose, hemicellulose, lignin, and pectin materials which are useful in the production of biofuels and chemicals.¹⁴ For conversion of biomass to biochemicals, the bonds between the lignocellulosic materials need to be broken. Figure 3¹⁵ shows the release of the three lignocellulosic components after pretreatment. The treatment of lignocellulosic materials leads to monomers and low molecular weight organic compounds. Pretreatment of lignocellulosic materials largely results in cellulose, hemicellulose, and lignin formation, with some oligomers and small amounts of

monomer sugars, aromatic compounds, acetic acids, and other organic acids.

Pretreatment methods reduce moisture, remove extractives, and make separation of the biomass components possible, as well as prevent reaction-inhibitory tendencies in the treatment stages. There are a few lignocellulosic pretreatment methods that result in the formation of monomers and low molecular weight organic compounds, for example thermochemical pretreatment or pyrolysis of grass. Other pretreatment methods such as chemical and hydrothermal hydrolysis have been employed in actual treatment processes.

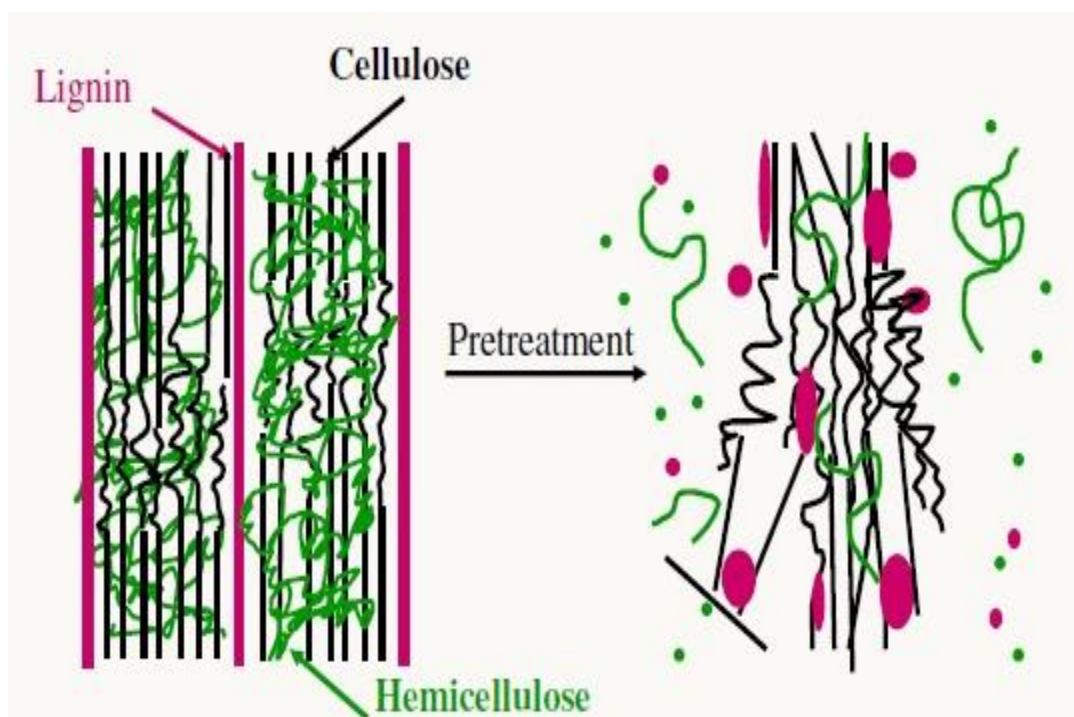


Figure 3. The impact of pretreatment of lignocellulosic biomass.¹⁵

There is a great challenge in separating the three lignocellulosic materials because of the crosslinkages formed between them. There are four main types of bonds that exist within the lignocellulosic materials. These are ether, ester, hydrogen, and carbon-carbon bonds. These four bonds form the linkages within each of the three major components

themselves (intrapolymer crosslinkages) and in the interpolymer crosslinkages that connect the cellulose, hemicellulose, and lignin components of the lignocellulosic biomass as indicated in Table 1.¹⁶

1.2.1. Intrapolymer crosslinkages of lignocellulosic materials

The cellulose polymer is made up of glucose monomers. To make available these glucose monomers for biofuels and chemicals, the bonds within the cellulose need to be degraded. The cellulose is a great source of ethanol production. There are two types of linkages that connect the monomers of cellulose, hydrogen and ether bonds. The ether bonds within the cellulose are formed by glycosidic linkages (1-4 β D-glycosidic) between the glucose moieties. These ether bonds are the bonds that initiate the polymerization in cellulose. The hydrogen bonds connect the hydroxyl groups on different glucose monomers and are responsible for the crystalline nature of the cellulose.¹⁷ The hydroxyl groups are evenly distributed on both sides of the glucose monomer, which allow hydrogen bonds to be formed between different hydroxyl groups on adjacent polymer chains leading to a formation of a well-arranged cellulose polymer in long parallel straight chains as demonstrated in Figure 4.¹⁶

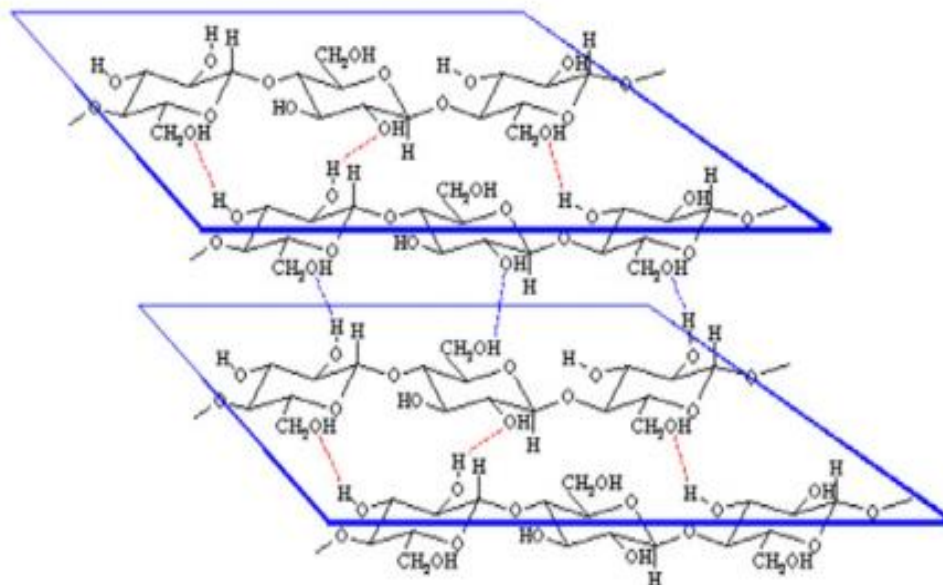


Figure 4. Hydrogen bonding in cellulose polymer of lignocellulosic biomass.¹⁶

Hemicellulose is a heterogeneous polysaccharide unlike cellulose. The hemicellulose is mainly made up of glucose and xylose, with fructose, rhamnose, mannose, arabinose, and galactose depending on the type of wood. The ether bonds in hemicellulose are mostly glycosidic and fructosic linkages. Hydrogen bonds are not present in the monomers that make up the hemicellulose. Hemicellulose produces less ethanol by weight of the starting material as compared to cellulose because of the presence of five-member rings within the hemicellulose polymer. There is no crystalline structure in the hemicellulose because of the highly branched polymer-chain structure and the presence of a high amount of carboxyl groups.¹⁸ The carboxyl groups on the pentose monomers in the polymer chains of the hemicellulose are responsible for the ester bonds. Degradation of the pentoses and hexoses results in ethanol and an array of bio-based chemicals, such as aromatic, aldehydes, sugars, and other hydrocarbons.

Ether and carbon-carbon crosslinkages are the main types of bonds found in the monomer units that make up the lignin as shown in Table 1. The ether linkages form the majority of the bonds in lignin molecules (about 70 % of total bonds in lignin monomer units).¹⁸ The rest of the bonds within the monomer units are made up of carbon-carbon linkages. The ether linkages may exist within two allylic carbons, aryl to aryl carbon atoms and allylic and aryl carbon atoms in the monomer units of lignin polymer. The carbon-carbon bonds may also occur between two aryl carbon atoms and an aryl carbon and an allylic carbon atom.¹²

1.2.2. Interpolymer crosslinkages of lignocellulosic materials

The plant polymer is considered a fibril-matrix length scale of cellulose, which is interspersed with lignin and hemicellulose within the cell-wall layers.¹⁹ It is very difficult to definitively establish the crosslinkages connecting the three components of lignocellulosic materials in plants. In order to determine the bonds that connect the lignin and the polysaccharides, the lignocellulosic materials have to be separated from each other. However, the separation processes used to break the bonds of the lignocellulosic complex changes the original structure of the three polymers (lignin, hemicellulose, and cellulose).

Bonding in the form of ether and ester crosslinkages have been identified between lignin and polysaccharides.¹⁸ Lignin is reported to be bonded to hemicellulose via ester linkages, whereas ether bonding couples lignin and polysaccharides.¹⁸ Hydrogen bonds between lignin and cellulose and with hemicellulose have also been identified. The hydrogen bonds formed between hemicellulose and cellulose is weak because of lack of a primary alcohol on the external side of the pyranose ring found in the hemicellulose.¹⁸

Table 1. The different crosslinkages formed between the monomers of cellulose, hemicellulose, and lignin

Bonds formed within lignocellulosic components (Intrapolymer)	
Ether bonds	Lignin, hemicellulose, cellulose
Carbon-carbon	Lignin
Hydrogen bonds	Cellulose
Ester bonds	Hemicellulose
Bonds connecting cellulose, hemicellulose, and lignin (Interpolymer)	
Ether bonds	Cellulose-lignin
	Hemicellulose-lignin
Ester bonds	Hemicellulose-lignin
Hydrogen bonds	Cellulose-hemicellulose
	Hemicellulose-lignin
	Cellulose-lignin

1.2.3. Physical pretreatment

Drying, chipping, and milling are important pretreatment techniques that help reduce the amount of water, the level of cellulose crystallinity, and the overall lignocellulosic crystallinity. Chipping is usually done during the biomass collection to reduce the size of the biomass and make packing easy in order to reduce transportation costs. The biomass size is considerably reduced as compared to its original size after chipping. Milling or grinding is performed on the lignocellulosic materials after chipping to alter biomass structure and reduce crystallinity, and it is usually done by simple machines to reduce the amount of time spent by manual grinding. Different types of milling machines are often used, but the vibrating ball is found to be most effective in improving the digestibility and in reducing the crystallinity of the biomass.²⁰

The reduction in lignocellulosic crystallinity increases enzyme accessibility to polysaccharides and results in more effective recovery of lignin from the biomass.²¹ Chipping of the biomass results in particle sizes of about 10 - 30 mm, whereas milling causes the size to be reduced to 0.2 - 2 mm. Almost all of the other pretreatment processes for biomass employ drying, chipping, and milling or grinding.

1.2.4. Biological pretreatment

Microorganisms such as fungi have been used to pretreat lignocellulosic biomass.²²⁻²³ White-rot, brown-rot, and soft-rot fungi, have been used for biomass pretreatment to release the polysaccharides and lignin.²⁴⁻²⁶ Lignin is resistant to microorganism degradation as compared to other lignocellulosic materials, and therefore, a higher amount of lignin is maintained after the pretreatment without degradation. The use of microorganisms for biomass pretreatment is always performed under low temperature and requires no additional energy, making it environmentally benign.²⁷ Biological pretreatment, however is not economically viable, and thus, it is not often considered on an industrial scale. Some portions of the biomass, such as cellulose, hemicellulose, and pectin, are often lost in the process by consumption from the microorganisms used.²⁸

1.2.5. Chemical pretreatment

a. Hydrolysis using acids

Several acids have been used to pretreat lignocellulosic materials from different grasses and other plants. Acidic-hydrolysis pretreatment has effectively improved ethanol production as well as delignification.²⁹ Acid hydrolysis has been used in combination with heating. The temperature used ranges from 50 °C to 260 °C with atmospheric

pressure.^{22,30} Low acid concentrations usually require higher temperatures and the application of mechanical force, whereas high concentrations of acid use less mechanical force with lower temperatures.³¹⁻³³ The most common acids used for lignocellulosic biomass hydrolysis are hydrochloric acid, sulfuric acid, and phosphoric acid, as well as organic acids such as oxalic, maleic, and fumaric acids.³⁴⁻³⁷ Most of the polysaccharides are depolymerized into monomers and oligomers, leaving the lignin polymer during acid hydrolysis making lignin recovery achievable by precipitation. Recovery of the acids after hydrolysis makes the process economical.³⁸

b. Alkaline hydrolysis

Alkaline solutions such as sodium, ammonium, potassium, and calcium hydroxides, as well as sodium sulfides, are used to break the bonds that link lignocellulosic materials into lignin, polysaccharides and sugars. Alkaline pretreatment is often performed at ambient temperature to temperatures a little above 100 °C.³⁹⁻⁴⁰ The lignin is then removed to allow subsequent degradation of the polysaccharides and sugars to fermentable sugars or to pyrolyze to fuel and other chemicals. The biomass is often soaked in the alkaline solution which causes swelling, increasing the internal surface area of the molecules leading to a decrease in crosslinkages between the lignin and polysaccharides, as well as disruptions within the polymers. The continuous instability increases the bond breakages in the polymers of the lignocellulosic materials.⁴¹ Most alkaline pretreatment is used for delignification of agricultural residues and herbaceous plants, such as grasses. Alkaline delignification of wood chips with hot water by kraft lignin is highly used in industry and leads to cheap and high purity lignin. The four

preferred alkaline agents used for biomass hydrolysis are sodium, calcium, potassium, and ammonium hydroxides, but the most studied is sodium hydroxide.⁴²⁻⁴⁵

c. Organosolv process

Organic solvent or a mixture of organic solvents is used to dissolve the lignin in lignocellulosic materials leaving the cellulose and hemicellulose in the biomass residue. Different groups of organic solvents have been used: ketones, phenols, esters, organic acids, etc. The organic solvents are mixed and heated with lignocellulosic biomass at pressures above atmospheric pressures to force the lignin molecules to dissolve into the organic solvent. Acids such as hydrochloric and sulfuric acids are usually added to the organic solvent mixtures as catalysts to break the bonds between the lignin and hemicellulose molecules.⁴⁶⁻⁴⁸ Phase separation is created when water is added at the end of the reaction, this removes any sugar arising from the hydrolysis of polysaccharides.⁴⁶ Lignins extracted using this pretreatment is considered to high purity lignin.⁴⁸

d. Ozonolysis hydrolysis

Ozone has been used as pretreatment for removal of hemicellulose and lignin in lignocellulosic materials in order to produce biochemicals. Morrison and Akins⁴⁹ used ozone to oxidize grasses to produce levulinic acid, vanillin, *p*-hydroxybenzoic acid, and hexanoic acid, malonic acid, hydroquinone, and *p*-hydroxybenzaldehyde. The degradation mostly attacks the bonds within the lignin and slightly affects hemicellulose, while the cellulose remains intact. Ozone oxidation pretreatment has been used to pretreat different lignocellulosic material such as green hay, pines, poplar sawdust, cotton straw, and wheat straw. Ozonolysis pretreatment reaction is performed at room temperature and

atmospheric pressure and produces no toxic residues.⁵⁰⁻⁵³ The only drawback is a large amount of ozone is required, which makes the reaction expensive.

Other oxidative delignification pretreatments that are similar to ozonolysis have been studied. Schmidt et al.⁵⁴ used wet oxidation to pretreat wheat straw to degrade lignin and hemicellulose at 185 °C and 1.2 MPa O₂ with water. Azzam et al.⁵⁵ also used hydrogen peroxide as an oxidative delignification agent to pretreat agrocellulosic waste, sugarcane bagasse at 30 °C.

1.2.6. Physicochemical pretreatment

a. Torrefaction

Torrefaction is a thermochemical process employed to pretreat lignocellulosic materials using temperatures from 200 – 300 °C in an inert or nitrogen atmosphere, thereby forming a solid uniform product (torrefied biomass) with less moisture but high calorific values compared to the raw biomass.⁵⁶ Devolatilization of lignocellulosic materials occurs at temperatures above 200 °C leading to torrefied biomass, depending on the conditions of the process. Torrefaction process causes the removal of hemicellulose, hydroxyl groups, cleavage of aryl ether linkages, demethoxylation of lignin, degradation of cellulose, and an overall increase in aromaticity of biomass, while increasing the energy value or energy density of the torrefied biomass.⁵⁷⁻⁵⁸ Studies have shown that torrefied biomass is about 70 % of the mass of the starting biomass.⁵⁹ Dehydration of the biomass during the torrefaction process reduces the ability of the torrefied biomass to uptake moisture. The hydrophobicity of the torrefied biomass is due to the removal of hydroxyl groups in the initial biomass by the dehydration reactions, which leads to the

inability of the torrefied biomass to form hydrogen bonds with water. The moisture uptake of torrefied biomass ranges from only 1 % to 6 %.⁵⁹⁻⁶⁰

Torrefaction is a promising pretreatment technique because of high process efficiency (94 %) as compared to pyrolysis (64 %).⁶⁰ There are many advantages of torrefied biomass over the raw biomass. The change in chemical and physical property of the torrefied biomass reduces the cost of transportation and logistics. The increase in hydrophobicity properties of the torrefied biomass provides suitable long-term storage. The torrefaction process increases carbon content and reduces oxygen and hydrogen content thereby lowering O/C. Torrefaction also result in better grinding of the biomass.^{57, 61}

b. Pyrolysis

Unlike torrefaction, in pyrolysis the lignocellulosic material is thermochemically converted to form vapor in the absence of oxygen at elevated temperatures, which produces bio-oil when the volatile gases generated are rapidly cooled.⁶²⁻⁶³ Pyrolysis can be used as pretreatment and treatment techniques for lignocellulosic materials at a desired temperature. This process uses high temperatures usually above 300 °C to 800 °C to convert lignin, cellulose, and hemicellulose to lower molecular weight liquid products, bio-oil, gas products (H₂, CO, CO₂, and CH₄ etc.), and bio-char. Bio-oil from pyrolysis is made up of a mixture of aqueous and organic compounds. Bio-oil is a renewable liquid fuel and in a well-controlled environment can also be converted to other forms of chemicals.^{64 65} The amount and structural compositions of pyrolytic products is dependent on the type of biomass and pyrolytic conditions used. The type of reactor, temperature program, particle size, reaction time, maximum temperature used, and

amount of water present in the biomass determines the yield and structural composition of pyrolytic products.

Bio-oils produced at temperatures lower than 350 °C are reported to have high water content and low weight organic compounds such as acetic acid, furan aldehydes, formaldehydes, hexanoic acid, and phenolic monomers (*p*-cresol, phenol, guaiacol, vanillin, etc.). Pyrolysis of biomass at temperatures above 400 °C to 800 °C usually results in a lower amount of water, high amount of organic compounds, and high amount of non-condensable gases (CO₂, H₂, and CO).⁶⁶ Pyrolysis of lignin results heavily in aromatic moieties, especially methoxylated phenolic monomers, and a few oligomers and aliphatic compounds. On the other hand, pyrolysis of hemicellulose and cellulose results in esters, organic acids, aldehydes, and a few oligomers. Pyrolysis of lignocellulosic materials above 900 °C produces little or no oil, but noncondensable gases. The amount of char produced reduces as the temperature increases.

1.2.7. Explosion pretreatment

There are different explosion pretreatment techniques that have been used for separation of lignocellulosic material components. Methods such as steam (autohydrolysis) explosion, carbon dioxide explosion, ammonia fiber explosion (AFEX) all have been used to pretreat recycled papers, rice straw, grasses, and sugarcane bagasse.⁶⁷⁻⁶⁹ Explosion pretreatment combines chemical and physical processes using high pressures and temperatures. The pressure is first maintained steadily for the reaction and followed by a rapidly reduction in pressure which causes the reactants to undergo explosive decompression. Steam explosion uses acids for lignocellulosic material hydrolysis and solubilizes the hemicellulose, increasing enzymatic saccharification.

Ammonia fiber explosion uses alkaline solutions and does not solubilize the hemicellulose. Carbon dioxide explosion uses a supercritical carbon dioxide/water combination which results in carbonic acid to increase the rate of hydrolysis of lignocellulosic materials. The carbon dioxide explosion process is the most cost effective of all the explosive methods and does not produce inhibitory products to affect the downstream enzymatic hydrolysis.⁶⁷ Steam explosion is the next most cost-effective process, but it produces inhibitory products to the enzymes downstream.

1.2.8. Liquid hot water pretreatment

Liquid hot water pretreatment uses water under high pressure and temperature to penetrate lignocellulosic materials to hydrate cellulose by removing hemicellulose and lignin.⁶⁷ This is similar to the hydrothermal treatment except that chemicals are usually not used, resulting in less resistance to enzymes during enzymatic hydrolysis. Chemicals are only used in a few cases where catalysts are added to aid in breaking the bonds within the lignocellulosic materials. In liquid hot water pretreatment, long reaction times and large amounts of hot water are used as compared to hydrothermal treatment. Therefore, more energy is needed to separate the products.

1.3. Depolymerization of lignin for high-value biochemicals

1.3.1. Monomers of lignin

Lignin is the second most abundant biopolymer found in the plant cell wall, consisting of phenylpropanoid chains linked mostly by carbon-carbon and ether bonds. This complex of phenolic heteropolymers provides strong stiffness and fortification of secondary cell walls in the xylem tissues. The denser matrix that binds cellulose and hemicellulose provides mechanical support and limits elasticity to tissues in the plant

stems. It is very difficult to identify a complete structure of a lignin polymer because of the complex nature and inherent difficulties in characterization of lignin polymers. Figure 5 shows a model structure of softwood lignin.⁷⁰

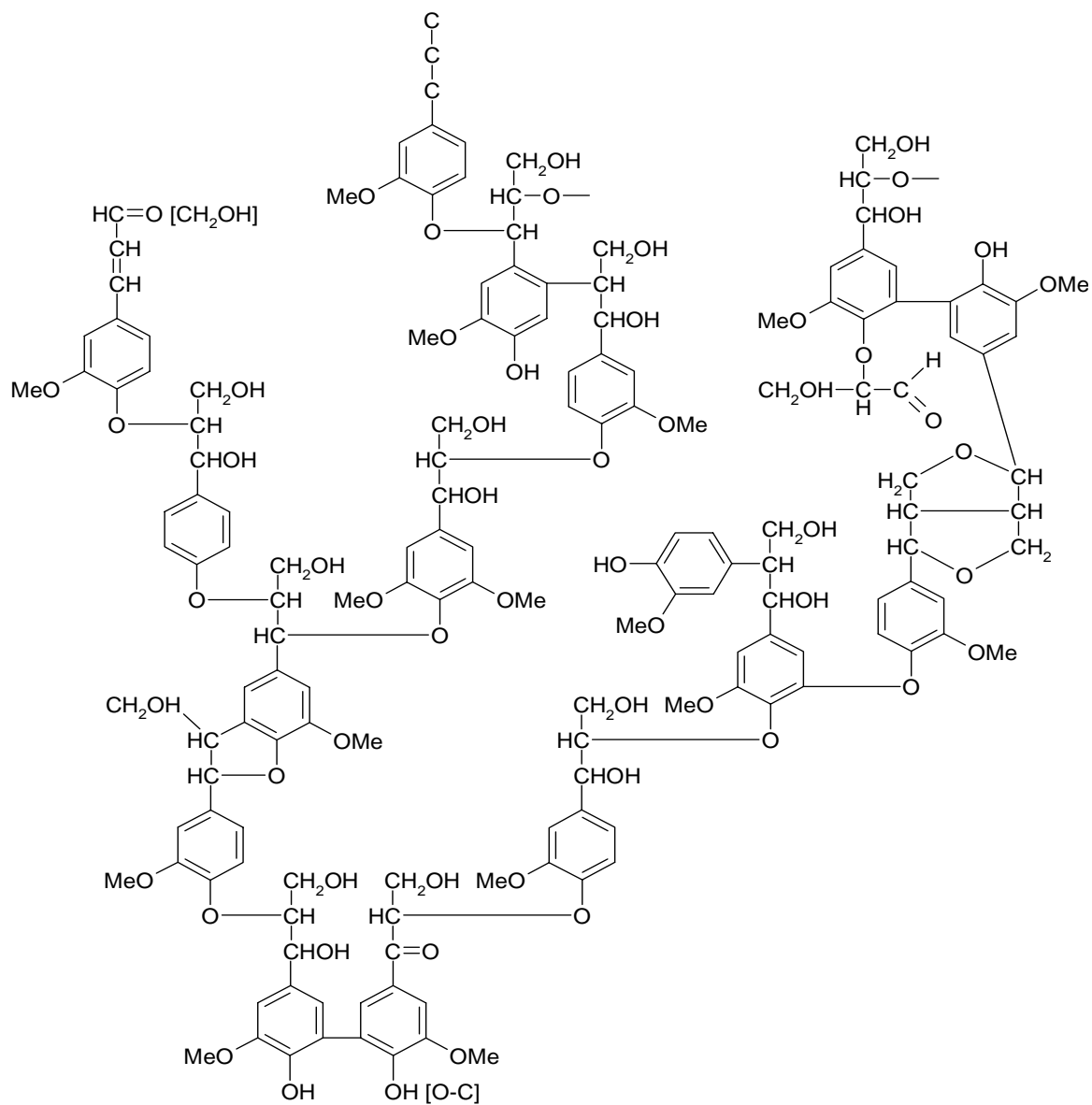


Figure 5. A model structure of lignin from softwood.⁷⁰

The three main phenolic monomers that make up the building blocks of a lignin polymer are *p*-hydroxyphenyl (H) moieties or *p*-coumaryl alcohol, coniferyl alcohol or guaiacyl (G) moieties, and sinapyl alcohol or syringyl (S) moieties as shown in Figure 6.⁷¹⁻⁷⁶ The propane side chains link the phenolic monomers in the lignin polymeric structure. The type of moieties present in the lignin polymer depend on the plant species, climatic conditions, age, the type of cultivation practices, and soil conditions under which the plant was grown. Pretreatment processes are employed to determine the amount of lignin in lignocellulosic biomass. Different lignin characterization methods are used to determine the phenylpropanoid moieties in the polymer. Lignins from softwood are predominately made up of guaiacyl (G) moieties while hardwoods are made up of both guaiacyl and syringyl moieties.⁷⁶ Lignins from grasses are predominantly *p*-hydroxyphenyl (H) moieties with guaiacyl (G) and syringyl (S) moieties.⁷⁶

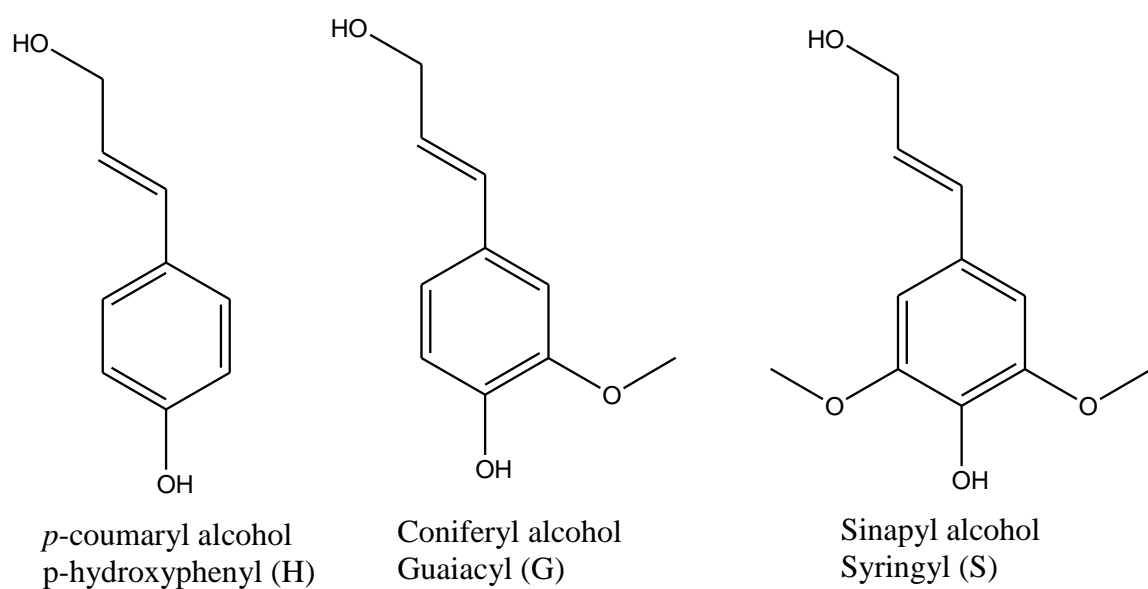


Figure 6. Structures of three basic phenolic monomers that form lignin.

1.3.2. Hydrotreatment or hydrothermal liquefaction of lignin

Lignin has been isolated in large quantities in the biorefinery, pulp, and paper industries because of its interference in the hydrolysis of polysaccharides. Unlike cellulose and hemicellulose, lignin is underutilized because of the difficulty in converting it to useful biochemicals. Lignin is rich in aromatic compounds and, therefore, can serve as a great source of phenolic compounds in order to replace petroleum products. There are several processes including pyrolysis previously described, hydrothermal gasification, wet oxidation, hydrotreatment or hydrothermal liquefaction (HTL) that are used to depolymerize lignin to bio-oil as a biochemical feedstock for the production of phenolic resins, epoxy resins, or phenolics for food and pharmaceutical additives. For the purpose of this study, the focus will be on conversion of lignin by hydrotreatment or HTL using subcritical water.

Subcritical water exists in a wide-temperature range, from the normal boiling point, 100 °C, and the critical temperature, 374 °C, as indicated in Figure 7.⁷⁷ Hydrotreatment uses temperatures between 200 °C and 374 °C and pressures between 10 and 25 MPa for physical and chemical transformation of lignin to produce value-added useful chemicals. The unique properties of subcritical and supercritical water allow it to behave as an acid-base catalyst because concentration of the ionic products (H_3O^+ and OH^-) increases by two orders of magnitude over that in water at room temperature while the pH remains neutral. The density of water decreases from 1000 kg/m³ at room temperature to 820 kg/m³ for subcritical water at 250 °C and 25 MPa⁷⁸, but the density

changes more significantly at temperature above 300 °C. The kinetic energy of the molecules of the liquid, as well as the intermolecular interactions, significantly affects how fast the liquid particles can vaporize. Liquid changes to a vapor when the kinetic energy of the liquid particles is higher than the intermolecular force of attraction between the particles of the liquid. The decrease in density of the water during hydrotreatment or HTL decreases the viscosity and increases the solubility of hydrophobic lignin in the superheated water. Even though increasing the temperature above 300 °C results in significant change in water density with pressure, the use of high pressure and superheated water below 300 °C with catalysts increases the rate of diffusion. Higher temperatures lead to char/coke formation, corrosion to the reaction vessel, damage to the catalyst, and increases in repolymerization. HTL has several advantages over other methods used for lignin depolymerization: (1) pre-drying of lignin from pulp, kraft, and papermaking is not necessary, reducing cost and energy usage. (2) hydrothermal treatment conditions produce hydrogen from the water which is necessary for lignin gasification,⁷⁹ (3) hydrothermal treatment temperatures are usually lower than other thermochemical methods including pyrolytic, supercritical, and gasification temperatures, and (4) nitrogen and sulfur are predominantly found in lignin, especially lignosulfonates. Other depolymerization methods release nitrogen oxide and sulfur oxides which require further treatment, incurring extra costs. In hydrotreatment, these oxides are dissolved in the water.

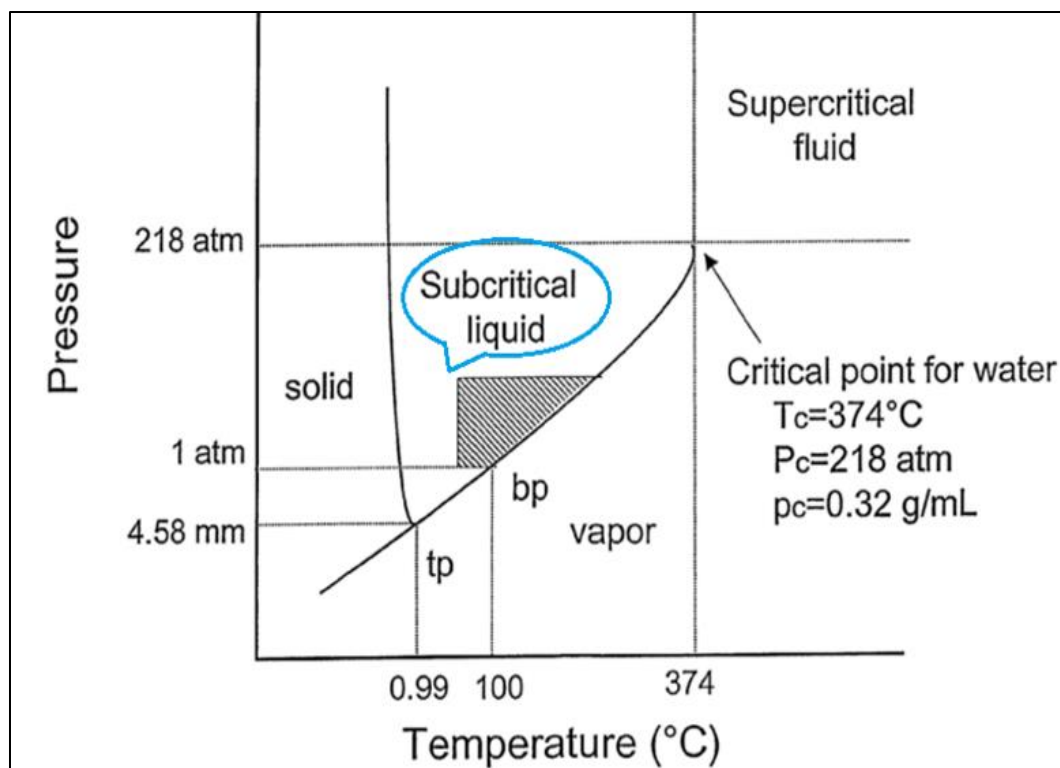


Figure 7. Changes in properties of water under different temperatures and pressures.⁷⁷

1.3.3. Catalysts

The primary aim of lignin depolymerization is to form phenolic monomers, but oligomers are also formed in the process. There are different operating conditions that affect the HTL of lignin. Temperature, pressure, resident time, and the concentration of the catalyst all affect the formation of phenolic monomers and oligomers, and repolymerization. Cheng et al.⁸⁰ indicated that the hydrotreatment process for lignin depolymerization needs stirring to reduce solid residue or char formation, but it is not affected by the rate of stirring. The catalyst is one of the operating conditions which affect the yields of HTL of lignin depolymerization in terms of breaking the C-C and C-O bonds (mainly β -O-4 ether bonds), which is usually accompanied by dealkylation of side chains and hydrolysis of methoxyl groups for desired products as well as reduction in

coke/char formation and repolymerization.⁸¹ Zeolite metal catalysts have two roles in lignin depolymerization: (1) acidic sites and (2) pores help control the reaction in the mixture in order to achieve the more stable, desired products, as well as to increase yields.⁸² The acidic sites are responsible for the breaking down crosslinkages, leading to the desired products, while the volume created by the pores helps prevent repolymerization and the formation of cokes in the reaction⁸². The combination of zeolite metal catalysts with desired changes in the properties of water at high temperatures and pressures during HTL process of lignin increases the yields of bio-based phenolic products.⁸⁰

1.3.4. Effect of hydrogen source in hydrothermal liquefaction

Hydrogen helps in reductive depolymerization of lignin when using supported-metal catalysts during hydrothermal liquefaction. The hydrogen breaks down to produce a hydrogen atom and a radical. The hydrogen radical initiates depolymerization of lignin while the hydrogen atom is donated to stabilize the intermediate phenolic moiety in the reaction solution. Several hydrogen-donating solvents such as formic acid, acetic acid, and 2-propanol have been employed in the application of reductive depolymerization of lignin.⁸³⁻⁸⁵ The hydrogen-donating solvents are usually added at the beginning of the reaction or during the extraction process. Large amounts of the hydrogen-donating solvents are needed when added during a depolymerization reaction process, but lesser amounts are needed if added at the extraction stage. When a hydrogen-donating solvent is added to a reaction mixture during the extraction process to be used only as a protonating agent, it is environmentally benign.

In the HTL process, the hydrogen gas produced *in-situ* gets adsorbed by the supported-metal catalysts surfaces, which cause the dissociation of the hydrogen gas into a hydrogen atom or a radical ⁸⁶. The hydrogen radical attacks the ether cross-linkages within the lignin polymer, as shown in Figure 8. ⁸⁶ The cleavage of the ether bonds results in the production of monomers and oligomers from the lignin polymer. The hydrogen atoms in the solution protonate the intermediate phenolic compounds, stabilizing them.

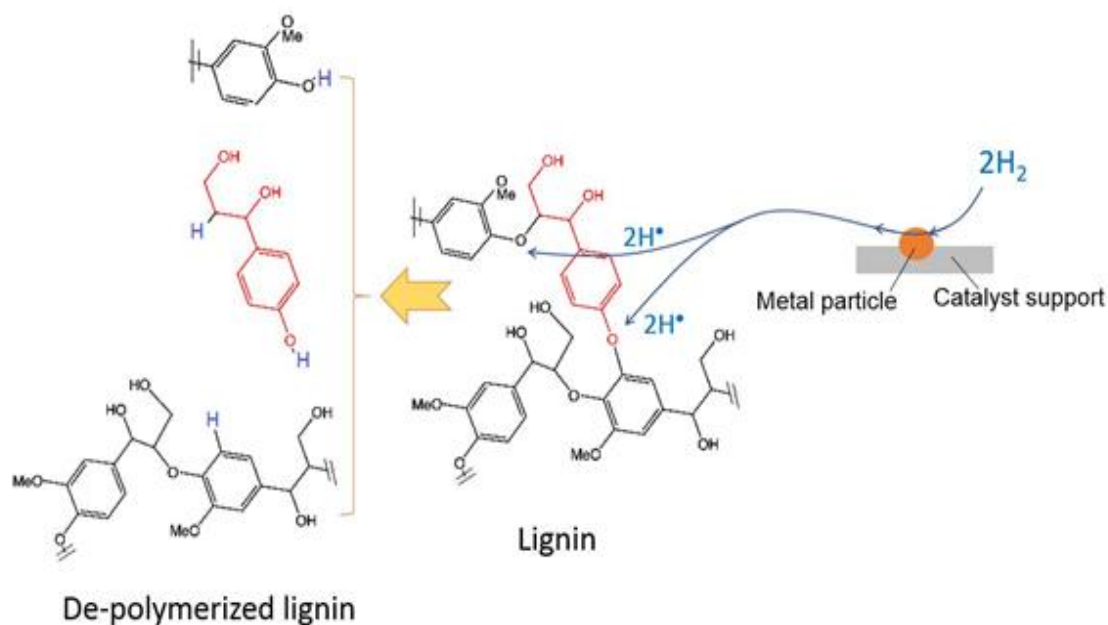


Figure 8. Lignin depolymerization reaction mechanism involving metal catalysts in hydrothermal liquefaction process. ⁸⁶

1.4. The purpose of this study

This dissertation proposes that subcritical water at elevated temperatures of 200 °C and 240 °C and pressures between 10 and 25 MPa will depolymerize kraft lignin to the desired phenolic monomers without side reactions when using a zeolite metal oxide catalyst and a liquid-liquid extraction method. At higher temperature near the critical point, the hypothesis is supported by an increased yield of phenolic monomers. This dissertation also proposes the identification of lignin in torrefied biomass and extracted

phenolic monomers obtained from the torrefaction of prairie cordgrass. The hypothesis is supported by lignin recovered from torrefied biomass as compared to the availability of lignin recovered by pyrolysis of prairie cordgrass. The specific objectives are summarized as:

1. Develop hydrothermal liquefaction methods using subcritical water and zeolite metal oxide catalysts (MoO, CoO, and LaO) to depolymerize kraft lignin into phenolic monomers. The phenolic monomers will be extracted from the reaction mixture by liquid-liquid extraction using ethyl acetate and acetic acid as protonating agents. The phenolic moieties will be characterized by GC-MS and UHPLC analysis.
2. Quantify lignin from the torrefied biomass of prairie cordgrass at 250 °C, 300 °C, and 350 °C using NREL lignin determination methods and compare it to the bio-char from pyrolysis at 600 °C and 900 °C.
3. Determine the phenolic monomers produced during pretreatment of prairie cordgrass using torrefaction at 250 °C, 300 °C, and 350 °C compared to phenolic monomers produced by pyrolysis at 600 °C and 900 °C. The phenolic moieties will be extracted by Accelerated Solvent Extraction (ASE) and characterized by GC-MS analysis.

This dissertation will characterize the kraft lignin before it is used for hydrothermal liquefaction to form phenolic monomers. This dissertation also aims to determine the effects the torrefaction pretreatment method has on ash, moisture, extractives, and lignin recovery from prairie cordgrass, as well as the elemental analysis and heating values of the biofuels resulting from the torrefaction method.

CHAPTER 2

HYDROTREATMENT OF KRAFT LIGNIN INTO PHENOLIC MONOMERS USING SUBCRITICAL WATER AND SUPPORTED-ZEOLITE METAL OXIDES

2.1. Introduction

The polyphenolic nature of lignin makes it a great source for production of useful phenolic compounds⁸⁷, which are renewable in nature.⁸⁸⁻⁹⁰ The main phenolic moieties found in lignin are *p*-hydroxyphenyl (H), guaiacyl (G), and syringyl alcohol (S).⁷²⁻⁷⁶ Lignin separation from other lignocellulosic materials involves two processes, sulfur and non-sulfur lignin extraction.⁹¹ Sulfur-free lignin extraction consists of the use of organic solvents and alkaline solutions.⁹² The sulfur process involves the use of sulfite to produce lignosulfonate and kraft lignins from extraction using sodium sulfite and sodium hydroxide mixtures. Kraft lignin has been produced as a byproduct in large quantities by the paper and pulp industry and forms 15-30 % by weight of the starting biomass. Lignin is usually burned as fuel in industrial burners and only small amounts are used as additives.⁹²⁻⁹⁴ About 50 million tons of lignin are produced as a byproduct annually in the paper and pulp industry.⁹⁵ However, there have been limitations in the direct use of kraft lignin because of high steric hindrances and lower reactivity caused by different crosslinkages. Utilization of kraft lignin for the production of biofuels and biochemicals will help generate additional revenue for the paper and pulp industry.

Lignin extraction methods are able to break the weak hydrogen and ether linkages between lignocellulosic materials in biomass, leading to separation of carbohydrates and lignin, but it does little on the bonds within lignin. The methoxylated phenylpropane units are cross-linked by C-C and C-O-C bonds. Ether linkages form two-thirds of the total

linkages in most lignins and the rest of the linkages are C-C bonds.⁸² The main ether linkages include the α -O-4 (α -aryl ether), 4-O-5 (diaryl ether), and β -O-4 (β -aryl ether), as shown in Figure 9, based on the positions of carbon and oxygen atoms forming the bond. The most abundant ether linkage is β -O-4 with lower percentages of α -O-4 and 4-O-5.⁹⁶⁻¹⁰¹ C-C linkages are more difficult to break than ether bonds in lignin because of higher bond dissociation energies in C-C bonds.¹⁰²⁻¹⁰⁴ Even though ether linkages are readily cleaved compared to C-C linkages in lignin, its chemical reactivity considerably dictates lignin resistance to thermochemical degradation.⁸² Functional groups within native lignin such as methoxyl, benzyl alcohol, phenolic and aliphatic hydroxyl, noncyclic benzyl ether, carboxyl, and carbonyl also affect reactivity and resistance of lignin to be transformed to useful compounds.⁸²

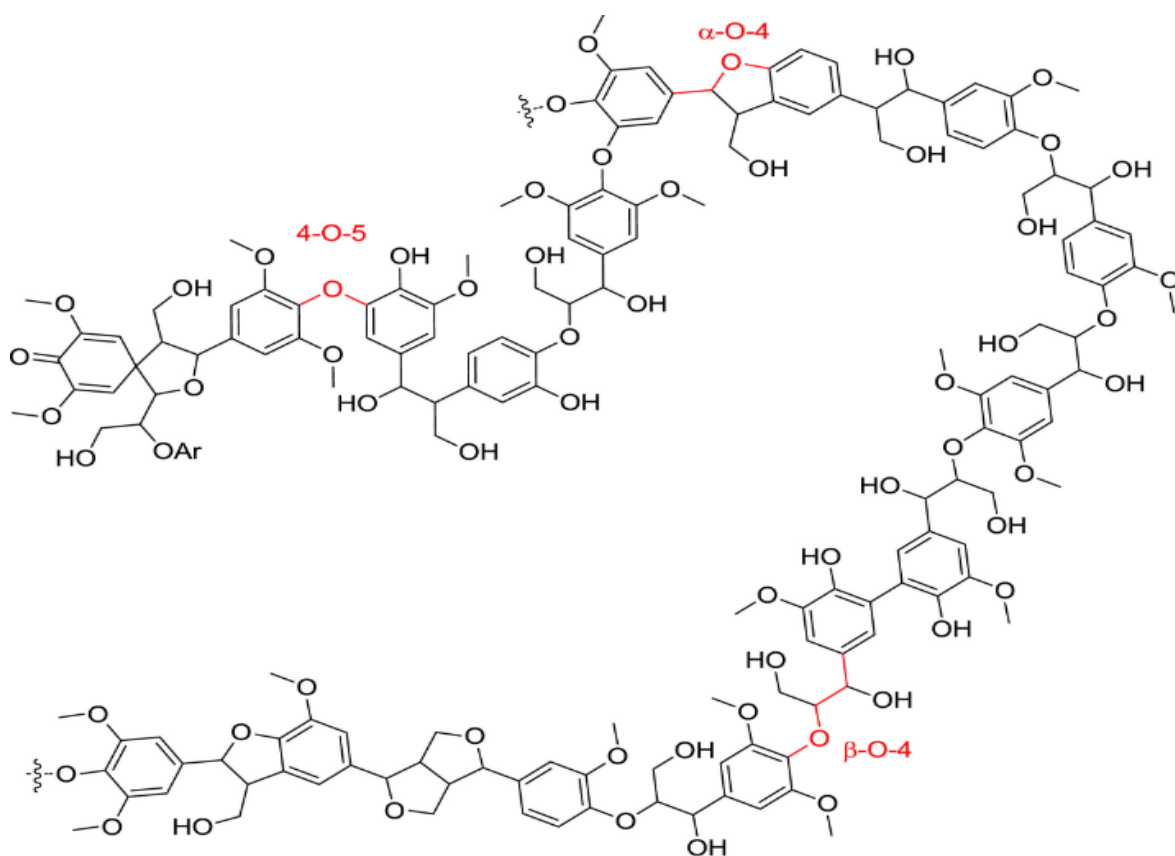


Figure 9: Schematic structure of a model compound bearing typical lignin linkages from hardwood.⁹⁷

The fragmentation of lignin during extraction and the multiplicity of various functional groups in lignin give rise to the complexity of lignin structure. Products produced from lignin depends largely on the characteristics of the starting material, therefore lignin characterization is necessary before any useful transformation is done. Studies have shown that the characteristic structure and functional groups of lignin significantly depend on the extractions methods employed.¹⁰⁵ Transformation of lignin to generate commodity chemicals requires cleavage of the linkages in the native lignin.¹⁰⁶ An appropriate catalytic method is needed to depolymerize lignin to useful aromatic compounds such as vanillin, vanillic acid, acetovanillone, guaiacol, syringol, etc. Several

studies have been conducted to depolymerize kraft lignin and other isolated lignins to valuable products to make the biorefinery industry economically viable.^{97, 107-110}

Recent developments of chemical depolymerization of lignin, including base-catalyzed, acid-catalyzed, metal-catalyzed, ionic liquid-assisted, and supercritical fluid-assisted, has been discussed by Wang et al.¹¹¹ Catalysts are employed in lignin depolymerization process to reduce high char yields and repolymerization. Base-catalyzed depolymerization, including the use of KOH, NaOH, Ca(OH)₂, LiOH, Ba(OH)₂, and CsOH with water/methanol or ethanol under supercritical conditions, for phenolic compounds (syringol, phenols, catechol, *p*-cresol, guaiacol, etc.) production at temperatures higher than 260 °C was studied by different researchers.^{47, 112-116} A near-neutral condition with the use of acetone/CO₂/water or phenol under supercritical temperatures above 300 °C and high pressure was utilized to depolymerize organosolv lignin.¹¹⁷⁻¹¹⁸ The use of Lewis acids (NiCl₂ and FeCl₂) and other acids (formic and boric) with different solvents were also used to convert lignin to phenolic compounds at temperatures above 300 °C.^{115, 119} Co, Ni, Ru, Mo, Cu, Au, Pt, and Pd are used on different supported media (C, Al₂O₃, SiO₂, SiO₂-Al₂O₃, and zeolite) in addition to bases, acids, subcritical, supercritical, and pyrolytic conditions to reduce repolymerization and to increase yield of organic compounds from lignin.^{107, 119-127} Zeolite H-ZSM-5-supported catalysts are known to favor production of aromatic hydrocarbons.¹²⁸ Co, Mo, and Ni have been the most studied catalysts to increase yield and hydrogenation in hydrotreatment.^{120, 129-130} Hydrotreatment of kraft lignin using Mo catalyst at different times (15 - 60 min), catalysts concentrations, and temperatures has been studied.¹³¹ Oasmaa and Johansson found out that Mo catalysts resulted in high yields of oils from

kraft lignin by hydrotreatment and that the concentration of the catalyst did not affect the change in yield, but high temperatures (430 – 450 °C) and long residence time (60 mins) showed lowest yield.¹³¹ Cheng et al also have reported that long residence times do not influence the properties and product yield using metal catalyst.⁸¹ Yuan et al have reported repolymerization of lignin fragments from the products of hydrotreatment at high temperatures.¹³²

Most of the methods discussed above involve model compounds where tetramers, trimers, and dimers are used. There is difficulty in repeating these experiments. In addition to the difficulty of using model compounds is the use of high temperatures and pressures which led to coke/char formation and corrosion on the internal surface of the reactor. The use of high amount of catalysts has made lignin depolymerization economically unattractive.¹⁰⁷ An environmental and economical benign process is needed to generate phenolic monomers from kraft lignin. In this study, we hypothesize that the use of inexpensive supported-zeolite metal oxides (CoO, LaO, and MoO)¹³³ with subcritical water at 200°C and 240°C will convert lignin to value-added phenolic monomers to serve as a feedstock for production of resins and additives for the pharmaceutical and food industries. Thus, to determine the phenolic monomers from the reaction, the approach is: (1) characterize the starting material (kraft lignin) using fourier transform infrared spectroscopy (FTIR), differential scanning calorimetry (DSC), pyrolysis-gas chromatography–mass spectrometry (Py-GC-MS), and thermogravimetric analysis (TGA) to understand the characteristics of the phenolic moieties in the lignin polymer, (2) use ultra-high-performance liquid chromatography (UHPLC), gas

chromatography–mass spectrometry (GC-MS), and FTIR to analyze the phenolic monomers from kraft lignin.

2.2. Experimental

2.2.1. Materials and reagents

Kraft lignin was purchased from Sigma-Aldrich (St. Louis, MO). Kraft lignin was oven dried at 105 °C for 48 hours and stored in a desiccator after cooling to room temperature. Supported-zeolite (H-ZSM-5) metal oxides, CoO, LaO, and MoO, were obtained from the Agricultural and Biosystems Engineering Department of South Dakota State University. 99 % nitrobenzene, 97.5 % cupric oxide, 99.9 % ethyl acetate, 99.9 % methanol, 99 % sodium hydroxide, and 99.8 % anhydrous acetic acid were all obtained from Sigma-Aldrich (St Louis, MO) and used without any further purification. Ultra-purified water used was obtained by using a Thermo Fisher Scientific 18 Ω M/cm⁻¹ Barnstead Ultrapure water system. 99 % phenol, 99 % catechol, 98 % guaiacol, 99 % p-cresol, 99 % 4-propyl-guaiacol, 98 % ethyl- guaiacol, 98 % methyl-guaiacol, 98 % eugenol, 97 % vanillin, 98 % acetovanillone, and 99.9 % o-terphenyl and acetic acid were purchased from Sigma-Aldrich (St. Louis, MO) and 98 % homovanillic from Acros Organics (NJ, USA).

2.2.2. Methods

Different characterization methods were employed to analyze the starting material and phenolic monomers extracted from HTL of the kraft lignin. Figure 10 shows the outline of the various characterization methods.

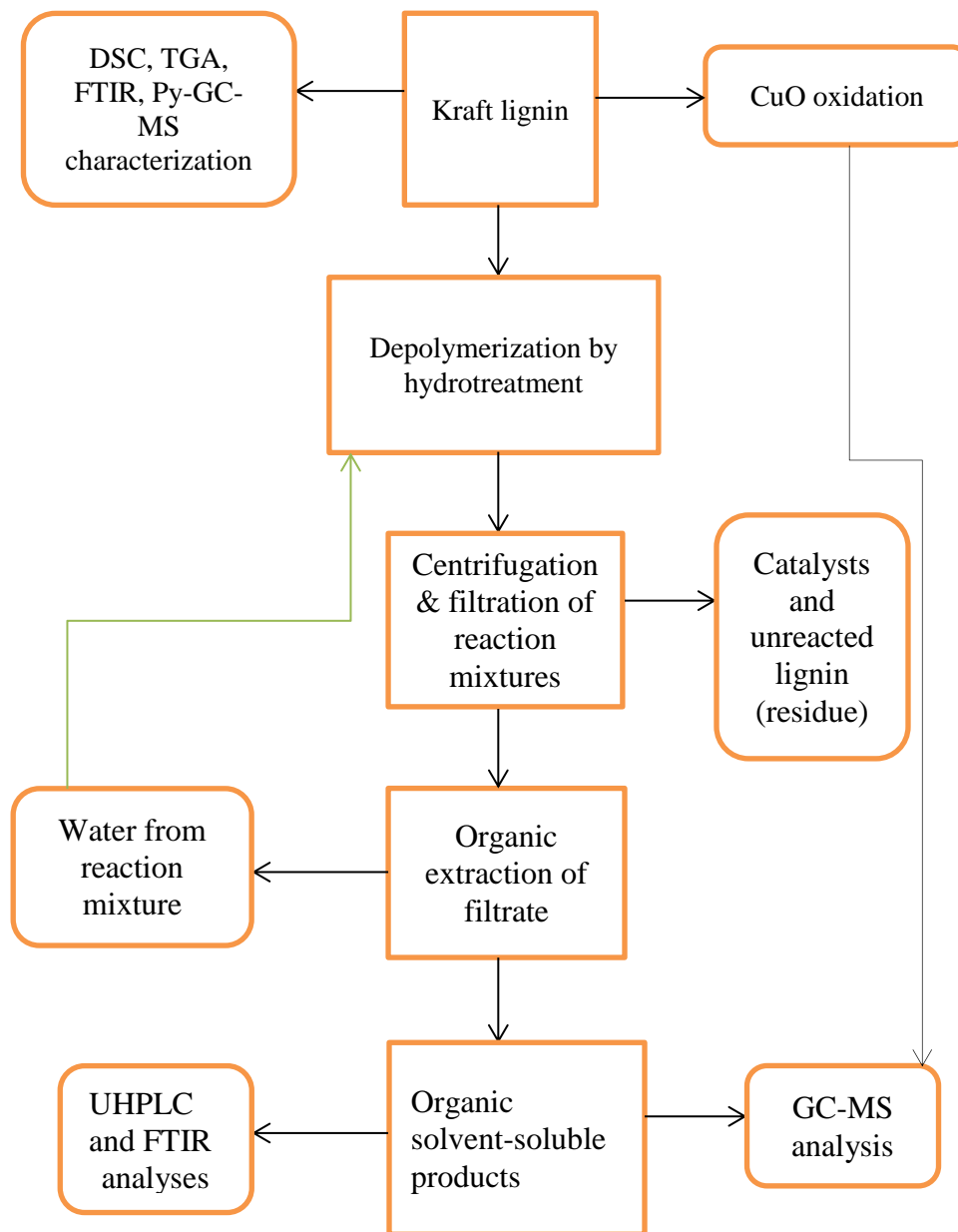


Figure 10. Outline of kraft lignin characterization and analysis of depolymerization processes.

a. Lignin characterization

i. Cupric oxide oxidation analysis

The Pearl cupric oxide oxidation method was used to elucidate the structure of the lignin with slight modification.¹³⁴ Base, 15-mL 2-M NaOH, was added to 100 mg of lignin in a 50-mL round-bottom flask and purged with nitrogen. The mixture was degassed and then filled with nitrogen gas to maintain an inert atmosphere. The reaction mixture was stirred uniformly and continuously until the lignin dissolved at room temperature. One gram of cupric oxide was added to the reaction mixture and refluxed for 150 minutes at 175 °C. The oxidized reaction was cooled to room temperature using cold water and then washed with 15-mL methylene chloride to remove the impurities. The reaction mixture was acidified to pH 3-4 using hydrochloric acid. The acidified mixture was washed three times using 15-mL methylene chloride. All methylene chloride extracts were concentrated using rotary evaporation under controlled vacuum and stored for GC-MS analysis of phenolic monomers.

ii. DSC analysis

DSC measurements of kraft lignin were performed using a DSC Q200 from TA Instruments (Newcastle, DE). Five to ten milligrams samples were loaded in the covered hermetic pans, sealed, and then run against the empty reference pan. DSC scans were measured at a dynamic heating rate of 15 °C/min from 20 to 400 °C under nitrogen. All samples were performed in duplicate. Logger Pro 3.8.6 software was used for the analysis of the different phase changes.

iii. Py-GC-MS Analysis

Py-GC-MS analysis of kraft lignin was performed. Py-GC-MS experiments were carried out using a CDS Analytical Inc. Pyroprobe 5000 (Oxford, PA) heated filament pyrolyzer directly coupled to an Agilent 7890A gas chromatography with Agilent 5975C triple-axis mass detector and electron-impact ionization at 70 eV (Newcastle, DE). Agilent DB-5 %-phenyl-methylpolysiloxane capillary column (30 m x 0.25 mm x 0.25 μ m) was used to separate the compounds. Hydrogen was used as a carrier gas. Approximately one mg of lignin was added to the quartz wool in the 20-mm quartz tube. The samples were subjected to pyrolysis at a set temperature range between 60 °C and 600 °C at a ramp rate of 20 °C/ms and held for 1 minute. The initial temperature was held for 5 s. The pyrolyzed gases were introduced into the GC at an interface temperature of 300 °C with splitless injection and an MS ion-source temperature at 200 °C. An initial oven temperature of 60 °C held for 2 min was ramped to 280 °C at of 10 °C/min and held for 5 min at 280 °C. The inlet and auxiliary lines were kept at 300 °C. Peaks were identified by NIST Mass Spectral library and mass spectra from standards. The mass spectral data was obtained using electron ionization at 70 eV over the m/z range from 50 to 550 amu.

iv. TG analysis

Kraft lignin samples were analyzed using a Perkin Elmer Pyris-1 TGA thermogravimetric analyzer (Shelton, CT). The TGA were obtained in terms of TG and DTG curves. The TG data were recorded as percent mass loss of the lignin samples as a function of temperature, whereas the DTG curve is first derivative of the TG curve. Thermal decomposition of lignin was performed using an aluminum crucible under nitrogen

atmosphere with dynamic conditions of 25 to 900 °C at a heating rate of 15 °C/min in a nitrogen atmosphere at a flow rate of 18 mL/min. Five to ten milligram samples were used for the analysis. The experiments were performed in duplicate. The data were automatically output through the integrated thermogravimetric analyzer system.

v. FTIR analysis

A Thermo Electron Corporation Nicolet 380 FT-IR spectrometer (Madison, WI) in the attenuated reflectance mode was used to obtain the FTIR spectra for the Kraft lignin to determine the functional groups present. Eight per centimeters resolution with 100 scans in the spectral range of 4000-700 cm^{-1} was used. The background spectra were collected for all trials before running all samples, as a control measurement. All data collection and analysis were done using OMNIC Spectra and Nicolet 380 OMNIC FT-IR spectrometer interpretation guide software.

a. Catalytic depolymerization of kraft lignin

i. Catalysts characterization

The surface area, pore sizes and total pore volumes of the catalysts were determined using Micromeritics Tristar 3000 automated N_2 adsorption-desorption analyzer. ASAP 2010 Micropore Analyzer with liquid nitrogen was used to carry out the analysis of the physisorption of the catalysts at 77 K. The catalysts were degassed using the Micromeritics FlowPrep 060 unit at 200 °C for 5h to remove moisture before nitrogen isotherm analysis. The specific surface areas of the catalysts were calculated by a Brunauer-Emmett-Teller (BET). The micropore and mesopore volumes were determined by Density Functional Theory (DFT) analysis.

ii. Hydrotreatment reaction

A supercritical fluid reactor from Applied Separations (Allentown, PA) was used for hydrothermal liquefaction of lignin, as shown in Figure 11. The lignin depolymerization was carried out in a 25-mL stainless steel reaction vessel.

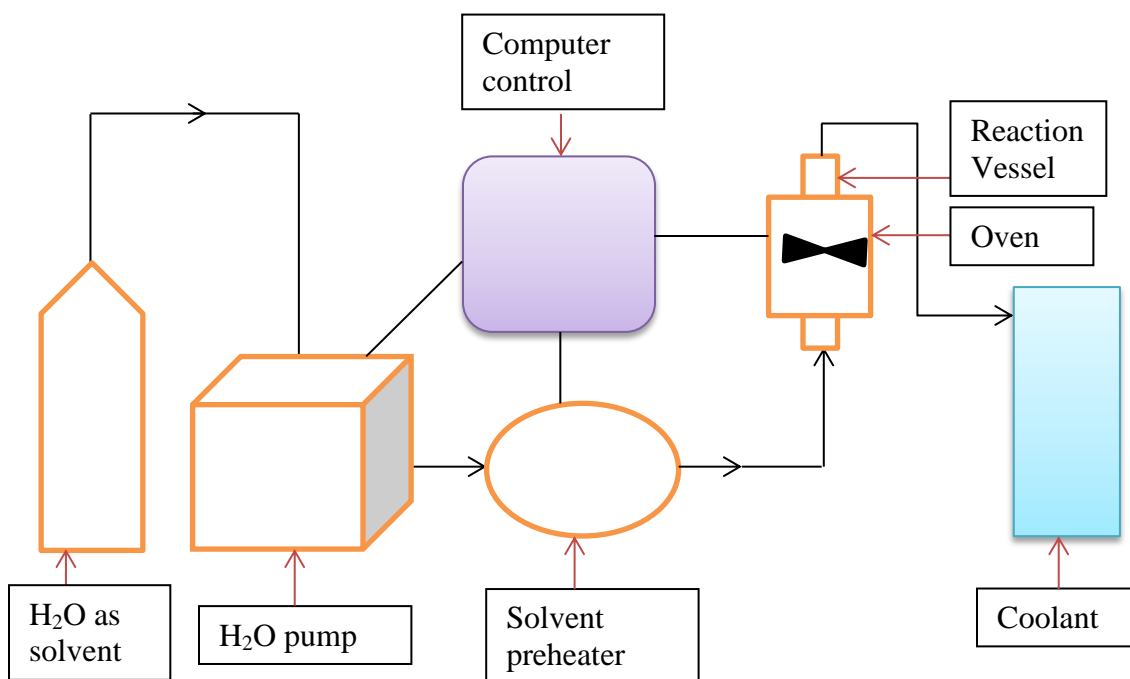


Figure 11. Helix SFE system used for hydrothermal depolymerization of Kraft lignin.

0.23 g of dry Kraft lignin was used for all hydrotreatment reactions. The catalysts (10 wt% with reference to the kraft lignin) were added to the Kraft lignin for all reactions and blanks. The three catalysts used were CoO, LaO, and MoO on the zeolite-support. 23-mL of deionized water was pumped into the reaction vessel. The water was preheated to 60 °C before reaching the reaction vessel. The oven was computer programmed to heat the reaction vessel to the required temperatures and pressures. Figure 11 shows the outline of the Applied Separations Supercritical Fluid reactor system used for the

hydrotreatment. The reaction conditions for the lignin depolymerization were 200 and 240 °C, 12 MPa, and 15 minute. The oven heated the reaction vessel to the desired temperature at 15 °C/min. The desired pressure was achieved as a result of temperatures reaching the maxima. The hydrothermal liquefaction reaction mixtures were emptied from the reaction vessel by rapid cooling of the reactor with water at room temperature. The product mixtures were collected in 50-mL centrifuge bottles and extracted. The solid residues (catalysts and unreacted lignin) were reused in the second hydrotreatment then dried and stored for further analysis.

iii. Extraction of phenolic monomers

Liquid-liquid extraction was used. The liquid reaction products were acidified using 0.02 mL of acetic acid to pH 2–3 from pH 5-6. Ethyl acetate was used for the extraction of phenolic monomers from the liquid reaction products.^{107, 135} Three mL of the liquid reaction mixture was measured and added to nine mL of ethyl acetate and vortexed for two min to obtain a uniform mixture. The mixtures were allowed to stand for 30 min before separation using a separatory funnel. The aqueous portion of the reaction mixtures were filtered and reused in the second depolymerization process. The organic-solvent soluble products (OSSP) were concentrated by nitrogen blow-down to one-third of the total extracted volume. 0.1 mL of 1000 ppm of internal standard (o-terphenyl) was added to the OSSP and the samples were then analyzed alongside the prepared standards on GC-MS and UHPLC. The blanks were also subjected to the extraction process and GC-MC, FTIR, and UHPLC analysis.

iv. Characterization of phenolic compounds

α. UHPLC analysis of phenolic monomers

The phenolic monomers present in the OSSP were determined at room temperature using a Thermo Fisher Dionex Ultimate 3000 UHPLC equipped with autosampler, pump, and diode array detector (DAD-300 RS) with ultraviolet visible (UV-Vis) wavelength range from 280 -720 nm. The Haghi et al. UHPLC method for phenolic compounds was employed to analyze the monomers present in the OSSP.¹³⁶ The injection volume was 1 μ L. Separation was conducted on a Agilent C18 column with dimensions of 150 mm x 4.6 mm (i.d.) x 5 μ m thickness using isocratic elution with a 2 % aqueous acetic acid and 0.5 % aqueous acetic acid: acetonitrile (50:50 v/v) with a flow rate of 0.8 mL/min. Phenolic standard compounds were injected into the column to identify the compounds present in the OSSP. The samples, standards, and blanks were run in triplicate. Five different concentration levels of standards were prepared using ethyl acetate as solvent. Thermo Scientific Dionex Chromeleon 7 software and the retention times of the standards were used for the identification of the phenolic monomers.

β. GC-MS analysis of phenolic monomers

The different phenolic compounds and their molecular weights in the reaction mixtures were determined using an Agilent 7890A GC equipped with an Agilent 5975C triple-axis mass detector with electron-impact ionization (Newcastle, DE). An Agilent DB-5 %-phenyl-methylpolysiloxane capillary column was used. The column dimension was 30 m x 0.25 mm x 0.25- μ m film and the oven temperature was initially programmed at 65°C for 1 min, ramped at 10°C/min up to 280°C with hydrogen gas as a carrier at 1.2

mL/min. A splitless 2 μ L injection of the standards and OSSP were used at injection temperature of 250°C. The mass spectrometry analysis was done in full-scan mode for m/z ranging from 50-550 amu using electron ionization at 70 eV. Analytical standards of the phenolic compounds present were prepared and used to identify the phenolic moieties present in the OSSP in connection with the NIST library and retention times of the known compounds on the MS Chemstation software. Quantification was achieved by internal standard methods using o-terphenyl as an internal standard.¹³⁷ Calibration curves were prepared by running five standard solutions with different concentration levels (31.25, 62.5, 125, 250, 500 ppm) and blanks in triplicates. Three masses corresponding to three major fragments of each compound were used for quantification from m/z values observed in the fragmentation pattern. The molecular weights and amounts of various phenolic moieties present in the OSSP were determined. The phenolic units present in the oxidation mixtures using cupric oxide oxidation were identified using the GC-MS method described for the OSSP.

2.3. Results and discussions

2.3.1. Catalysts characterization

Table 2 shows the lists of N₂ adsorption-desorption analysis for CoO/Al₂O₃, MoO/Al₂O₃ and LaO/Al₂O₃. The molecular cross-sectional areas were determined to be the same for all metal catalysts. The BET surface area increased while the total pore volumes decreased for all metal catalysts after loading of CoO, MoO, and LaO to Al₂O₃ as compared Al₂O₃ by Zhao et al.¹³⁸ The BET surface area and total pore volume of MoO/Al₂O₃ were higher than CoO/Al₂O₃ and LaO/Al₂O₃ metal catalysts. The possible explanation to the lower total pore volumes in CoO/Al₂O₃ (0.162 cm³/g) and LaO/Al₂O₃

(0.160 cm³/g) compared to MoO/Al₂O₃ is due to high filled up of metal oxides of the micropores and mesopores of the supporting medium after loading of CoO, LaO and MoO.¹³⁹ The high BET surface area of MoO/Al₂O₃ (380.89±5.14 m²/g) is as a result of interactions within MoO and aggregation of it deposition on the surface of Al₂O₃.

Table 2. Characterization of the three different catalysts by their textural properties; BET surface area, molecular cross-sectional areas, and total pore volume.

Catalysts	S _{BET} ¹ (m ² /g)	d ² (nm ²)	Total pore volume(cm ³ /g)
CoO/Al ₂ O ₃	353.13±2.88	0.162	0.162
MoO/Al ₂ O ₃	380.89±5.14	0.162	0.171
LaO/ Al ₂ O ₃	364.88±2.80	0.162	0.160

¹ BET surface area

² Molecular cross-sectional areas

2.3.2. Lignin characterization

a. Cupric oxide oxidation

The structural composition of lignin is characterized by the presence of *p*-hydroxyphenyl (H), guaiacyl (G), and syringyl (S) phenolic units distributed in the cross-linkages of the polymer. Cupric oxide and nitrobenzene oxidations are the main chemical degradative methods used to analyze the structure characteristics of lignin polymer.¹⁴⁰⁻¹⁴¹ Nitrobenzene is known to produce higher phenolic yields from lignin compared to cupric oxide. However, the harmful nature of nitrobenzene in its reduced form in the reaction mixture makes the use of cupric oxide lignin oxidation more preferable. The phenolic units present in the oxidation mixtures were determined by GC-MS as described for the separation of OSSP except that dichloromethane was used to prepare the standard and

there was no internal standard used. Figure 12 and Table 3 show the different phenolic monomers and the type of structural moieties.

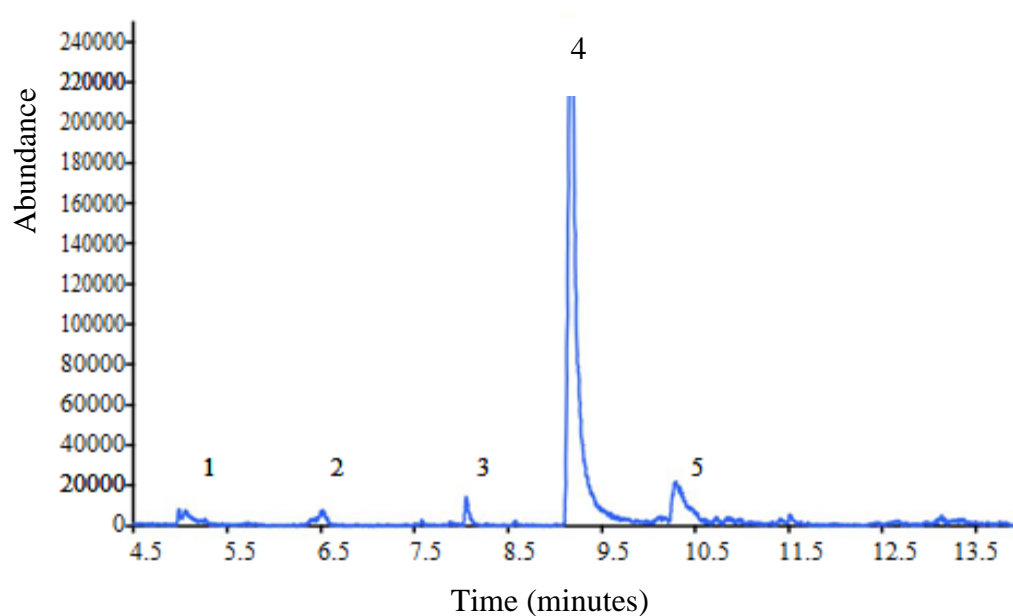


Figure 12. GC-MS total-ion chromatogram showing phenolic moieties produced from oxidation of Kraft lignin using cupric oxide.

Table 3. Structure of phenolic monomers in Kraft lignin produced during cupric oxide oxidation

Peak number	Compounds	Type of phenolic structure
1	Guaiacol	G
2	<i>p</i> -cresol	H
3	Vinyl-guaiacol	G
4	Vanillin	G
5	Acetovanillone	G

All the phenolic moieties are guaiacyl (G) units of the lignin resulting from cupric oxide oxidation, except *p*-cresol which is a hydroxyphenyl (H). Vanillin showed the highest abundance of all the phenolic moieties as indicated in Figure 12. The abundance of vanillin and other guaiacyl (G) moieties is an indication that the lignin polymer belongs to softwood origin. Cupric oxide oxidation of softwood lignins results in high yields of vanillin and other guaiacyl moieties, alongside a few hydroxyphenyl moieties.¹⁴²

b. Py-GC-MS Analysis

Kraft lignin was subjected to Py-GC-MS analysis. Figure 13 and Table 4 show the different phenolic moieties with molecular formula and weights obtained from pyrolysis at 600 °C. The compounds were identified by retention times of standards and the NIST library. The group type according to the arrangement of ether groups on the phenolic linkages (*p*-hydroxyphenyl, guaiacyl, and syringyl) was also determined.

Table 4. Phenolic monomers, groups, molecular weights and formula identified using Py-GC-MS analysis of Kraft lignin

Peak number	Compound	Formula	Molecular weight (g/mol)	Moiety type
1	Phenol	C ₆ H ₆ O	94	H
2	Guaiacol	C ₇ H ₈ O ₂	124	G
3	p-Cresol	C ₇ H ₈ O	108	H
4	2-methoxy-6-methylphenol	C ₈ H ₁₀ O ₂	138	G
5	Methyl guaiacol	C ₈ H ₁₀ O ₂	138	G
6	Ethyl guaiacol	C ₉ H ₁₂ O ₂	152	G
7	Catechol	C ₆ H ₆ O ₂	110	H
8	4-Propyl guaiacol	C ₁₀ H ₁₄ O ₂	166	G
9	Eugenol	C ₁₀ H ₁₂ O ₂	164	G
10	Vanillin	C ₈ H ₈ O ₃	152	G
11	Acetovanillone	C ₉ H ₁₀ O ₃	166	G
12	Homovanillic acid	C ₉ H ₁₀ O ₄	182	G

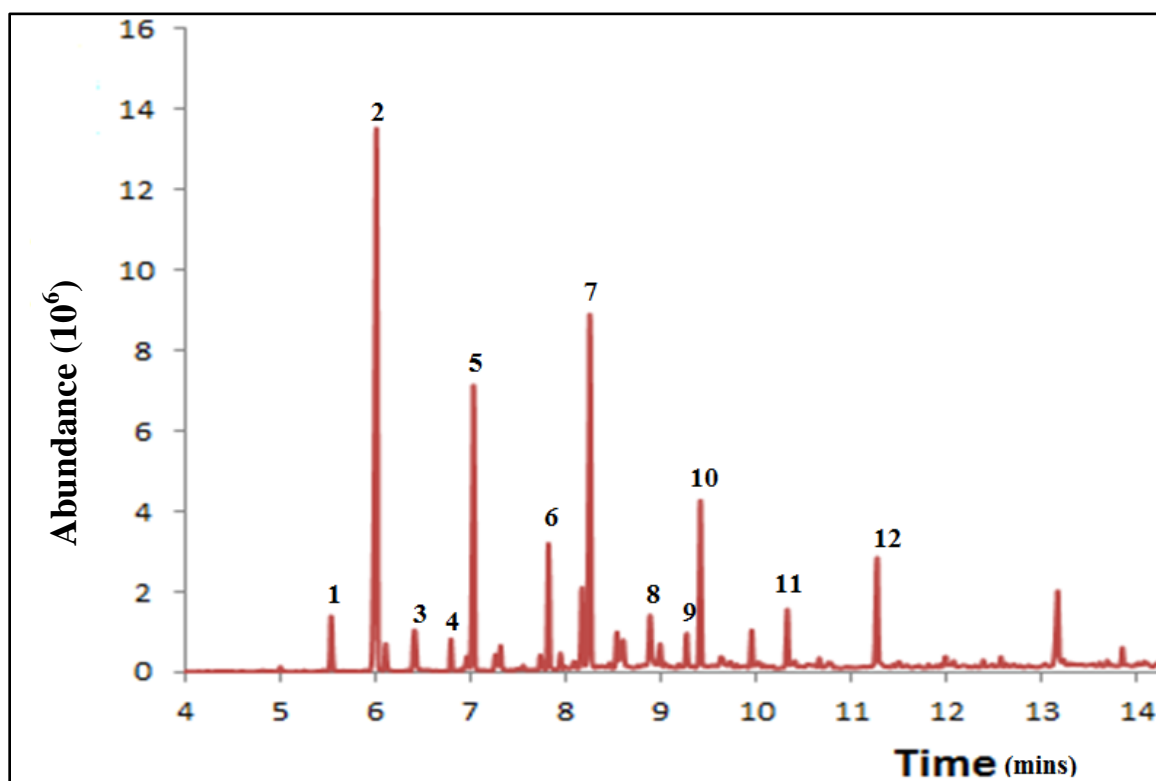


Figure 13: Chromatogram of phenolic compounds produced during Py-GC-MS analysis of Kraft.

The majority of the phenolic compounds are guaiacyl (G) moieties, with a hydroxyphenyl (H). This is in agreement with the results of cupric oxide oxidation reaction. The phenolic compounds obtained from the pyrolysis are characteristics of softwood lignin. Softwood lignins mostly contain guaiacyl moieties, hardwood lignins are mainly made up of hydroxyphenyl (H) and syringyl (S) moieties, whereas grass lignins exhibit characteristics of all the three different groups of moieties.¹⁴³ The large abundance of these phenolic compounds resulting from pyrolysis of Kraft lignin is indicative that many useful phenolic moieties, especially guaiacyl units, can be derived

from the crosslinked three-dimensional lignin polymer using catalysts in suitable conditions. Some of the phenolic compounds from the pyrolysis have the same chemical formula but because they differ in their structural arrangement, they elute from the column at different times.

c. TG analysis

Figure 14 shows the thermal decomposition of Kraft lignin as measured by TG and differential thermal gravimetric (DTG) with increasing temperature from 25 °C to 900 °C at a rate of 15 °C/min. The TG curve shows a measure of weight loss as a function of temperature whereas the DTG curve is the first derivative of the thermogravimetry curve with respect to temperature. The initial weight loss in the Kraft lignin which is considered as drying was observed to be 1.6 % from 25 to 120 °C due to the removal of moisture from the polymeric film of the lignin which is less than what is reported in the Sigma Aldrich website (5 %) for kraft lignin.¹⁴⁴⁻¹⁴⁵ The reduction in moisture content is due to the oven drying of the kraft lignin in our laboratory which helped in determining the dry weight mass of the lignin used in depolymerization. The first stage (S1) of the kraft lignin degradation started from 149 to 225 °C. The degradation at this stage is mainly as a result of devolatilization of functional groups and accounted for 2.5 % mass loss.

The second stage (S2) of degradation occurred from 225 - 520 °C with maximum (DTG_{max}) decomposition occurring at 360 °C as shown by broad peak on the DTG curve in Figure 14. The weight loss was determined to be 36 % and this is due to breakdown of crosslinkages within the lignin polymer.¹⁴⁶ The last stage of the degradation (S3) led to formation of char in the temperature range of 520 – 750 °C as result of the breakdown of

aromatic rings. The weight loss was observed to be 11.1 %. The residual carbon for the Kraft lignin was determined to be 48.4 % at temperatures above 750 °C. The high residual carbon yield shows that kraft lignin has high resistance to degradation. The degradation profile is comparable to Sigma Aldrich degradation analysis.¹⁴⁵

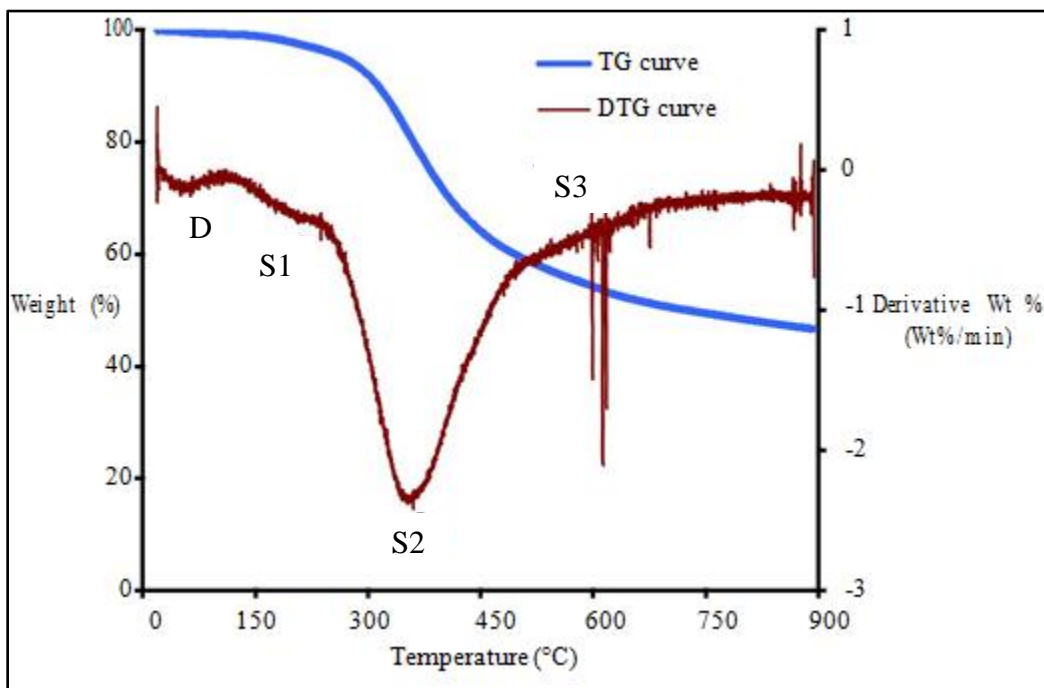


Figure 14. TG and DTG analysis curves of Kraft lignin performed at 900 °C under nitrogen atmosphere at constant heating rate of 15 °C/min.

d. DSC Analysis

The enthalpy change of Kraft lignin was determined by obtaining a differential scanning calorimetry (DSC) heating curve within a temperature range of 20 to 400 °C at a constant heating rate of 15 °C/min under nitrogen atmosphere. Figure 15 shows the DSC curve of Kraft lignin of heat flow as a function of temperature. The glass transition (T_g), melting temperature (T_m), and crystallization temperature (T_c) were determined from the DSC heating curve.

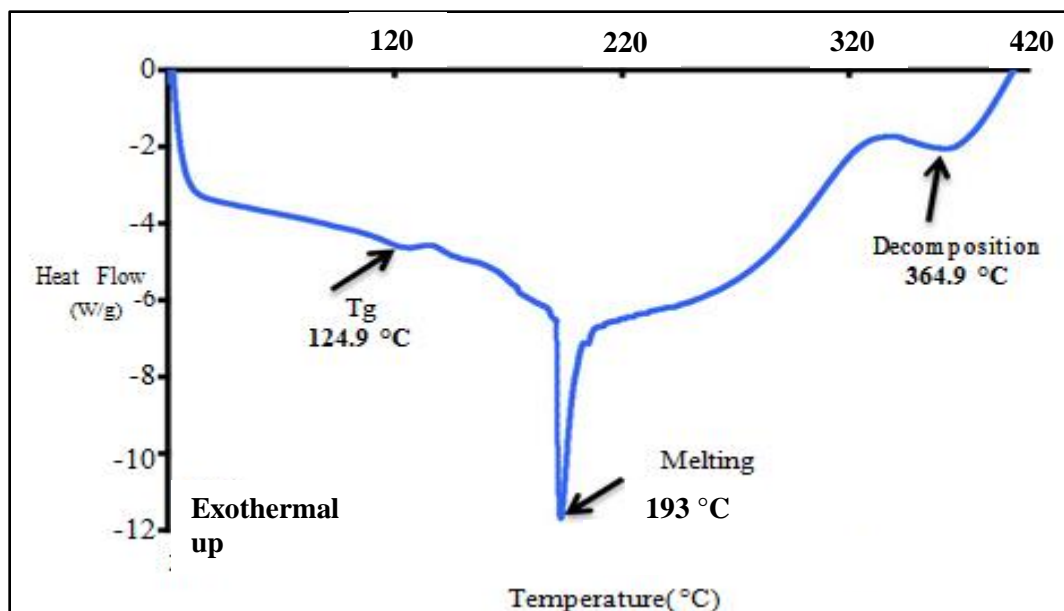


Figure 15. Heating curve of differential scanning calorimetry analysis of kraft lignin from 20 to 400 °C at a constant heating rate of 10 °C/min.

All the enthalpy changes for the Kraft lignin DSC analysis were endothermic.

Figure 15 shows the three endothermic peaks. The first endothermic peak occurred at 124.9 °C which corresponds to the glass transition temperature (T_g), whereby the brittle hard state of amorphous materials in the lignin polymer is converted to rubbery material. The glass transition temperature determined is comparable to literature values under similar conditions for lignins from *Eucalyptus nitens* (140 °C) and *Pinus radiata* (120 °C).¹⁴⁷ The second endothermic peak was observed at 193 °C which shows the melting temperature of the Kraft lignin which is consistent with the first thermal degradation range observed (149 – 225 °C). The last endothermic peak was observed 365 °C due to decomposition of hydroxyl and epoxy groups in the polymer of the lignin.¹⁴⁸ The decomposition temperature from the DSC analysis is in agreement with the maximum degradation, DTG_{max} value (360 °C).

2.3.3. Catalytic hydrotreatment of lignin

The functional groups in the Kraft lignin and the OSSP were compared using FTIR analysis. The extracted phenolic monomers in the organic solvent ethyl acetate were characterized using GC-MS and UHPLC. The identification and quantification of the phenolic monomers were done using GC-MS. UHPLC identification analysis was performed at oven temperature of 30 °C to confirm that the phenolic monomers were produced from the depolymerization reaction rather than resulting from breaking down of oligomers that might be present in the organic solvent during GC-MS analysis.

a. FTIR analysis

FTIR analysis of the starting material and OSSP, as well the lignin residue after the hydrotreatment, was performed to determine the correlation between their functional groups in the wavenumber region of 4000- 650 cm^{-1} . FTIR is one of the methods that can be used to investigate changes in structure of lignin. The characteristic spectra were assigned using Thermo Electron Corporation Nicolet 380 OMNIC FT-IR spectrometer interpretation guide software and literature spectra studies of lignin and its product analysis.^{105, 149-152} Figures 16 and Table 4 show the FTIR absorption spectra of Kraft lignin, untreated lignin, and OSSP. The FTIR spectra for the starting material show similarities in functional groups and absorption intensities to the unreacted lignin except in absorption band regions of 1045-1032 cm^{-1} and 1090-1078 cm^{-1} where an unreacted lignin showed stronger absorption intensities than kraft lignin. The strong absorption intensities in the unreacted lignin in these two regions are as result of C-O deformation in the secondary alcohol and aliphatic ethers caused by the hydrotreatment. Apart from these two absorption band regions, which reveal cleavage of ether linkages and

disorientation in the C-C linkages, the unreacted lignin is able to maintain most of the characteristics of the starting material and therefore, can be reused to produce useful phenolic monomers, because it did not transform into coke or char during the depolymerization reaction. The unreacted lignin and the OSSP all have absorptions between 2985-2336 cm^{-1} and 1738-1702 cm^{-1} which indicate the presence of methyl, methylene, and aromatic carbonyl. The major difference between the unreacted lignin and the OSSP is the strong absorption at 3389.8 cm^{-1} indicating the presence of alcohol in the unreacted lignin peak but not in the OSSP peak.

A careful study of the OSSP shows that there is a disappearance of the peak at 3390-3382 cm^{-1} which confirms that the broad peak exhibited by Kraft lignin and unreacted lignin was as result of O-H stretching of alcohols in the lignin polymer but not O-H stretching of aromatics. The strong guaiacyl rings plus C=O stretching at 1269-1239 cm^{-1} coupled with C=O stretching in aromatic carbonyl at 1738-1702 cm^{-1} for OSSP without peak formation at 1224-1221 cm^{-1} for C-C and C=O stretch for condensed guaiacyl moieties, confirms that Kraft lignin underwent depolymerization by hydrotreatment to form phenolic monomers. The FTIR analysis correlates well with the GC-MS, copper oxide oxidation, HPLC, and Py-GC-MS analysis that the phenolic monomers produced in the reactions are mainly guaiacyl type.

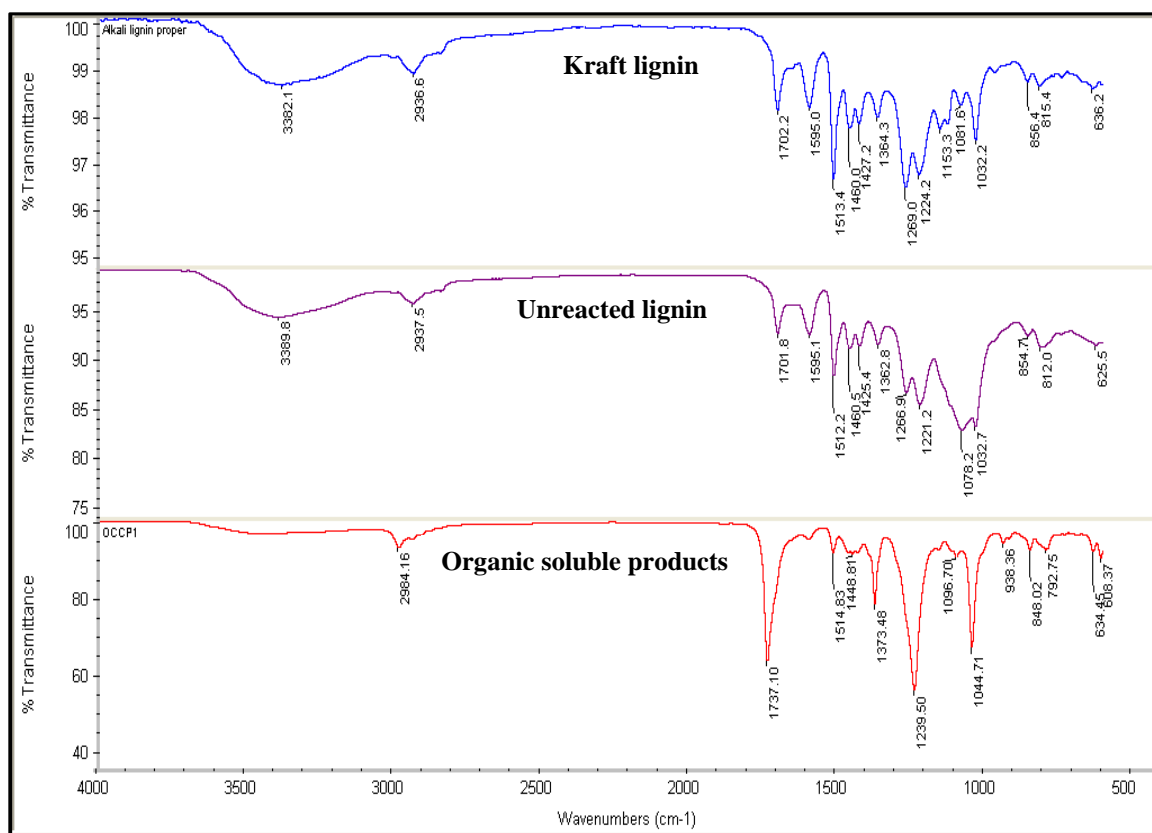


Figure 16. FTIR analysis spectra of Kraft lignin (blue), unreacted lignin (purple) from the hydrotreatment, and organic-solvent soluble products (red) showing similarities and differences in peak absorption intensity.

Table 5. Functional group assignment of FTIR analysis of Kraft lignin, unreacted lignin and organic solvent soluble products.

Absorption bands (cm ⁻¹)	Functional groups	Kraft lignin and products		
		1	2	3
3390-3382	O-H stretching vibration due to alcohols	s	s	-
2985-2336	C-H stretching in methyl and methylene groups	m	m	m
1738-1702	C=O stretching in aromatic carbonyl	m	m	s
1595	Aromatic skeletal vibration plus C=O stretch	m	m	-
1515-1513	Aromatic skeletal vibrations; Guaiacyl (G)	s	s	w
1461-1444	Aliphatic CH ₂ deformation	w	w	w
1427-1425	Aromatic skeletal vibrations plus C-H in plane deformation	w	w	-
1373-1362	Aliphatic C-H stretch in CH ₃	w	w	m
1269-1239	Guaiacyl rings plus C=O stretch	m	m	s
1224-1221	C-C, and C=O stretch Guaiacyl (G) condensed	m	m	-
1090-1078	C-O deformation in secondary alcohols and aliphatic ethers	w	s	w
1045-1032	Aliphatic ether C-O and alcohol C-O stretching	m	s	s
860-840	Aromatic C-H out of plane deformation	w	w	w
634-608	Phenol O-H out of plane deformation	w	w	w

1- Kraft lignin: 2- unreacted lignin: 3- organic soluble product: s-strong intensity: m-medium intensity: w-weak intensity

b. GC-MS Analysis

All the samples and standards were subjected to GC-MS analysis. There were up to six phenolic compounds that were extracted. The analytical standards and internal standards were purchased commercially and were used in GC-MS for phenolic monomer characterization after preparation using ethyl acetate as solvent. All of the retention times and fragmentation patterns of phenolic monomers from hydrotreated depolymerized kraft

lignin matched the analytical standards analyzed on GC-MS. The molecular weight of all the analyzed phenolic monomers were less than 190 g/mol ranging from 124 to 183 g/mol and only one unidentified peak on the GC-MS analysis for both temperatures, as shown in Figures 17 and 18 was observed. GC-MS run time was increased from 13 min to 45 minute to accommodate possibility of detecting more peaks, but no peaks were found after 12.5 min. This shows that the extraction method is able to extract mainly the phenolic monomers. Ethyl acetate eluted before all the phenolic monomers, but the internal standard eluted after the analytes.

The phenolic monomers produced were guaiacol, 3-methoxyacetophenone, vanillin, 4-propylguaiacol, acetovanillone, and homovanillic acid. There were more phenolic monomers and higher yields in hydrotreatment depolymerization at 240 °C than 200 °C as shown in Figures 17, 18, 19 and 20. The reaction conditions without catalyst produced only one and two phenolic monomers at 240 °C and 200 °C respectively. An increase in temperature without catalyst decreased the yield in phenolic monomers from 1 wt% to 0.6 wt%. Moreover, the use of catalyst increased the phenolic monomers from 0.6 wt% to 15 wt% (use of MoO) at 240 °C and from 1 wt% to 5 wt% for temperature of 200 °C (use of MoO). The highest yield of product was recorded for MoO (15 wt%) for all the mixtures of the two hydrotreatment reactions performed on the same Kraft lignin followed by LaO (9 wt%) and, CoO (3.4 wt%) at 240 °C. Under the first reaction conditions using MoO, LaO, and CoO the yields in phenolic monomers were 6.8 wt%, 4.8 wt%, and 0.9 wt% respectively.

The increase in number and amount of phenolic monomers in the catalyzed depolymerization reactions conditions at 240 °C is indicative that the catalysts were able

to cause depolymerization to more phenolic monomers from the lignin polymer and subsequently stabilize them to prevent repolymerization. Repolymerization has been a major issue in the production of phenolic monomers from lignin. The oxo species of MoO, CoO and LaO cycle between multiple oxidation states, in the process release and transfer hydrogen and oxygen atom within the lignin polymer.¹⁵³ The oxidation states affected the yield of phenolic monomers. The Mo metal has highest unpaired electrons in the d-orbital (up to +6 oxidation state) compared to Co and La metals which aided more hydrogen generation to stabilize more intermediate phenolic moieties and therefore, we speculate this is why it led to high yield of phenolic monomers.¹⁵³ The surface area of the metal oxides after the formulation also affected the yield of phenolic monomers. Higher surface area of the supported-zeolite metal oxides led to higher yields.

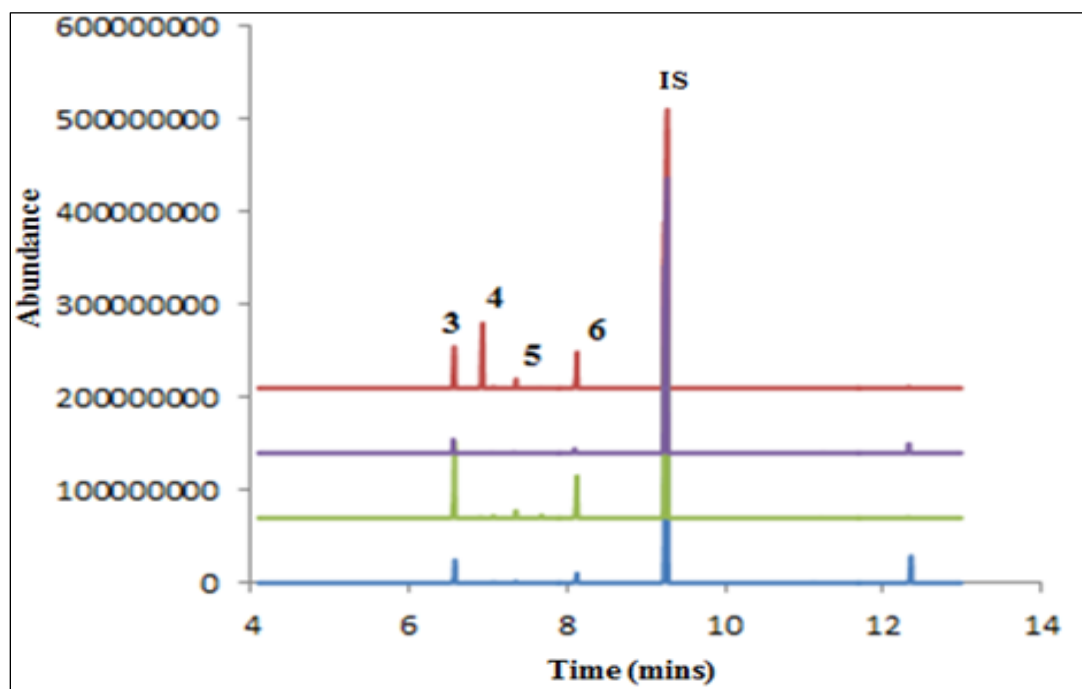


Figure 17. GC-MS total-ion chromatogram of vanillin (3), 4-propylguaiacol (4), acetovanillone (5), and homovanillic acid (6) obtained from Kraft lignin hydrotreatment at 200 °C

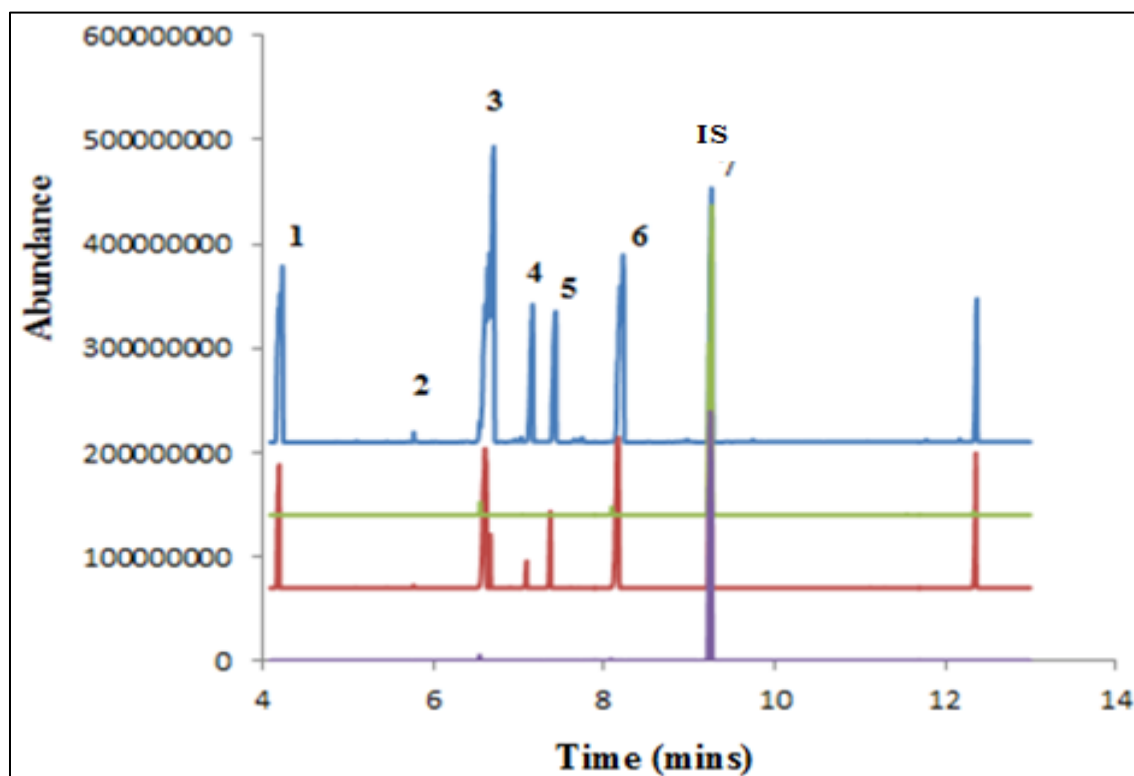


Figure 18. GC-MS total-ion chromatogram of guaiacol (1), 3-methoxyacetophenone (2), vanillin (3), 4-propylguaiacol (4), acetovanillone (5), and homovanillic acid (6) obtained from Kraft lignin at 240 °C.

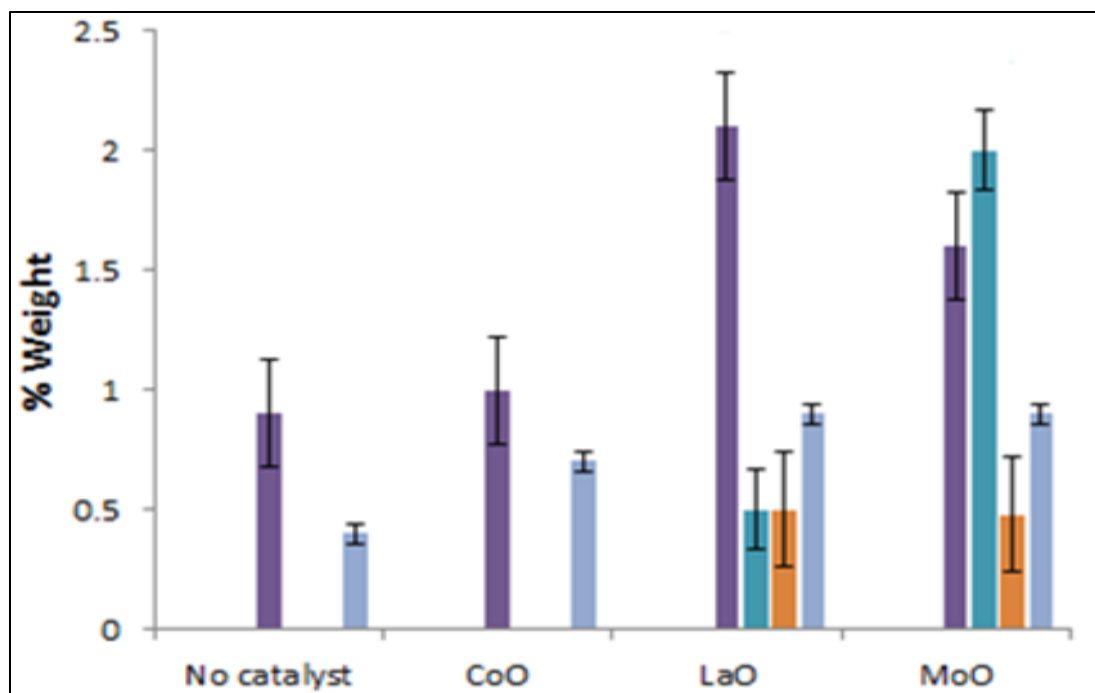


Figure 19. Yields of phenolic monomers - vanillin (purple), 4-propylguaiacol (dark blue), acetovanillone (orange) from hydrothermal liquefaction of Kraft lignin at 200 °C.

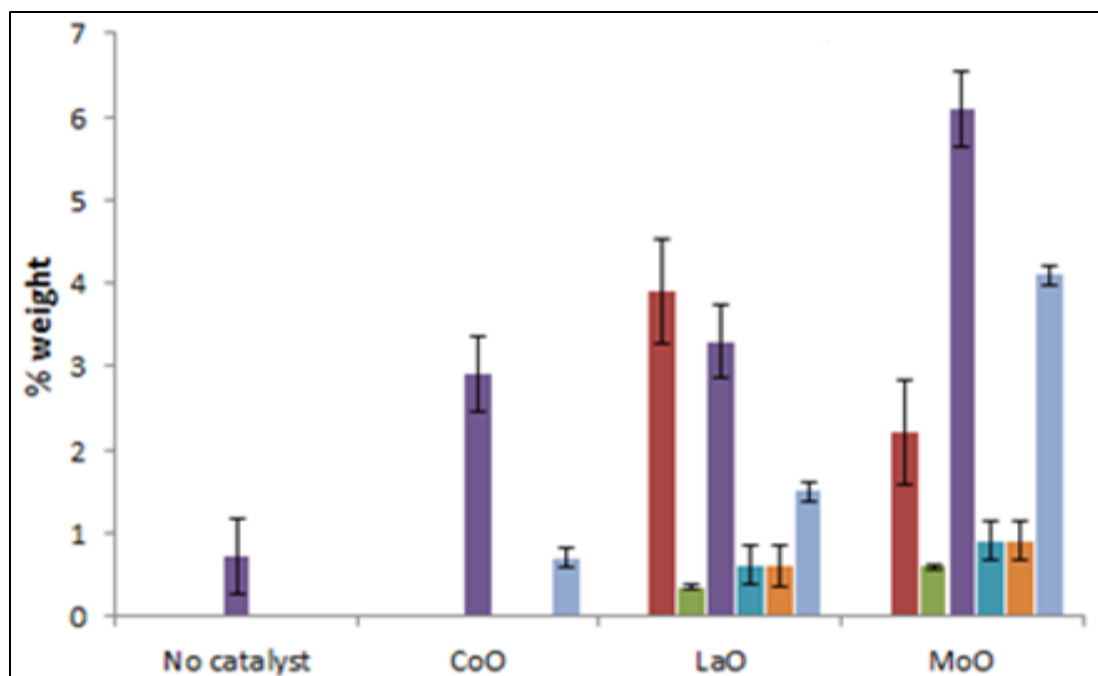


Figure 20. Yields of phenolic monomers: guaiacol (red), 3-methoxyacetophenone (green), vanillin (purple), 4-propylguaiacol (dark blue), acetovanillone (orange), and homovanillic acid (light blue) from hydrothermal liquefaction of Kraft lignin at 240 °C.

c. UHPLC analysis of phenolic monomers

The OSSP were analyzed by injecting them and the standards into the HPLC column. Figure 21 shows the peaks of phenolic monomers and the internal standard. The phenolic compounds were identified using HPLC analysis are similar to those analyzed by GC-MS. Deepa et al. confirmed that no oligomers are extracted during phenolic monomers extraction using organic solvent extraction.¹⁰⁷

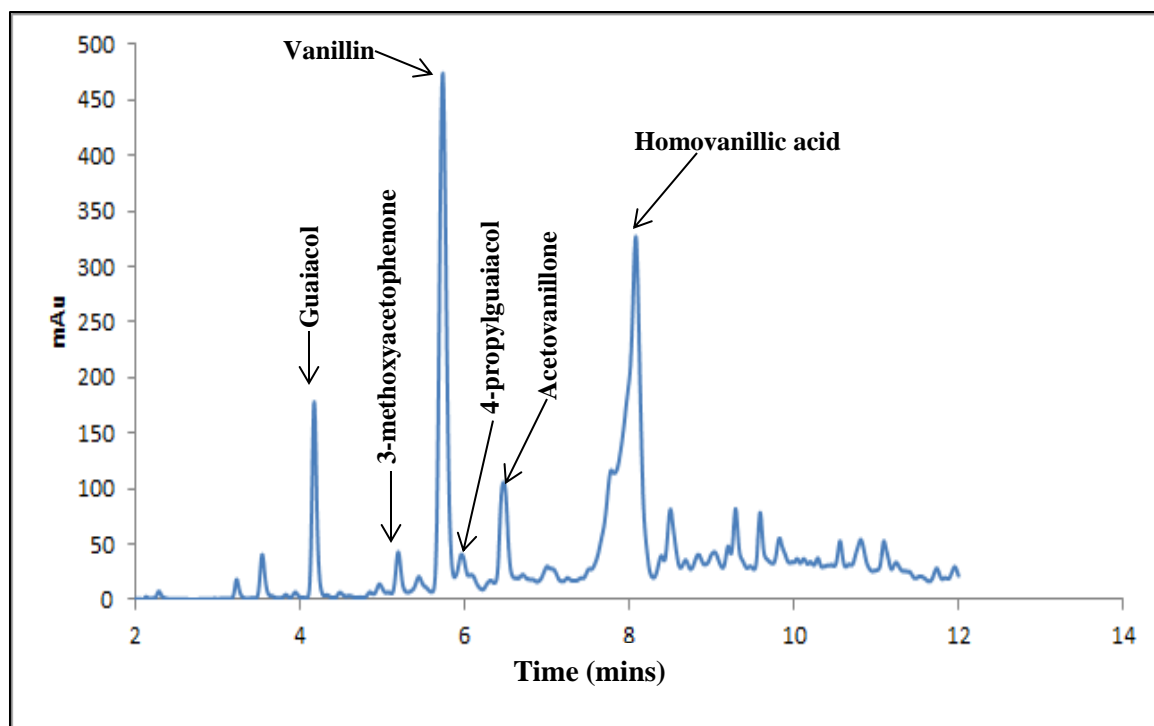


Figure 21. HPLC analysis of phenolic monomers in the ethyl acetate extract of depolymerized Kraft lignin at 240 °C using MoO catalyst

2.4. Conclusion

The result obtained and discussed for the hydrothermal liquefaction demonstrated that subcritical water at 250 °C and 12 MPa with MoO using a reaction time of 15 mins is able to depolymerize Kraft lignin. The BET surface area ($380.89 \pm 5.14 \text{ m}^2/\text{g}$) and total pore volume (0.171 cm^3) contributed to high yields of monomers for MoO/Al₂O₃ at 240°C than CoO/Al₂O₃, and LaO/Al₂O₃. The extraction of the reaction mixtures using ethyl acetate produced six useful phenolic monomers: guaiacol, vanillin, 3-methoxyacetophenone, acetovanillone, 4-propylguaiacol and homovanillic acid. Subcritical water and MoO supported-zeolite catalysts reaction provides a viable alternative to depolymerize lignin.

CHAPTER 3

AROMATIC MONOMERS GENERATED FROM TORREFACTION AND PYROLYSIS OF PRAIRIE CORDGRASS

3.1. Introduction

The constant growing concern for an alternative renewable, abundant, greener and cleaner source for fuels and chemicals has resulted in many studies into lignocellulosic materials as another source of energy rather than continuous reliance on petroleum products^{110, 154}. Lignocellulosic biomass, of which prairie cordgrass forms part, accounts for about 50 % of world's biomass, and it is readily available from agricultural waste, energy crops, and woody and grassy materials at low cost¹⁵⁵⁻¹⁵⁸. Lignin from biomass has a great potential for production of biochemicals, renewable energy, and control of CO₂ emissions therefore reducing global warming.¹⁵⁹

In recent developments, lignin is used as a co-polymer in bio-composites for plastic and polylactide materials to enhance their thermal and mechanical strength.¹⁶⁰⁻¹⁶¹ Studies have shown that lignin-based co-polymer electrodes display electrochemical properties that are comparable to commercial anodes at low production cost, meaning lignin can serve as energy storage in batteries.¹⁶²⁻¹⁶³ Lignin is now used as a biobased alternative for carbon precursors. The rich carbon structure of lignin allows it to be used as renewable, low-cost graphitic carbon compared to the high cost of producing other carbon-fiber precursors such as polyacrylonitrile and its associated environmental issues.¹⁶⁴⁻¹⁶⁵ The many hydroxyls and polar groups exist in the lignin structure leading to the formation of strong intramolecular and intermolecular hydrogen bonding, therefore

making the intrinsic lignin insoluble in any solvent. However, chemical hydrolysis of the separated lignin enables it to be divided into soluble lignin and insoluble lignin.¹⁶⁶

Torrefaction and pyrolysis processes cause thermal decomposition of cellulose, hemicellulose and lignin at temperatures above 200 °C, but pyrolytic temperatures used for production of bio-oil and biochar effectively range from 250-800°C.^{62, 167} Drying of biomass is done at temperatures above 105 °C for several hours to reduce water in pyrolytic bio-oil. Water content is highest at the initial stage of pyrolysis when temperatures are in the range of 100-300 °C.¹⁶⁸ Torrefaction is a thermochemical pretreatment process where raw biomass is heated at lower temperatures ranging between 200-300 °C under an inert atmosphere in order to remove bound and unbound water, thereby reducing moisture content.^{61, 158, 169-171} However torrefaction biochars below 250 °C have poor grindability.⁵⁹ Torrefaction is one of the pretreatment techniques employed in recent times to increase heating value, density, grindability and hydrophobicity of the feedstock to reduce logistic cost.^{61, 169-170, 172-173} Torrefaction study on bio-char from prairie cordgrass at 250, 300, and 350 °C by Wei et al¹⁷³ shows that an increase in temperature lowered the moisture content, leading to an increase in carbon content from 44.27 to 66.28 wt%, along with a subsequent increase in heating value (7.25 to 28.75 MJkg⁻¹). Bio-char from torrefaction has high polycyclic aromatic hydrocarbons as compared to bio-char from pyrolysis at temperatures above 360 °C.¹⁷⁴

The undesirable characteristics of bio-oil from torrefaction and pyrolysis is mostly due to high water and oxygen content, which makes it an ineffective fuel source for transportation.¹¹⁰ The oxygenated content is mostly made up of aromatic organic compounds. These aromatics compounds are rich in useful furfurals and phenolic

monomers from the lignin of the biomass which can serve as feedstock for polymer synthesis.¹⁷⁵⁻¹⁷⁷

Reduction in moisture content occurs mainly at low temperature, below 220 °C during torrefaction. Hemicellulose is the component of lignocellulosic material that degrades at the lowest temperatures, from 200-260 °C, followed by cellulose degradation from 240 °C - 360 °C. Lignins decompose slowly to volatiles in the background during torrefaction and pyrolysis starting at a 160 °C and continuing until 900 °C.^{56, 63, 168}

Degradation of cellulose and hemicellulose result in a low pH in bio-oil because of the formation of organic acids¹⁷⁸, but favors the extraction of aromatic compounds in the bio-oil. Bio-oil produced from biomass shows a lot of similarities to petroleum-based fuels in terms of usage and storage. It contains diverse chemical compounds, such as hydroxyaldehydes, carboxylic acids, ketones, and aromatic compounds, all having different polarities. Most of the phenolic groups exist as monomers, dimers and tetramers, contributing to the difficulty in using traditional refinement processes.¹⁷⁹⁻¹⁸⁰ However, an understanding into the physical and chemical properties of bio-oil will help with the isolation of useful fractions. Mohan et al.⁶³ have presented several manual methods for the solvent separation of bio-oil components. Manual extraction of bio-oil components takes a substantial amount of time to perform and also uses a large amount of solvent.

Pressurized solvent extraction uses less solvent at elevated temperatures for the extraction of desirable components of bio-oil. The extraction kinetics and solute solubility are increased by the elevated temperatures, while the high pressures prevent the solvent from boiling. This reduces the solvent consumption by up to 90%.¹⁸¹ This

pressurized solvent extraction technique can selectively extract specific compounds in bio-oil based on the chosen solvent. Accelerated solvent extraction (ASE) increases the reproducibility of solute extraction and reduces human exposure to solvent because it is automated. Ethyl acetate and dichloromethane have been used by Mantilla et al ¹³⁵ to extract phenolic compounds of bio-oil from agricultural biomass waste, but the use of dichloromethane for extraction has health and environmental concerns.

To date, the amount of lignin remaining in biochar from prairie cordgrass during torrefaction is not known. A stepwise procedure is needed to determine the amount of lignin, ash, moisture, extractives, and total solids in biochar at different pretreatment temperatures (250, 300, 350, 600, and 900 °C) without interferences in analysis. In this study, lignin determination from torrefaction of prairie cordgrass at 250 °C, 300 °C, and 350 °C is compared to the pyrolysis of prairie cordgrass at 600 °C and 900 °C. We hypothesize that National Renewable Energy Laboratory (NREL) procedure for lignin determination in biomass can be used to determine lignin from biochars at different pretreatment temperatures (250, 300, 350, 600, and 900 °C), as well as raw prairie cordgrass (PCG). Lignin determination includes the use of acid hydrolysis which isolates the lignin to acid-soluble and acid-insoluble portions. The acid-insoluble portion contains most of the pure lignin compared to the acid-soluble. Lignin from different pyrolysis temperatures was recovered using the organosolvent (organosolv) method to obtain amount of pure lignin. FTIR, high heating value (HHV) analysis, Elemental analyzer, and TGA were used to characterize the recovered lignin. This work also uses ethyl acetate as a solvent during ASE for the extraction of the bio-oil components and characterization by

GC-MS. FTIR was used to confirm the presence of aromatic compounds in the bio-oil.

Figure 22 shows the overview of various pathways used in this work.

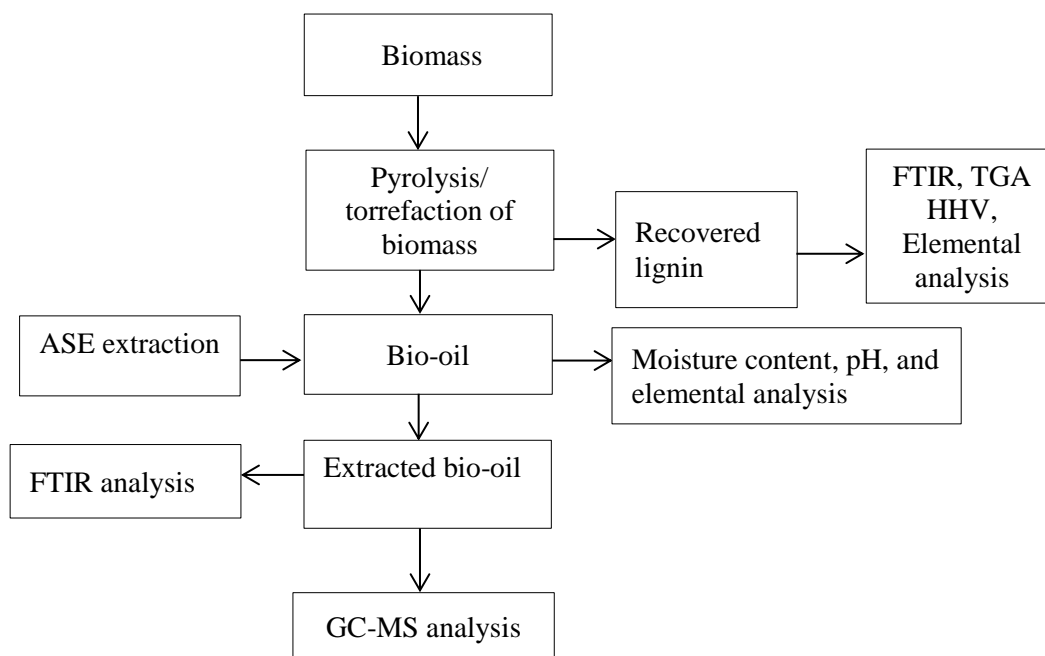


Figure 22. Outline for pyrolysis of prairie cordgrass and separation and analysis of pyrolytic products

3.2. Experimental

3.2.1. Materials and Reagents

Ethanol (200 proof), and 8M sulfuric were purchased from Thermo-Fisher Scientific in Dubuque (Iowa, USA). Methyl isobutyl ketone (MIBK), 1, 3, 5-trioxane, 99.8 % anhydrous ethyl acetate and deuterated dimethyl sulfoxide were purchased from Sigma-Aldrich in St. Louis, MO, USA. A Thermo-Fisher Scientific Barnstead Ultrapure water purification systems set at $18\Omega\text{M cm}^{-1}$ was used to produce ultrapure water. Prairie cordgrass was harvested in Brookings, SD, USA and air dried for two weeks. The prairie cordgrass was knife milled with 1-mm screen sieving pans to obtain uniform 1-mm

pieces. Ice cubes obtained from ice making machine in the Dr. Lin Wei laboratory located in the Agricultural and Engineering Department of South Dakota State University Brookings, SD, USA. The balance for weighing was constantly checked with standard masses of 1, 2, 5, 10, 20, 50, and 100 g from Will Corporation, Rochester, NY, USA. All analytical grade chemicals acquired were used without further purification. Analytical aromatic compound standard 99 % vanillin, 98 % guaiacol, 99 % m-cresol, 99 % p-cresol, 99 % catechol, 98.5 % American Chemical Society (ACS) grade xylene, 99 % ACS grade phenol, 98 % ethyl-guaiacol, 99 % syringol, 99 % ethyl-phenol, 98 % furan-2-one, 97 % 3-furancarboxaldehyde, and o-terphenyl were purchased from Sigma Aldrich in St Louis, MO.

3.2.2. Methods

a. Torrefaction and pyrolysis of biomass

A 310 stainless steel reactor, 27cm in length, internal diameter of 12.5cm, and 13.5cm outer diameter that can withstand a maximum temperature of 1125 °C was used for torrefaction and pyrolysis of the prairie cordgrass. An isothermal, programmable, forced-draft muffle furnace with microprocessor control of linear heating and cooling was used to provide heat and cooling to the reactor. Copper tubes were connected from the nitrogen gas supply through the reactor to the bio-oil collection containers and Tedlar bag outlet for exit of the pyrolysis gas from the system as shown in Figure 23. The reactor and copper tubing systems were cleaned before each experiment. Each experiment was carried out in triplicate and the reported yield is the average. The samples were knife milled with 1-mm screen sieving pans to obtain uniform 1-mm particles

before each run. The sample (100 g) was weighed for each experiment and placed in an airtight reactor.

The heating rate of the reactor was 10 °C/min starting from 19 °C to the required temperature and held for 1 hour. The prairie cordgrass was subjected to torrefaction at 250 °C (Tor250), 300 °C (Tor300), 350 °C (Tor350), and pyrolysis at 600 °C (Pyro600) and 900 °C (Pyro900). The system was purged right before the start of the experiment until its completion. Nitrogen (N₂) was used as an inert gas to purge the system at a flow rate of 1L/min. Gas produced from the biomass samples were carried out through the reactor outlet to bio-oil collection flasks because of the direction of the flow of nitrogen gas from the nitrogen tank (Figure 23). The condensable gases were condensed to bio-oil and collected by corked Erlenmeyer flasks over ice at 0 °C. The copper tube connected to the Tedlar bag helped remove the non-condensable gases (NCG) from the reactor. The bio-oils and biochars (solid residues) were collected and weighed to determine the percent yield from the starting material. The bio-oils were collected in airtight 300-mL centrifuge bottles and stored in a refrigerator at a temperature of 0 °C for subsequent analysis. The percent yields of bio-oils, biochars, and noncondensable gases were determined from the starting material. Equation 1 was used to calculate the final yield of bio-oils, biochars and noncondensable gases as the ratio of the weight of desired product (WDP), bio-oils and bio-char) to the weight of initial sample (WIS). The yield of the NCG was determined by Equation 2. The bio-chars were stored in polyethylene bags at room temperature prior to analysis.

$$\%Yield = \frac{WDP}{WIS} \times 100 \quad (1)$$

$$\%Non - condensable\ gases = 100 - (yield\ of\ bio - oil\ and\ biochar) \quad (2)$$

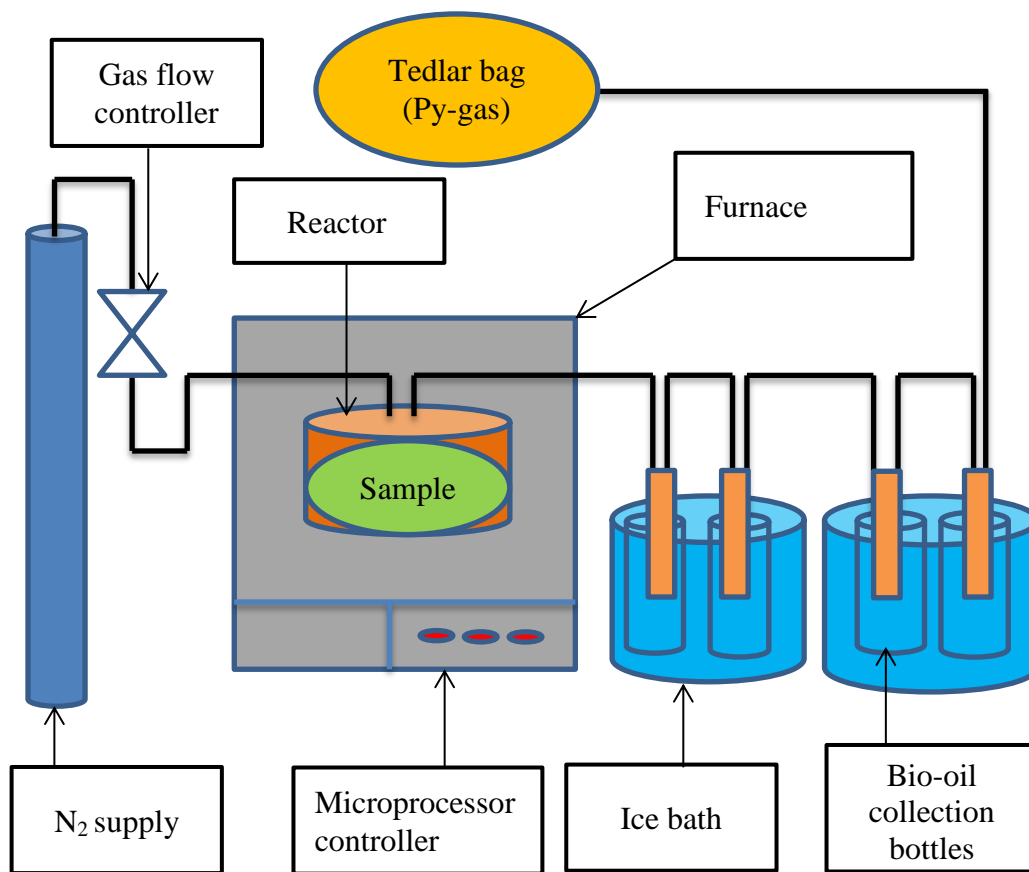


Figure 23. Pyrolysis-reactor system used for torrefaction and pyrolysis of prairie cordgrass.

b. Determination of lignin content in bio-chars of prairie cordgrass at different temperatures

i. Sample Preparation

The National Renewable Energy Laboratory method for lignocellulosic sample preparation (NREL/TP-510-42620)¹⁸² was used for the sample preparation for lignin determination analysis of PCG and bio-chars obtained from Tor250, Tor300, Tor350, Pyro600, and Pyro900. The bio-char samples were oven dried at 45 °C for 48 hours and cooled to room temperature in a desiccator prior to lignin determination analysis experiment.

ii. Total solids and moisture content determination in prairie cordgrass bio-chars

The National Renewable Energy Laboratory method (NREL/TP-510-42621) was used for moisture content and total solids determination in the samples.¹⁸³ 200-mL aluminum pans were used as weighing containers. The containers were first oven dried for four hours at 105 °C. The hot, dry containers were removed and placed in the desiccator for cooling to room temperature. The weights of the empty aluminum pans were measured. Once the aluminum pans were cooled, 4.5g of samples were weighed into each and oven dried for four hours at 105 °C. After which, the samples were cooled to room temperature in a desiccator and the weights of each were recorded. The samples were oven dried for an additional four hours at 105 °C until a constant weight was obtained. The final weights of aluminum pans and samples were recorded to determine the sample weight. The dried samples were stored in a desiccator for further analysis. The percent average total solids and moisture in the samples were calculated in equation 3 and

4, respectively, using oven-dry weight (ODW) of weighing pans and ODW of samples and weight of air dry samples.

$$\% \text{ Total solids} = \frac{\text{ODW of pan plus sample} - \text{ODW of pan}}{\text{Weight of air dry sample}} \times 100 \quad (3)$$

$$\% \text{ Moisture} = 100 - \frac{\text{ODW of pan plus sample} - \text{ODW of pan}}{\text{Weight of air dry sample}} \times 100 \quad (4)$$

iii. Determination of amount of extractives in prairie cordgrass bio-chars

The amount of extractives in PCG and bio-chars were determined using the National Renewable Energy Laboratory method (NREL/TP-510-42619).¹⁸⁴ Extractives in samples (Tor250, Tor300, Tor350, Pyro600, Pyro900, and PCG) were determined by exhaustive extraction in a two-step process, with water and ethanol as solvents, using a Dionex ASE 350 (Sunnyvale, CA) and 250- mL ASE collection vessels. Oven dried samples at 105 °C for four hours were weighed (5.5 g) and loaded into extraction cells. The dead volumes in the extraction cell were filled with glass beads which provided a uniform flow for water and ethanol during extraction. The parameters used for the extraction were 1500 psi, 100 °C, 7-min static hold, 120 s purge, three static cycles, and 150 % flush volume. Samples were collected and oven dried at 105 °C for six hours after the extraction cells were cooled to room temperature. The weights of the dried samples were recorded. The samples were stored in a desiccator. Equation 5 was used to calculate the percent extractives in the samples. The average percent extractives were determined

from the triplicate experiments using the difference in ODW of pan plus samples and ODW of pans.

$$\% \text{ Extractives} = \frac{\text{ODW of pan plus extractives} - \text{ODW of pan}}{\text{Weight of air dry sample}} \times 100 \quad (5)$$

iv. Determination of ash content in prairie cordgrass bio-chars

The National Renewable Energy Laboratory method (NREL/TP-510-42622) was used to determine the ash content in PCG and bio-chars samples from Tor250, Tor300, Tor350, Pyro600, and Pyro900. The porcelain crucibles were placed in a muffle furnace at 575 °C for four hours and then cooled in a desiccator to room temperature. Porcelain crucibles were dried at 575 °C in the muffle furnace for an additional four hours to achieve a constant weight for the empty crucibles. The muffle-furnace-dried porcelain crucibles were cooled and stored in the desiccator. The furnace-dried weights (FDW) of the porcelain crucibles were recorded. The extractive-removed biochar samples (0.5 g) were placed in dried porcelain crucibles and subjected to ashing at 575°C in the muffle furnace for 24 hours. The porcelain crucibles with the ashes were removed from the muffle furnace and cooled to room temperature in the desiccator. The weights of ash samples were recorded. The ash samples were subjected to additional ashing in the muffle furnace at 575°C for six hours. The weights of the ash samples were recorded after they were cooled in the desiccator to room temperature. The average ash content in samples was calculated in percentages using Equation 6.

$$\% \text{ Ash} = \frac{\text{FDW of crucibles plus ash} - \text{FDW of crucibles}}{\text{ODW extractives free samples}} \times 100 \quad (6)$$

v. Lignin content determination and recovery in bio-chars from prairie cordgrass

The amount of lignin in prairie cordgrass bio-chars was determined by National Renewable Energy Laboratory method (NREL/TP-510-4618).¹⁸⁵ Lignin determination by this method accounts for both the acid-insoluble lignin (AIL) and acid-soluble lignin (ASL) of the biomass sample through hydrolysis, filtration, and ashing.¹⁸⁶ The extractives free biochar samples and PCG were knife milled with 1-mm screening pans to obtain uniform particles size of 1-mm. Extractives free PCG, Tor250, Tor300, Tor350, Pyro600, and Pyro900 biomasses were each added (300 mg) to 3 mL of 72% sulfuric acid in an Ace glass pressure tube with a Teflon cap and an O-ring. The pressure tubes were removed sealed tightly and shook for 60 minutes at 30°C in an incubator. The pressure tubes were removed from the incubator after 60 minutes and 84 ml of deionized water was added to each sample to obtain a 4% sulfuric acid solution. The Teflon caps were tightly screwed on and sample contents were vigorously mixed to eliminate any concentration gradient. The content of the airtight sealed pressure tubes were autoclaved at 120 °C for 60 minutes. The samples were removed and cooled to room temperature at the completion of the reaction for analysis of acid-soluble and acid-insoluble lignin.

Porcelain filtering crucibles were dried at 575°C for four hours in a muffle furnace. The porcelain-filtering crucibles were then removed from the furnace and placed in the desiccator to cool to room temperature. After which, the FDW were recorded. The porcelain-filtering crucibles were further dried in the muffle furnace at 575 °C for four

hours to attain a constant weight. The final weights of dried porcelain-filtering crucibles were recorded. The autoclave-hydrolyzed sample mixtures were vacuum filtered using the oven-dried porcelain-filtering crucibles into filtrate and solid residues. The remaining solids in the pressure bottles were rapidly washed by hot deionized water and transferred into porcelain filtering crucibles. 45 mL of the filtrates were then transferred into 50 mL centrifuge bottles for acid-soluble lignin analysis. Triplicate UV spectrometer analyses of the filtrates were done using 4% of sulfuric acid as a blank solution on the same day to prevent breakdown of lignin in the hydrolyzed solutions. Absorbance of the aliquots was recorded at 320 nm using a 1-cm cuvette.

The acid-insoluble lignin was determined by using the collected solid residues in the porcelain filtering crucibles. The solid residues were dried in an oven at 105°C for 24 hours until a constant weight was achieved. The samples were removed and stored in the desiccator to attain room temperature. The weights of the crucibles plus the samples were measured. The porcelain-filtering crucibles containing the samples were subjected to ashing at 575°C for 24 hours in the muffle furnace. The samples were removed from the muffle furnace and cooled to room temperature in the desiccator. The samples were further subjected to ashing at 575 °C for six hours in the muffle furnace. The samples were finally removed and stored in the desiccator, after which the weights were recorded at room temperature. Equations 7 and 8 were used to calculate the percentages of lignin in bio-char samples in terms of acid-insoluble lignin (AIL) and acid-soluble lignin (ASL).

$$\% \text{ AIL} = \frac{\text{FDW of crucibles with lignin plus ash} - \text{FDW of crucibles with ash}}{\text{ODW extractives free samples}} \times 100 \quad (7)$$

$$\%ASL = \frac{UVabs \times Volume \text{ of filtrate} \times dilution}{Absorptivity \text{ at } 320 \text{ nm} \times ODW \text{ sample} \times Path \text{ length}} \times 100 \quad (8)$$

Lignins determined from PCG, Tor250, Tor300, and Tor350 were further extracted by the organosolv method using a Dionex Accelerated Solvent Extractor ASE 350¹⁸⁷ to determine the percentage purity of the lignin. MIBK was used as a solvent for the lignin whereas H₂SO₄ acted as an acid promoter to dissolve the lignin in the ternary mixture. Samples were each weighed (15 g) and then loaded into 33-mL extraction cells having a filter at the bottom. The ternary mixture (200 mL) prepared in the ratio of MIBK: EtOH: H₂O (52:35:13 v/v/v) with 0.5 % H₂SO₄ was placed into the ASE 350 bottle (reservoir). All the extractions were performed at 140 °C (preheating time of 5min) with 56-min static hold, 150 % flush volume, 1500 psi, 300-sec purge, and two static cycles. Phase separation was created by diluting the extracts with 200 mL of water, creating an organic phase containing lignin and an aqueous phase. The weights of empty beakers were measured after oven drying at 45 °C. The organic phase was further washed with water, and the organic solvent was subsequently evaporated to obtain the extracted lignin. The extracted lignin was ground and placed in the weighed, empty beakers. The extracts were further washed with benzene: methanol mixture in a ratio of 5:1 and oven dried at 45 °C for 48 hours. The total weights of the beaker plus lignin extracts were measured, and the percentage lignin recovered was determined using Equation 9. The extracted lignins were stored in an airtight Ziploc bags for characterization.

$$\%Lignin \text{ recovery} = \frac{Weight \text{ of beaker plus lignin} - weight \text{ of dry beaker}}{Weigh \text{ of sample}} \times 100 \quad (9)$$

c. ASE extraction of bio-oil from torrefaction and pyrolysis of prairie

cordgrass

Bio-oils obtained from torrefaction and pyrolysis of prairie cordgrass at different temperatures (250 °C, 300 °C, 350°C, 600 °C, and 900 °C) were extracted for aromatic monomers by ethyl acetate using a Dionex ASE 350, 300-mL collection vessels, 33-mL extraction cells, and glass fiber filters. Five grams of bio-oil samples were weighed and mixed with diatomaceous earth and loaded into the extraction cells with a filter at the bottom and top. The dead volume in the extraction cell was filled with glass beads. All extractions were performed at 140 °C with five-minute preheating, 10-min static hold, 150 % flush volume, 1500 psi, three-minute purge, and two static cycles. All collection vessels were weighed separately before and after the extraction to determine the weight of the bio-oil fraction. The bio-oil extracts were concentrated by gentle nitrogen blow-down.

d. Characterization of bio-oil and lignin from bio-char of prairie cordgrass

i. Characterization of bio-oil from torrefaction and pyrolysis of prairie

cordgrass

α. Water content, density, and pH of bio-oils

The pH of the bio-oils was determined using a Fisher Scientific Accumet Basic AB15 pH meter (Waltham, Massachusetts) at room temperature. The density of the bio-oil was determined by dividing the mass of the bio-oil by its volume. The volume was determined using a 25-mL pycnometer and the mass was measured as well. All the measurements were done at room temperature. The moisture content in the bio-oil was

determined with a Mettler Toledo V20 compact volumetric Karl Fischer Titrator (Columbus, OH).

β. FTIR bio-oil extracts analysis

Fourier transform infrared spectrometry (FTIR) experiments were performed using a Nicolet 380 FTIR spectrophotometer from Thermo-Fisher Scientific (USA). The absorption spectra were determined in the region of 4000-600 cm^{-1} at 8 cm^{-1} resolution with 100 scans. Aliquots of bio-oil extracts were all subjected to FTIR analysis. Background spectra were collected for the experiments before running samples. All data collection and analysis were done using OMNIC Spectra software.

γ. GC-MS bio-oil extracts analysis

The gas chromatographic analysis for all the extracts were done using an Agilent 7890A equipped with an Agilent 5975C triple-axis mass detector and electron-impact ionization (Newcastle, DE) . An Agilent DB-5 phenylmethylpolysiloxane capillary column was used. The column dimensions were 30 m x 0.25 mm (0.25- μm film) and the oven temperature was initially held at 65°C for 1 min, ramped at a 10°C/min up to 280°C with a hydrogen carrier at 1.2 mL/min. Two-microliter splitless injections of the standards and bio-oil extracts were done at an injection temperature of 250 °C. The mass spectrometer analysis was done in the full-scan mode ranging from m/z 50-550 using electron ionization at 70 eV. Agilent Chemstation software was used to auto-tune the mass detector frequently. Analytical standards of the compounds present in the bio-oil extracts, as shown in Table 5, were prepared using ethyl acetate and used to identify the phenolic and furfural moieties present in the bio-oil samples in connection with the NIST library and retention times of known compounds. Quantification was achieved using the

internal standard method and o-terphenyl as an internal standard.¹³⁷ Calibration curves were prepared by running five standard solutions in triplicate with different concentration levels (31.25, 62.5, 125, 250, and 500ppm). Three masses corresponding to the three major fragments of each compound were used for quantification.

ii. Characterization of lignin from bio-char of prairie cordgrass

α. Elemental analysis and Higher Heating Value (HHV)

Organosolv-extracted lignin samples were used for elemental analysis. EA440 E, Exeter Analytical Incorporation elemental analyzer (North Chelmsford, MA, USA) was used to measure the C, H, and N contents in the extracted lignin. The O content was determined by the difference as follows: $O = 100 - (C + H + N)$. The elemental composition of lignin samples were reported as percentage of dry weight of the starting lignin. The higher heating values (HHV) of the lignin samples were determined by C2000 calorimeter systems from IKA-Works Incorporation (Wilmington, N.C, USA)

β. FTIR spectroscopic analysis

PCG, Tor250, Tor300, Tor350 organosolv-extracted lignin were used for FTIR spectroscopic analysis. Thermo Electron Corporation Nicolet 380 FT-IR spectrometer (Madison, WI, USA) with 8 cm^{-1} resolution with 100 scans in an absorption spectra range $4000\text{-}600\text{ cm}^{-1}$. Background spectra were collected for the experiments before running all samples as control measurement. All data collection and analysis were done using OMNIC Spectra software.

γ. Thermogravimetric analysis (TGA)

TGA analysis for organosolv-extracted lignin samples from PCG, Tor250, Tor300, and Tor350 were analyzed using TG/DTA 220U system from Seiko Instruments

(California, USA). The TGA data was recorded as change in mass of the lignin sample as a function of temperature. Thermal-decomposition behavior of lignin was performed using an aluminum crucible under a nitrogen atmosphere with dynamic conditions of 25 to 500 °C at a heating rate of 20 °C/min. 10 mg sample size was used for the analysis. The experiments were performed in duplicate with a RSD less than 5 %. Logger Pro 3.8.6 software was used for the analysis of the weight loss curves.

3.3. Results and discussion

3.3.1. Yield of pyrolysis products

The total yield of bio-oil, bio-char, and non-condensable gases determined were based on the initial dry weight of the prairie cordgrass.¹⁸⁸ Table 6 shows the distribution of products (condensate, noncondensate, and biochar) obtained after torrefaction of prairie cordgrass at 250, 300, and 350 °C compared to pyrolysis at 600 and 900 °C. There was an increase in bio-oils and non-condensable gases with a corresponding decrease in biochar yield as temperatures increased, with the exception of 900 °C, where a decrease in biochar did not lead to an increase in bio-oil, but did result in a significant increase in noncondensable gases. Bio-oil yields at 350 and 600 °C were comparably high (34.24±1.10 and 36.50±6.13 wt%)¹⁸⁹ due to the breakdown of cellulose, hemicellulose, and lignin to condensable gases as compared with 900 °C, which composed mainly of volatile matter¹⁹⁰ and less bio-oil yields. This is because of the degradation of higher molecular weight compounds into noncondensable gases at 900 °C.¹⁹¹ A higher amount of noncondensable gases was determined at 300 °C (32.73±1.30 wt%) compared with 350 °C (27.86±1.01 wt%) must be due to the rapid degradation of cellulose and hemicellulose that did not result in the condensation of those volatile compounds.

Table 6. Yield of products obtained from torrefaction and pyrolysis of prairie cordgrass at different temperatures

<i>Sample</i>	<i>Bio-oil</i> (wt%)	<i>Biochar</i> (wt%)	<i>Noncondensable gases</i> (wt%)
Tor250	13.51±2.27	71.00±2.66	15.49±2.02
Tor300	21.88±1.03	45.39±1.10	32.73±0.87
Tor350	34.24±1.10	37.90±0.19	27.86±0.64
Pyro600	36.50±6.13	30.23±5.10	33.27±4.60
Pyro 900	26.60±3.87	23.41±8.30	49.99±5.29

3.3.2. Lignin content and recovery in prairie cordgrass bio-chars

All experiments were performed in triplicate and the results were recorded as an average with standard deviation. Table 7 shows the total amount of solids, moisture content, extractives, ash content, acid-soluble lignin, and acid-insoluble lignin. Lignin determination is largely affected by amount of ash, particle size and extractives in the biomass. Ash contents increased as extractives and moisture contents in the torrefied biomass decreased compared to PCG due to evaporation at higher temperatures. The moisture content in all biomass samples were less than 10 % and the use of extractives free samples reduced interferences in lignin determination. The determined ash content of PCG (4.78±0.10 wt%), Tor250 (6.37±0.09 wt%), Tor300 (7.00±0.04 wt%) are comparable to what was determined by Cybulska et al ¹⁹² for raw prairie cordgrass (5.7 wt%), but ash content in biochars from temperatures above torrefaction, Tor350 (12.09±0.10 wt%), Pyro600 (12.57±0.45 wt%), and Pyro900 (14.72±0.15 wt%) were higher than 10 % due to an increase in the amount of inorganic matter and char.

Table 7. Amount of total solids, moisture, extractives, ash, and total lignin with % RSD determined for torrefaction biochar samples at 250 °C (Tor250), 300 °C (Tor300), 350 °C (Tor350) and pyrolysis biochar samples at 600°C (Pyro 600) and 900°C (Pyro 900).

Sample	wt% Total solids	wt% Moisture	wt% Extractives	wt% Ash	wt% Lignin	wt% Lignin recovered
Tor250	95.37±1.27	4.6±2.2	9.44±0.03	6.37±0.09	23.5±1.6	92.3±1.0
Tor300	95.42±0.63	4.9±1.1	8.37±0.06	7.00±0.04	5.4±6.8	92.9±2.7
Tor350	96.69±1.79	3.3±3.1	2.65±0.13	12.09±0.22	4.1±7.3	93.1±3.2
Pyro600	97.47±0.64	2.5±1.1	1.25±0.01	12.57±0.45	-	-
Pyro900	98.56±1.04	1.4±1.8	1.22±0.05	14.72±0.15	-	-
PCG	93.63±0.81	6.4±1.4	16.78±0.41	4.78±0.10	20.3±2.6	89.2±2.5

The total amount of determined soluble lignin was small in quantity compared to insoluble lignin, as expected. At 250 °C, the amount of lignin in the bio-char is higher than lignin in PCG but as the temperature increases to severe torrefaction, 300 °C and 350 °C and pyrolysis temperatures, the amount of lignin decreases to a point where there is no detectable lignin in the bio-char (Pyro600 and Pyro900). This is because from 300 °C and above most of the three lignocellulosic materials are degrading. At 250 °C there is degradation of hemicellulose and cellulose but less lignin degradation. Thus the biochar at Tor250 is rich in lignin as compared to PCG.^{56, 168, 174} The percentage lignin determined using the organosolv method are Tor250 (92.3±1.0 wt%), Tor300 (92.9±2.7 wt%), and Tor350 (93.1±3.2 wt%). Recovered lignin percentages are comparable to the literature on prairie cordgrass and studies have shown that lignins recovered by organosolv method is considered native lignin because it is less than 5 % carbohydrate.¹⁹²

The high percentage of lignin recovered from the torrefied biochar is due to less interference by carbohydrates.

3.3.3. Characterization of bio-oil and lignin from prairie cordgrass bio-chars

a. Characterization of bio-oil from torrefaction and pyrolysis of prairie cordgrass

i. Water content, pH, Density of bio-oils

Table 8 shows the water content, density, and pH of the bio-oil obtained at different torrefaction and pyrolytic temperatures. As seen in Table 7 pH range of the bio-oils is 2.6 ± 0.3 to 3.2 ± 0.4 . The acidic nature of the bio-oils aided extraction of aromatic compounds by aromatic ring hydrogenation.¹¹² The water content for the torrefaction temperatures (250-350 °C) were high, ranging from 65 to 75 wt%, but was reduced in bio-oils for pyrolytic temperatures of 600 °C (41.73 ± 8.20 wt%) and 900 °C (42.77 ± 1.30 wt%). The high water content at torrefaction temperatures is a good indication that those conditions can be used to pretreat the biomass to remove a large amount of water before pyrolysis at higher temperatures, as studied by Wei et al.¹⁷³ The lower water content for torrefaction at 350 °C (65.43 ± 1.01 wt%) is consistent with the water content Cheng et al. determined for the same biomass at 350 °C.¹⁹³ The densities of bio-oils from torrefaction are comparable to the density of water at room temperature, 0.997044 g/cm^3 because of the high amount of water in the bio-oils. The densities of bio-oils at 600 and 900 °C were determined to be the same (1.42 g/cm^3), and higher than densities of bio-oils obtained from torrefaction because of the presence of higher molecular weight compounds from lignin degradation at higher temperatures during pyrolysis.¹⁹⁴

Table 8. Physicochemical properties of pyrolysis of prairie cordgrass at different temperatures.

<i>Sample</i>	<i>Water content (wt%)</i>	<i>Density (g/cm³)</i>	<i>pH</i>
Tor250	75.11±2.24	1.08±0.16	2.61±0.30
Tor300	71.06±0.16	1.02±0.61	2.62±0.20
Tor350	65.43±1.01	1.04±0.20	2.91±0.01
Pyro600	41.73±8.20	1.42±0.11	2.90±0.68
Pyro900	42.77±1.30	1.42±0.36	3.25±0.48

ii. FTIR bio-oil extracts analysis

FTIR spectroscopic analysis was performed to determine the functional groups present in the bio-oil samples. Table 9 shows characteristics assignment of typical FTIR absorption bands, main functional groups, and compounds. Figure 24 shows FTIR spectra analysis of bio-oil fractions after ASE extraction. FTIR spectra of different bio-oil samples show similar functional groups indicating that they have similar chemical bonds within the samples. There is a strong absorption from 3600 -3200 cm⁻¹ as a result of the stretching H-bonded of O-H groups, along with an intense band at 1290-1220 cm⁻¹ due to C-O stretching indicating the presence of phenols and alcohols¹⁹⁵ in bio-oil extracts as determined by Abnisa et al.¹⁹⁶ This is consistent with our GC-MS results. The phenolic compounds present in all the bio-oil samples are due to lignin breakdown during the pretreatment process.¹⁹⁷ The presence of methylene and methyl groups are indicated by the strong absorbance peaks of C-H vibrations between 3000 and 2600 cm⁻¹. The intense absorption bands present between 1750-1650 cm⁻¹ are due to C=O stretching of ketones, aldehydes, and carboxylic acids as a result of breakdown of hemicellulose and cellulose.¹⁹⁸ Absorption from 1170-1020 cm⁻¹ is due to C-O-C stretching vibrations from the

pyranose ring skeleton as a result of the breakdown of hemicellulose during pyrolysis to form 3-furancarboxaldehyde and furan-2-one in all bio-oil samples¹⁹⁹, which is in agreement with the GC-MS results shown in Figure 24 and Table 9.

On the other hand, the absorption bands at 1500 cm^{-1} are due to C=C stretching of aromatic skeletal vibrations. C-H in-plane deformation as a result of peak bands at 1125 cm^{-1} , a C=O vibration of esters at 1167 cm^{-1} , and aromatic C-H out of plane vibration at $650\text{-}950\text{ cm}^{-1}$ indicate the presence of aromatic compounds in all bio-oil samples and confirms the presence of guaiacyl and syringol moieties^{198, 200-201} in the prairie cordgrass.

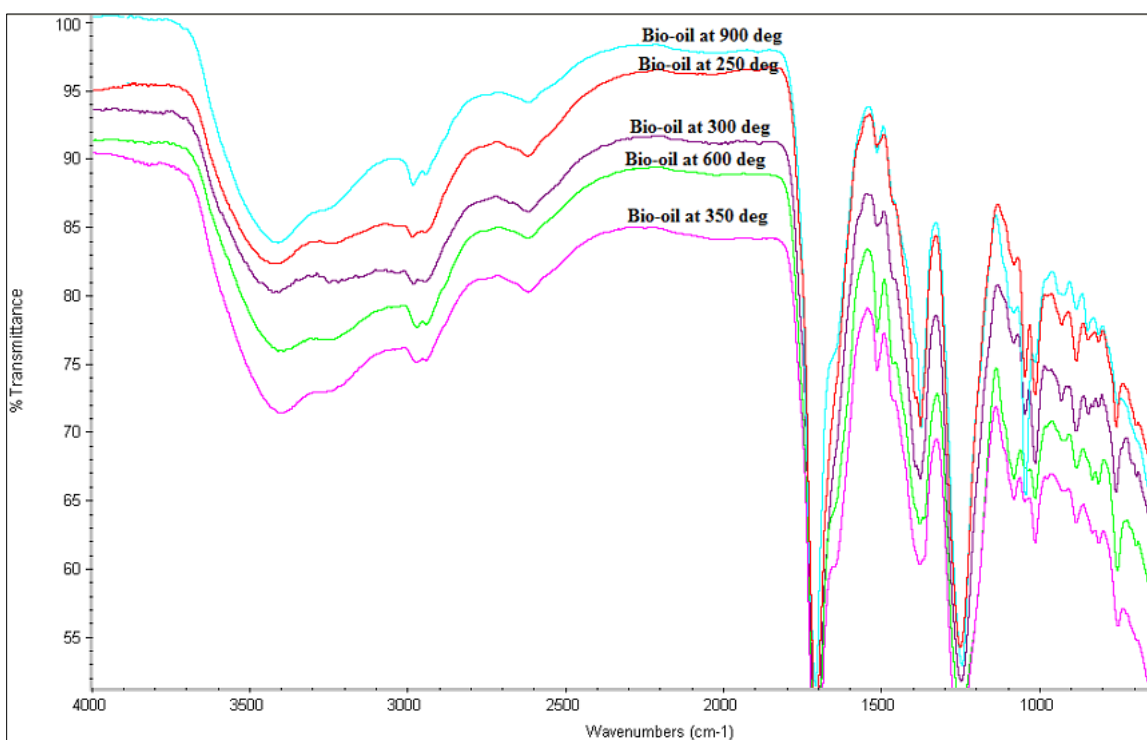


Figure 24. FTIR spectra of bio-oil extracts from Pyro900 (blue), Tor250 (red), Tor300 (purple), Pyro600 (green), and Tor350 (pink) of prairie cordgrass.

Table 9: Assignments of FTIR absorption bands of lignin from Tor250, Tor300, Tor350, and PCG and bio-oils from torrefaction and pyrolysis

Absorption bands (cm ⁻¹)	Functional groups and compounds
3460-3200	O-H stretching
3000-2842	C-H stretching in methyl and methylene groups
1738-1709	C=O stretching in unconjugated ketone, carbonyl
1675-1655	C=O stretch in conjugated aryl ketones
1605-1593	Aromatic skeletal vibrations plus C=O stretch
1515-1505	Aromatic skeletal vibration; Guaiacyl
1470-1460	Aromatic methyl group vibrations
1430-1422	Aromatic skeletal vibrations
1370-1365	Aliphatic C-H stretch in CH ₃
1330-1325	Syringyl ring breathing with C-O stretching
1270-1266	Guaiacyl ring plus C=O stretch
1230-1221	C-C, and C=O stretch Guaiacyl condensed
1165	C=O in ester groups conjugated typical for <i>p</i> -hydroxyphenyl, Guaiacyl, Syringyl
1135	Aromatic C-H in-plane deformation for syringyl type
1043	Aromatic C-H in-plane deformation for guaiacyl type
835	Aromatic C-H out of plane bending
691	Aromatic C-H stretching

iii. GC-MS analysis of bio-oil fractions

The identification and quantification of the major components of bio-oils obtained from torrefaction and pyrolysis of prairie cordgrass at different temperatures has been analyzed by GC-MS. Figure 25 shows the GC-MS chromatograms of the different bio-oil extracts analyzed using *o*-terphenyl as an internal standard. For the purposes of determining the high acidity (pH from 2.6-3.2) of bio-oil samples, acetic acid and hexanoic acids GC-MS peaks were identified in Figure 25 as A and B, respectively,

which is in agreement with FTIR peaks showing strong absorption bands for organic acids.

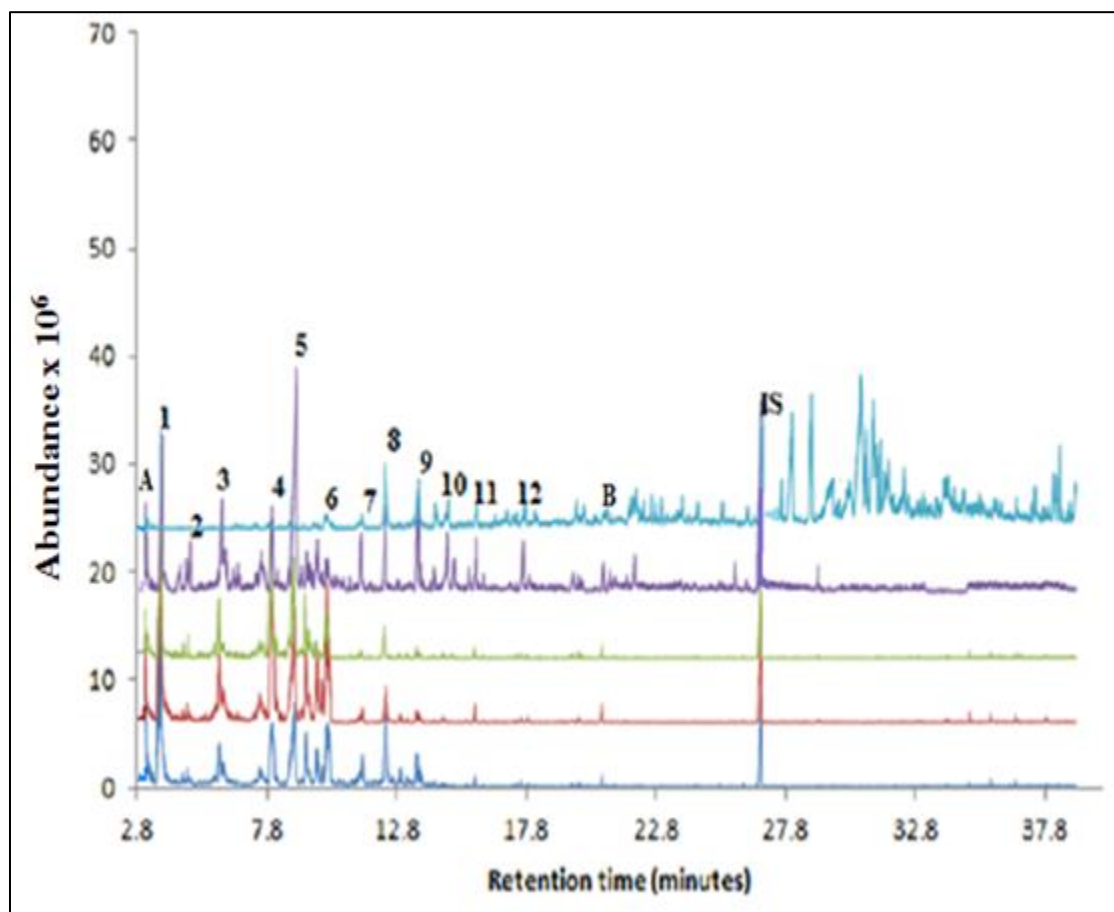


Figure 25. GC-MS chromatograms of bio-oil extracts from Pyro900, Pyro600, Tor250, Tor300, and Tor350 of prairie cordgrass

Table 10. GC-MS aromatic composition of bio-oils obtained from torrefaction and pyrolysis of prairie cordgrass at different temperatures

Numbers	Compounds	Retention time(mins)	250 °C (wt%)	300 °C (wt%)	350 °C (wt%)	600 °C (wt%)	900 °C (wt%)
1	3-Furancarboxaldehyde	3.01	0.32	0.30	0.38	0.52	-
2	Furan-2-one	3.21	0.03	0.06	0.07	0.10	-
3	Phenol	5.11	0.30	0.31	0.37	0.51	-
4	Guaiacol	7.81	0.77	0.85	1.01	1.39	-
5	m-Cresol	8.01	0.83	2.33	2.76	3.82	-
6	p-Cresol	9.88	0.17	1.18	1.32	1.83	0.03
7	Xylenol	11.22	-	0.17	0.19	0.27	0.01
8	Ethyl-phenol	12.80	-	0.76	0.90	1.24	0.07
9	Ethyl-guaiacol	13.32	-	0.09	0.12	0.16	0.01
10	Catechol	14.01	-	0.13	0.15	0.21	0.01
11	Syringol	14.45	-	0.09	0.10	0.14	0.01
12	Vanillin	17.81	-	0.01	0.01	0.17	0.05
	Total aromatic compounds		2.42	6.28	7.38	10.36	0.19

The major compounds identified and quantified were aromatic compounds involving useful furanic and phenolic moieties in the bio-oils as listed in Table 10. Table 10 shows retention times and amounts of aromatic compounds contained in the bio-oil extracts. All bio-oil extracts showed the presence of organic acids and aromatic moieties. Bio-oils at 250 and 900 °C gave less aromatic compounds while 300, 350, and 600 °C produced more aromatic compounds. For torrefaction at 250 °C, water was evaporated and only a small portion of the lignocellulosic materials degrading, leading to high water content in the bio-oils and less aromatic moieties as indicated in Tables 6 and 7. An increase in torrefaction temperature led to degradation of more polysaccharides and lignin, resulting in an increase in the amount of aromatic compounds, but at 900 °C

further breakdown of aromatic compounds, resulted in less furanic and phenolic compounds, as seen in Figure 25 and Table 10. The amount of aromatic compounds determined for 250, 300, 350, 600, and 900 °C were 2.42, 6.28, 7.38, 10.36, 0.19 wt% respectively.

b. Characterization of lignin from bio-char of prairie cordgrass

i. Elemental and HHV analysis

The elemental composition and HHV of extracted lignin from PCG, Tor250, Tor300, and Tor350 were analyzed by an elemental analyzer and calorimeter respectively. The elemental analysis and HHV were carried out in duplicates and the averages with standard deviations were reported, as shown in Table 11. Lignin extracted from raw prairie cordgrass have high O content (39.8 ± 10.6 %), but lower C and H contents compared to lignin from torrefaction. Elemental compositions of lignin from torrefaction were comparable. Carbon content in the extracted lignin increased from 53.4 % to 68.3 % as the amount of oxygen content decreased from 39.8 % to 20.8 %. Torrefaction at 250 °C have the highest C and H contents. Even though torrefaction led to a significant increase in C and H content and reduction in oxygen content, severe torrefaction temperatures (300 and 350 °C) turned the trend around. The HHV of torrefied lignin (23.1-29.8 MJ/kg⁻¹) were comparable to the lignin from PCG (25.8 MJ/kg⁻¹). Lignin from Tor250 has the greatest HHV while lignin from Tor300 and Tor350 has lower HHV than lignin from PCG. This is due to degradation of lignin polymer to form lower molecular weight compounds at higher temperatures.

Table 11: Elemental compositions and High Heating Values (HHV) of lignin extracted from PCG, Tor250, Tor300, and Tor350

Sample	% C	% H	% N	% O	HHV(MJkg ⁻¹)
PCG	53.4 ± 1.8	5.7 ± 16.7	1.1 ± 7.6	39.8 ± 10.6	25.8 ± 1.5
Tor250	68.2 ± 1.4	7.4 ± 13.1	0.5 ± 2.9	23.9 ± 7.7	29.8 ± 1.3
Tor300	64.8 ± 1.4	6.9 ± 13.8	0.4 ± 2.6	27.9 ± 8.1	24.4 ± 1.6
Tor350	62.1 ± 1.5	6.7 ± 14.4	0.7 ± 2.1	30.5 ± 8.4	23.1 ± 1.7

ii. FTIR spectroscopic analysis

The lignin recovered by the organosolv method from torrefied bio-chars and raw prairie cordgrass were analyzed by FTIR spectroscopy in the wavenumber region of 4000-600 cm⁻¹, as shown in Figure 26. Table 9 shows typical characteristic assignments of lignin FTIR absorption bands and functional groups of possible compounds associated with the signals as a reference.²⁰²⁻²⁰⁵ The results of the FTIR spectra of Tor250, Tor300, Tor350, and PCG lignins are essentially similar in absorption bands from 4000-1600 cm⁻¹ but differ in signal profiles from 1515-844 cm⁻¹, and are comparable to earlier studies on extracted lignins from different plants,²⁰⁴⁻²⁰⁶ The similarities in the spectral profile for all the four extracted lignins are the result of broad intense absorption at 3460-3200 cm⁻¹ due to O-H groups and at 3000-2842 cm⁻¹ as a result of C-H stretching in methylene and methyl groups. The difference in absorption spectral in the fingerprint region is due to modifications caused by torrefaction of the PCG at different temperatures. The PCG, Tor250, Tor300, and Tor350 show spectral absorption bands at 1605-1422 cm⁻¹ due to aromatic vibrations plus C=O stretching. An aromatic C-H in-plane deformation present at 1135-1043 cm⁻¹ and intense absorption band ranging from 1230-1221 cm⁻¹ due to the C=O stretching. The C=O vibration in ester groups led to an intense absorption band at

1165 cm^{-1} . All of these confirm the presence of guaiacyl, *p*-hydroxyphenyl, and syringyl moieties in the lignins.²⁰⁵

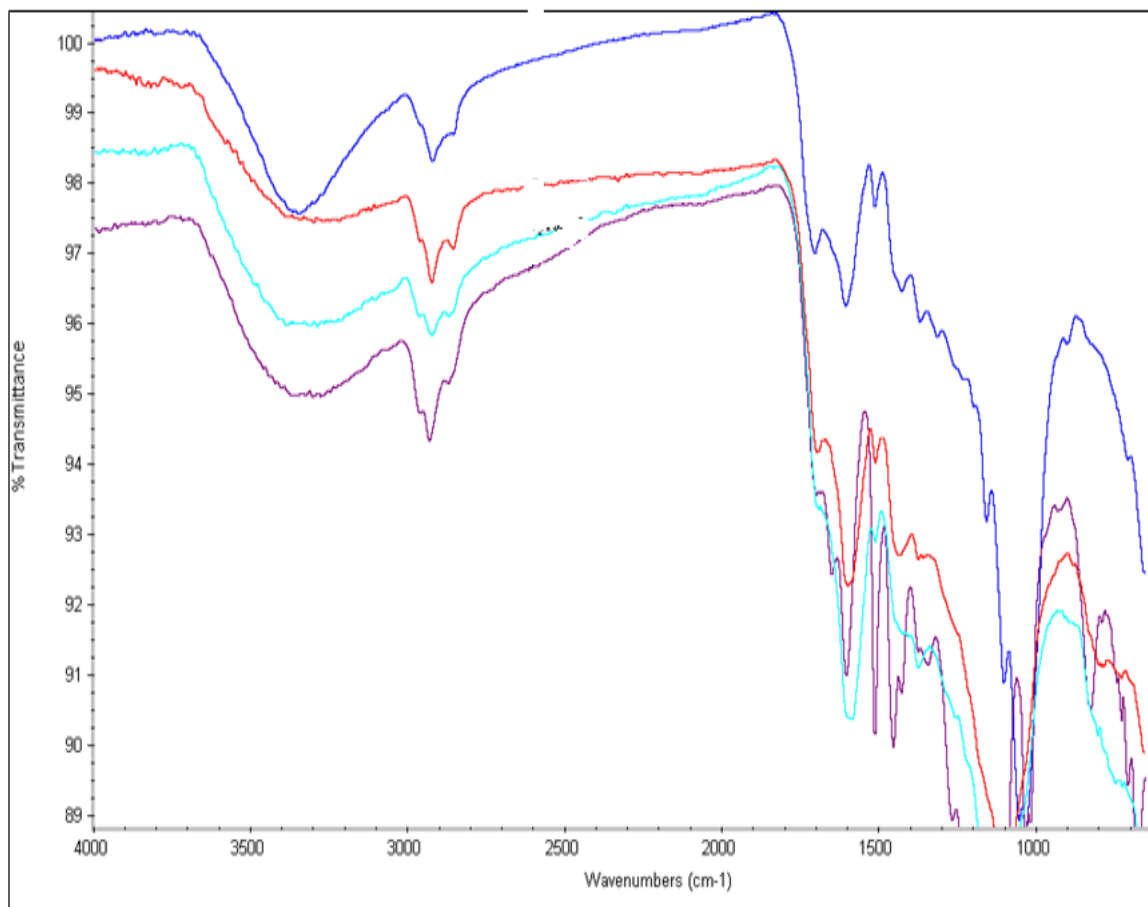


Figure 26. FTIR spectra for extracted lignin from Tor250 (blue), Tor300 (red), Tor350 (green), and PCG (violet).

iii. Thermogravimetric analysis

Thermal stability of differently extracted lignins was measured using their thermogravimetric analysis (TGA). Thermal decomposition of PCG, Tor250, Tor300, and Tor350 were determined by a temperature range from 25 to 500 $^{\circ}\text{C}$ at a rate of 20 $^{\circ}\text{C}/\text{min}$ under an inert nitrogen atmosphere. Weight loss was recorded as a function of

increasing temperature. Figure 27 shows the TGA curves of the different extracted lignin. Table 12 shows the measurement of weight losses at different stages of the TGA curves.

The first stage of weight loss occurred from 45 to 120 °C as a result of the evaporation of moisture from the polymeric films of the extracted lignin.¹⁴⁴ The loss of water may also be due to the release of unbound and bound water in the polymeric films of the extracted lignin. The amount of water evaporated from PCG, Tor250, Tor300, Tor350 lignin were 4.12 %, 5.72 %, 4.51 %, and 4.21 % respectively. The high water content in all lignin compared to the starting biomass may be due to insufficient drying of lignins. The second stage of weight loss in the lignin happened at a temperature range of 160-280 °C due to devolatilization of carbohydrates associated with lignin samples and due to the conversion of lower molecular lignin compounds to volatile gasses like CO, CO₂, and CH₄.^{56, 199, 207} As shown in Table 12, the weight loss was highest in lignin extracted from raw prairie cordgrass, PCG (13.14%), whereas lignin extracted from torrefied prairie cordgrass showed less mass loss, ranging from 6.06-11.18 %. The low amount of devolatilization in lignin from torrefied prairie cordgrass at this stage is a good indication that there is less association of carbohydrates, and confirms the high percentage of lignin recovery in Tor250 (92.3 %), Tor300 (92.9 %), and Tor350 (93.1 %) compared to PCG (89.2 %).

The third stage of degradation occurred as a result of continuous devolatilization at a temperature range of 280-403 °C for all the extracted lignin. The lowest degradation was observed in lignin from Tor300 (27.5 %) and the highest degradation in PCG (35.0 %) lignin with Tor250 and Tor350 lignins recording 32.9 % and 30.4 % degradation respectively. This suggests that torrefaction of biomass affects lignin thermal properties.

After 400 °C of pyrolysis the amount of carbon residue of PCG, Tor250, Tor300, and Tor350 were 47.8 %, 50.18 %, 59.40 %, and 59.04 % respectively. There are higher yields of residual carbon in lignin from torrefied prairie cordgrass than the raw prairie cordgrass. Within the third stage, the devolatilization products are mainly from the lignin compounds such as phenolics, alcohols, aldehydes, and ketones.²⁰⁷ Cleavage of β -O-4 linkages and the devolatilization of functional groups present in the extracted lignin led to mass losses within the second and third stages of the TGA.^{146, 208}

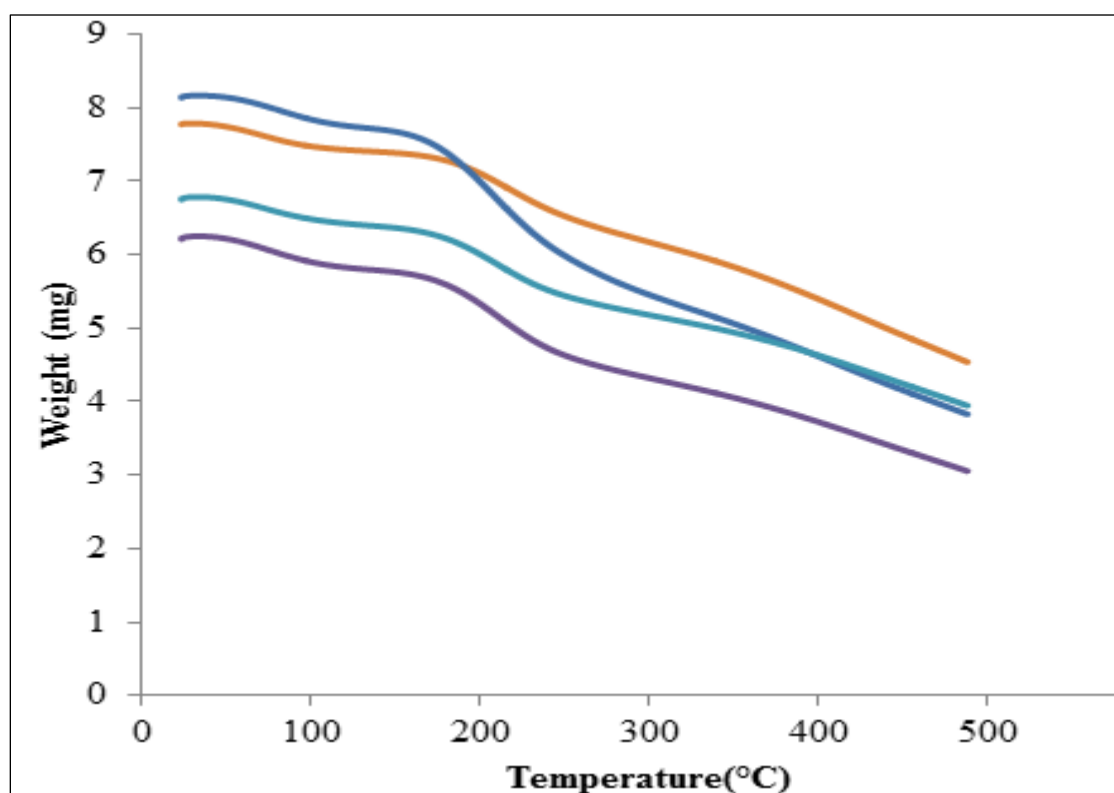


Figure 27: Thermogravimetric analysis curves obtained for organosolv lignin extracted from Tor250, Tor300, PCG and Tor350 (from bottom to top) with a temperature range from 25 to 500 °C.

Table 12. Thermogravimetric analysis of extracted lignins from PCG, Tor250, Tor300, and Tor350 showing mass losses at different degradation stages.

Degradation Stages	PCG % Mass loss	Tor250 % Mass loss	Tor300 % Mass loss	Tor350 % Mass loss
Stage 1	4.1±1.6	5.7±1.0	4.5±1.5	4.2±0.5
Stage 2	13.1±1.9	11.1±1.9	8.6±1.8	6.1±1.8
Stage 3	35.0±1.5	33.0±1.9	27.5±2.2	30.6±2.1
Carbon residual	47.8±1.4	50.2±0.6	59.4±0.6	59.0±0.1

3.4. Conclusion

In order to determine the amount of lignin in the torrefied prairie cordgrass, torrefaction in a pyrolysis reactor was performed with a working temperature of 250 °C, 300 °C, 350 °C and compared to pyrolysis at 600 °C and 900 °C. The extracted lignin from the torrefied prairie cordgrass yielded 4.1 to 23.5 wt%. The organosolv recovered lignin for the torrefaction temperatures yielded in the range between 92.3-93.1 %. The result for evaluated bio-oil from the torrefaction of the prairie cordgrass demonstrated that torrefaction produces useful aromatic compounds, furan and phenolic moieties. Torrefaction at 250 °C yielded the highest lignin (23.5±1.6 wt%), but the lowest aromatic monomers (2.42 wt%) while the torrefaction at 350 °C yielded the lowest lignin (4.1±7.3 %) but high lignin purity (93.1±3.2) and 7.38 wt% aromatic monomers. Increase in temperature led to corresponding increase in aromatic monomers but decrease in lignin amount. Pyrolysis at 600 °C produced the highest amount of aromatic monomers (10.36 wt%) but no lignin determined at 600 °C and above.

CHAPTER 4

CONCLUSIONS AND FUTURE WORK

Feedstocks for production of biochemicals from lignocellulosic materials are cheap and renewable and can replace diminishing petroleum products. The uses of biochemicals from the lignocellulosic materials are environmentally benign. Lignocellulosic materials are complex and dynamic structure mainly consists of cellulose, hemicellulose and lignin. The main challenge is to develop methods and technologies to efficiently hydrolyze the components of the lignocellulosic materials. Torrefaction is one of the pretreatment methods used to process prairie cordgrass. Lignin is a potential source for value-added biochemicals. Torrefied prairie cordgrass can serve as a large source of lignin and bio-oil from torrefaction process has aromatic compounds. Kraft lignin is cheap and produced in large amounts in paper and pulp industries. In this study we determined and characterized lignin and bio-fuels from torrefied prairie cordgrass. We also depolymerized and characterized the products from hydrothermal liquefaction of Kraft lignin

In the first part of this dissertation, characterization of the Kraft lignin showed mainly guaiacyl and hydroxyphenyl moieties which is indicative of softwood lignin origin.²⁰⁹ All the phenolic monomers identified by the GC-MS and UHPLC analysis show guaiacyl moieties (G) which is supported by cupric oxide oxidation and pyrolysis GC-MS analysis. No hydroxyphenyl moieties were detected in the GC-MS or UHPLC analysis for the organic solvent soluble products. Hydrotreatment reaction conditions without catalyst at 200 °C resulted in two phenolic monomers (vanillin and homovanillic acid) and only vanillin at 240 °C due to repolymerization at this higher temperature. The

use of CoO catalyst yielded two phenolic monomers (vanillin and homovanillic acid) at 200°C and 240 °C. A separate hydrotreatment reaction conditions for LaO and MoO both yielded guaiacol, 3-methoxyacetophenone, vanillin, 4-propylguaiacol, acetovanillone, and homovanillic acid at 240 °C and the same phenolic products at 200 °C with the exception of guaiacol and 3-methoxyacetophenone. Vanillin yield was predominant in all the different hydrotreatment reaction conditions. There is more cleavage of ether linkages and propyl chains in the lignin polymers for the catalyzed hydrotreatment reaction that resulted in formation of more phenolic monomers than the non-catalyzed hydrotreatment reactions.

Increased in temperature resulted in an increased in phenolic monomers of the three reaction steps. The use of MoO on supported-zeolite medium at 240 °C yielded the highest products (15 wt%) as compared to low product yield (0.5 wt%) for non-catalyzed depolymerization reaction at the same temperature. The use of zeolite-supported metal catalysts reduced repolymerization in the product mixtures as shown in the noncatalyzed reaction where homovanillic acid repolymerized at higher temperature, 240°C. The decrease in reaction time to 15 minute prevented coke formation as shown by the lignin residue FTIR analysis. The reuse of the reaction solvents (water) and the lignin residue for the subsequent reactions brings economic and environmental advantages to depolymerization of kraft lignin. MoO supported-zeolite catalysts can be used to produce useful phenolic monomers under mild temperature and pressure conditions using hydrotreatment.

In the second part of this dissertation, torrefaction and pyrolysis of prairie cordgrass at different temperatures, 250, 300,350, 600, and 900 °C at 25 °C/min with

nitrogen as flow gas have been performed using simple laboratory reactor. The yields of different pyrolytic products were determined. The water content, density, pH of the bio-oils obtained from prairie cordgrass at different temperatures has been analyzed. ASE was used for extraction of useful aromatic components of the bio-oils. The low pH range of 2.6-2.9 aided the extraction. The type and amount of aromatic compounds in the bio-oil fractions were determined by GC-MS, ranging from 0.19-10.28 wt % of the bio-oil. Temperature at 900 °C showed the lowest amount of aromatic compounds 0.19 wt % while 600 °C gave the highest amount of aromatic compounds of 10.28 wt %. The functional groups of the aromatic groups were confirmed by FTIR analysis of the bio-oil fractions. The present study involves extraction of lignin from torrefied prairie cordgrass and raw prairie cordgrass using NREL lignin determination method, as well as lignin recovery by organosolv method. The lignins were characterized through FTIR, elemental analysis, HHV, and TGA methods. Lignin yield from torrefaction at 250 °C was the highest and comparable to lignin extracted from raw prairie cordgrass whereas there was a decrease in lignin amount as temperature increased above 250 °C. Therefore, 250 °C is the best torrefaction temperature for prairie cordgrass amongst the temperatures studied in this experiment. FTIR analysis shows that all the extracted lignins are made up of guaiacyl, p-hydroxyphenyl, and syringyl moieties which can be used for production of high commercial value biochemicals.²¹⁰

In addition, elemental compositions of extracted lignin from PCG, Tor250, Tor300 and Tor350 show that torrefaction decreased the oxygen content and increased the carbon content of lignin which makes it a good pretreatment method for extraction of lignin for production of co-polymers in bio-composites and carbon fiber precursors.^{160, 163}

Lignin from Tor250 has the highest carbon and lowest oxygen content that led to greatest HHV due to devolatilization of H₂O, CO₂, formic acids, aldehydes and phenols from lateral chains but at severe torrefaction temperatures (300 and 350 °C) there is an additional release of hydrocarbons, mainly CH₄ from methoxy and methylene groups in the lignin²⁰⁶. The TGA degradation curves exhibited by the extracted lignins are comparable to other lignin degradation curves and pyrolysis studies.^{208, 211} The evaporation of H₂O, devolatilization, and continuous devolatilization led to different decomposition phase changes. Lignin extracted from torrefied prairie cordgrass have high thermal resistance than lignin from raw prairie cordgrass because of high formation of residual carbon yields at temperatures above 400 °C during thermogravimetric analysis. Therefore lignin from torrefaction can be used for carbon fiber-based anode applications.²¹²

The methods described in this study are a step towards determination and thermal characteristics of lignin from torrefied prairie cordgrass. This study will serve as a background to determine amount of lignin in other torrefied biomass. The effect of seasonal changes in biomass on the amount of lignin in the torrefied prairie cordgrass should be investigated.

The economies and ergonomics on the hydrothermal liquefaction depolymerization of lignin using subcritical water and supported-zeolite catalyst need to be evaluated to determine the applicability of the process on industrial scale. The potential reuse of the solvents and catalysts as well as optimization process should be evaluated to ensure efficient production of aromatic monomers from lignin.

5. REFERENCES

1. Nashawi, I. S.; Malallah, A.; Al-Bisharah, M., Forecasting World Crude Oil Production Using Multicyclic Hubbert Model. *Energy & Fuels* **2010**, *24* (3), 1788-1800.
2. Harmsen, P. F. H.; Hackmann, M. M.; Bos, H. L., Green building blocks for bio-based plastics. *Biofuels, Bioproducts and Biorefining* **2014**, *8* (3), 306-324.
3. http://www1.eere.energy.gov/bioenergy/pdfs/Archive/abcs_biofuels.html (accessed on October 03, 2016).
4. Samuel, R.; Pu, Y.; Raman, B.; Ragauskas, A. J., Structural characterization and comparison of switchgrass ball-milled lignin before and after dilute acid pretreatment. *Applied biochemistry and biotechnology* **2010**, *162* (1), 62-74.
5. Farrell, A. E.; Plevin, R. J.; Turner, B. T.; Jones, A. D.; O'Hare, M.; Kammen, D. M., Ethanol can contribute to energy and environmental goals. *Science* **2006**, *311* (5760), 506-8.
6. Sheehan, J.; Aden, A.; Paustian, K.; Killian, K.; Brenner, J.; Walsh, M.; Nelson, R., Energy and Environmental Aspects of Using Corn Stover for Fuel Ethanol. *Journal of Industrial Ecology* **2003**, *7* (3-4), 117-146.
7. Nelson, R. G., Resource assessment and removal analysis for corn stover and wheat straw in the Eastern and Midwestern United States—rainfall and wind-induced soil erosion methodology. *Biomass and Bioenergy* **2002**, *22* (5), 349-363.
8. Wilhelm, W. W.; Johnson, J. M. F.; Karlen, D. L.; Lightle, D. T., Corn Stover to Sustain Soil Organic Carbon Further Constrains Biomass Supply. *Agronomy Journal* **2007**, *99* (6), 1665-1667.

9. Banowetz, G. M.; Boateng, A.; Steiner, J. J.; Griffith, S. M.; Sethi, V.; El-Nashaar, H., Assessment of straw biomass feedstock resources in the Pacific Northwest. *Biomass and Bioenergy* **2008**, *32* (7), 629-634.
10. <http://webcoist.momtastic.com/2008/11/02/biomass-thermal-power-systems/> (accessed on October 03, 2016).
11. <http://www.naylornetwork.com/ppi-otw/articles/index-v2.asp?aid=326138&issueID=42755> (accessed on September 30, 2016).
12. Lebo, S. E.; Gargulak, J. D.; McNally, T. J., Lignin. In *Kirk-Othmer Encyclopedia of Chemical Technology*, John Wiley & Sons, Inc.: 2000.
13. Galbe, M.; Zacchi, G., Pretreatment of Lignocellulosic Materials for Efficient Bioethanol Production. In *Biofuels*, Olsson, L., Ed. Springer Berlin Heidelberg: Berlin, Heidelberg, 2007; pp 41-65.
14. Yat, S. C.; Berger, A.; Shonnard, D. R., Kinetic characterization for dilute sulfuric acid hydrolysis of timber varieties and switchgrass. *Bioresour Technol* **2008**, *99* (9), 3855-63.
15. Mosier, N.; Wyman, C.; Dale, B.; Elander, R.; Lee, Y. Y.; Holtzapple, M.; Ladisch, M., Features of promising technologies for pretreatment of lignocellulosic biomass. *Bioresour Technol* **2005**, *96* (6), 673-86.
16. Faulon, J.-L.; Carlson, G. A.; Hatcher, P. G., A three-dimensional model for lignocellulose from gymnospermous wood. *Organic geochemistry* **1994**, *21* (12), 1169-1179.

17. Qian, X., The effect of cooperativity on hydrogen bonding interactions in native cellulose I β from ab initio molecular dynamics simulations. *Molecular Simulation* **2008**, *34* (2), 183-191.
18. Harmsen, P. F. H. Literature review of physical and chemical pretreatment processes for lignocellulosic biomass.
19. Lawoko, M.; Henriksson, G.; Gellerstedt, G., Structural differences between the lignin-carbohydrate complexes present in wood and in chemical pulps. *Biomacromolecules* **2005**, *6* (6), 3467-73.
20. Millett, M. A.; Baker, A. J.; Satter, L. D. In *Physical and chemical pretreatments for enhancing cellulose saccharification*, Biotechnol. Bioeng. Symp.;(United States), Dept. of Agriculture, Madison, WI: 1976.
21. Mais, U.; Esteghlalian, A. R.; Saddler, J. N.; Mansfield, S. D., Enhancing the Enzymatic Hydrolysis of Cellulosic Materials Using Simultaneous Ball Milling. *Applied biochemistry and biotechnology* **2002**, *98-100* (1-9), 815-832.
22. Brennan, A. H.; Hoagland, W.; Schell, D. J.; Scott, C. D., *High temperature acid hydrolysis of biomass using an engineering - scale plug flow reactor. Results of low testing solids.* ; Solar Energy Research Institute, Golden, CO 80401, USA: 1986; p Medium: X; Size: Pages: 53-70.
23. Lee, J., Biological conversion of lignocellulosic biomass to ethanol. *J Biotechnol* **1997**, *56* (1), 1-24.
24. Sun, Y.; Cheng, J., Hydrolysis of lignocellulosic materials for ethanol production: a review. *Bioresour Technol* **2002**, *83* (1), 1-11.

25. Fan, L.-t.; Gharpuray, M. M.; Lee, Y.-H., *Cellulose hydrolysis*. Springer Science & Business Media: 2012; Vol. 3.
26. Hatakka, A. I., Pretreatment of wheat straw by white-rot fungi for enzymic saccharification of cellulose. *European Journal of Applied Microbiology and Biotechnology* **1983**, *18* (6), 350-357.
27. Okano, K.; Kitagawa, M.; Sasaki, Y.; Watanabe, T., Conversion of Japanese red cedar (*Cryptomeria japonica*) into a feed for ruminants by white-rot basidiomycetes. *Animal Feed Science and Technology* **2005**, *120* (3-4), 235-243.
28. Wyman, C., *Handbook on bioethanol: production and utilization*. CRC press: 1996.
29. McWilliams, R. C.; van Walsum, G. P., Comparison of aspen wood hydrolysates produced by pretreatment with liquid hot water and carbonic acid. *Applied biochemistry and biotechnology* **2002**, *98-100*, 109-21.
30. Zhang, Y. H.; Ding, S. Y.; Mielenz, J. R.; Cui, J. B.; Elander, R. T.; Laser, M.; Himmel, M. E.; McMillan, J. R.; Lynd, L. R., Fractionating recalcitrant lignocellulose at modest reaction conditions. *Biotechnology and bioengineering* **2007**, *97* (2), 214-23.
31. Cahela, D. R.; Lee, Y. Y.; Chambers, R. P., Modeling of percolation process in hemicellulose hydrolysis. *Biotechnology and bioengineering* **1983**, *25* (1), 3-17.
32. Esteghlalian, A.; Hashimoto, A. G.; Fenske, J. J.; Penner, M. H., Modeling and optimization of the dilute-sulfuric-acid pretreatment of corn stover, poplar and switchgrass. *Bioresource Technology* **1997**, *59* (2), 129-136.

33. Converse, A. O.; Kwarteng, I. K.; Grethlein, H. E.; Ooshima, H., Kinetics of thermochemical pretreatment of lignocellulosic materials. *Applied biochemistry and biotechnology* **1989**, 20-21 (1), 63-78.
34. Bensch, E. C.; Mensah, M., Chemical Pretreatment Methods for the Production of Cellulosic Ethanol: Technologies and Innovations. *International Journal of Chemical Engineering* **2013**, 2013, 1-21.
35. Lu, X. B.; Zhang, Y. M.; Yang, J.; Liang, Y., Enzymatic Hydrolysis of Corn Stover after Pretreatment with Dilute Sulfuric Acid. *Chemical Engineering & Technology* **2007**, 30 (7), 938-944.
36. de Vasconcelos, S. M.; Santos, A. M.; Rocha, G. J.; Souto-Maior, A. M., Diluted phosphoric acid pretreatment for production of fermentable sugars in a sugarcane-based biorefinery. *Bioresour Technol* **2013**, 135, 46-52.
37. Lee, J. W.; Houtman, C. J.; Kim, H. Y.; Choi, I. G.; Jeffries, T. W., Scale-up study of oxalic acid pretreatment of agricultural lignocellulosic biomass for the production of bioethanol. *Bioresour Technol* **2011**, 102 (16), 7451-6.
38. von Sivers, M.; Zacchi, G., A techno-economical comparison of three processes for the production of ethanol from pine. *Bioresource Technology* **1995**, 51 (1), 43-52.
39. Tao, L.; Aden, A.; Elander, R. T.; Pallapolu, V. R.; Lee, Y. Y.; Garlock, R. J.; Balan, V.; Dale, B. E.; Kim, Y.; Mosier, N. S.; Ladisch, M. R.; Falls, M.; Holtzapfel, M. T.; Sierra, R.; Shi, J.; Ebrik, M. A.; Redmond, T.; Yang, B.; Wyman, C. E.; Hames, B.; Thomas, S.; Warner, R. E., Process and technoeconomic analysis of leading pretreatment technologies for lignocellulosic ethanol production using switchgrass. *Bioresour Technol* **2011**, 102 (24), 11105-14.

40. Falls, M.; Holtzapple, M. T., Oxidative lime pretreatment of Alamo switchgrass. *Applied biochemistry and biotechnology* **2011**, *165* (2), 506-22.
41. Taherzadeh, M. J.; Karimi, K., Pretreatment of lignocellulosic wastes to improve ethanol and biogas production: a review. *Int J Mol Sci* **2008**, *9* (9), 1621-51.
42. Soto, M. L.; Domínguez, H.; Núñez, M. J.; Lema, J. M., Enzymatic saccharification of alkali-treated sunflower hulls. *Bioresource Technology* **1994**, *49* (1), 53-59.
43. Fox, D. J.; Gray, P. P.; Dunn, N. W.; Marsden, W. L., Comparison of alkali and steam (acid) pretreatments of lignocellulosic materials to increase enzymic susceptibility: Evaluation under optimised pretreatment conditions. *Journal of Chemical Technology & Biotechnology* **2007**, *44* (2), 135-146.
44. Macdonald, D. G.; Bakhshi, N. N.; Mathews, J. F.; Roychowdhury, A.; Bajpai, P.; Moo-Young, M., Alkali treatment of corn stover to improve sugar production by enzymatic hydrolysis. *Biotechnology and bioengineering* **1983**, *25* (8), 2067-76.
45. Elshafei, A. M.; Vega, J. L.; Klasson, K. T.; Clausen, E. C.; Gaddy, J. L., The saccharification of corn stover by cellulase from *Penicillium funiculosum*. *Bioresource Technology* **1991**, *35* (1), 73-80.
46. Chum, H. L.; Johnson, D. K.; Black, S. K., Organosolv pretreatment for enzymic hydrolysis of poplars. 2. Catalyst effects and the combined severity parameter. *Industrial & Engineering Chemistry Research* **1990**, *29* (2), 156-162.
47. Thring, R. W., Alkaline degradation of ALCELL® lignin. *Biomass and Bioenergy* **1994**, *7* (1-6), 125-130.

48. Pan, X.; Arato, C.; Gilkes, N.; Gregg, D.; Mabee, W.; Pye, K.; Xiao, Z.; Zhang, X.; Saddler, J., Biorefining of softwoods using ethanol organosolv pulping: preliminary evaluation of process streams for manufacture of fuel-grade ethanol and co-products. *Biotechnology and bioengineering* **2005**, *90* (4), 473-81.
49. Morrison, W. H.; Akin, D. E., Water soluble reaction products from ozonolysis of grasses. *Journal of Agricultural and Food Chemistry* **1990**, *38* (3), 678-681.
50. Ben-Ghedalia, D.; Miron, J., The effect of combined chemical and enzyme treatments on the saccharification and in vitro digestion rate of wheat straw. *Biotechnology and bioengineering* **1981**, *23* (4), 823-831.
51. Neely, W. C., Factors affecting the pretreatment of biomass with gaseous ozone. *Biotechnology and bioengineering* **1984**, *26* (1), 59-65.
52. Ben-Ghedalia, D.; Shefet, G., Chemical treatments for increasing the digestibility of cotton straw: 2. Effect of ozone and sodium hydroxide treatments on the digestibility of cell-wall monosaccharides. *The Journal of Agricultural Science* **2009**, *100* (02), 401.
53. Vidal, P. F.; Molinier, J., Ozonolysis of lignin — Improvement of in vitro digestibility of poplar sawdust. *Biomass* **1988**, *16* (1), 1-17.
54. Schmidt, A. S.; Thomsen, A. B., Optimization of wet oxidation pretreatment of wheat straw. *Bioresource Technology* **1998**, *64* (2), 139-151.
55. Azzam, A. M., Pretreatment of cane bagasse with alkaline hydrogen peroxide for enzymatic hydrolysis of cellulose and ethanol fermentation. *Journal of Environmental Science and Health, Part B* **1989**, *24* (4), 421-433.
56. Prins, M. J.; Ptasinski, K. J.; Janssen, F. J. J. G., More efficient biomass gasification via torrefaction. *Energy* **2006**, *31* (15), 3458-3470.

57. Bourgois, J.; Bartholin, M. C.; Guyonnet, R., Thermal treatment of wood: analysis of the obtained product. *Wood Science and Technology* **1989**, *23* (4), 303-310.
58. Neupane, S.; Adhikari, S.; Wang, Z.; Ragauskas, A. J.; Pu, Y., Effect of torrefaction on biomass structure and hydrocarbon production from fast pyrolysis. *Green Chemistry* **2015**, *17* (4), 2406-2417.
59. Bergman, P. C.; Boersma, A.; Zwart, R.; Kiel, J., Torrefaction for biomass co-firing in existing coal-fired power stations. *Energy Centre of Netherlands, Report No. ECN-C-05-013* **2005**.
60. Uslu, A.; Faaij, A. P. C.; Bergman, P. C. A., Pre-treatment technologies, and their effect on international bioenergy supply chain logistics. Techno-economic evaluation of torrefaction, fast pyrolysis and pelletisation. *Energy* **2008**, *33* (8), 1206-1223.
61. Bourgeois, J.; Doat, J.; Egnéus, H.; Ellegård, A. In *Torrefied wood from temperate and tropical species. Advantages and prospects*, Bioenergy 84. Proceedings of Conference 15-21 June 1984, Goteborg, Sweden. Volume III. Biomass Conversion, Elsevier Applied Science Publishers: 1984; pp 153-159.
62. Guo, J.; Chong Lua, A., Characterization of chars pyrolyzed from oil palm stones for the preparation of activated carbons. *Journal of Analytical and Applied Pyrolysis* **1998**, *46* (2), 113-125.
63. Mohan, D.; Pittman, C. U.; Steele, P. H., Pyrolysis of Wood/Biomass for Bio-oil: A Critical Review. *Energy & Fuels* **2006**, *20* (3), 848-889.
64. Czernik, S.; Bridgwater, A. V., Overview of Applications of Biomass Fast Pyrolysis Oil. *Energy & Fuels* **2004**, *18* (2), 590-598.

65. Sukiran, M. A.; Kheang, L. S.; Bakar, N. A.; May, C. Y., Production and characterization of bio-char from the pyrolysis of empty fruit bunches. *American Journal of Applied Sciences* **2011**, *8* (10), 984.
66. Ferdous, D.; Dalai, A. K.; Bej, S. K.; Thring, R. W., Pyrolysis of lignins: Experimental and kinetics studies. *Energy & Fuels* **2002**, *16* (6), 1405-1412.
67. Zheng, Y.; Lin, H.; Tsao, G. T., Pretreatment for cellulose hydrolysis by carbon dioxide explosion. *Biotechnol Prog* **1998**, *14* (6), 890-6.
68. Vlasenko, E. Y.; Ding, H.; Labavitch, J. M.; Shoemaker, S. P., Enzymatic hydrolysis of pretreated rice straw. *Bioresource Technology* **1997**, *59* (2-3), 109-119.
69. Reshamwala, S.; Shawky, B. T.; Dale, B. E., Ethanol-Production from Enzymatic Hydrolysates of Afex-Treated Coastal Bermudagrass and Switchgrass. *Applied biochemistry and biotechnology* **1995**, *51-2* (1), 43-55.
70. Adler, E., Lignin chemistry?past, present and future. *Wood Science and Technology* **1977**, *11* (3), 169-218.
71. Pinkert, A.; Goeke, D. F.; Marsh, K. N.; Pang, S. S., Extracting wood lignin without dissolving or degrading cellulose: investigations on the use of food additive-derived ionic liquids. *Green Chemistry* **2011**, *13* (11), 3124-3136.
72. Collinson, S. R.; Thielemans, W., The catalytic oxidation of biomass to new materials focusing on starch, cellulose and lignin. *Coordination Chemistry Reviews* **2010**, *254* (15-16), 1854-1870.
73. Kuroda, K.-i., Analytical pyrolysis products derived from cinnamyl alcohol-end groups in lignins. *Journal of Analytical and Applied Pyrolysis* **2000**, *53* (2), 123-134.

74. Yaman, S., Pyrolysis of biomass to produce fuels and chemical feedstocks. *Energy Conversion and Management* **2004**, *45* (5), 651-671.
75. Tobimatsu, Y.; Chen, F.; Nakashima, J.; Escamilla-Trevino, L. L.; Jackson, L.; Dixon, R. A.; Ralph, J., Coexistence but independent biosynthesis of catechyl and guaiacyl/syringyl lignin polymers in seed coats. *The Plant cell* **2013**, *25* (7), 2587-600.
76. Buranov, A. U.; Mazza, G., Lignin in straw of herbaceous crops. *Industrial Crops and Products* **2008**, *28* (3), 237-259.
77. Asl, A. H.; Khajenoori, M., Subcritical Water Extraction. In *Mass Transfer - Advances in Sustainable Energy and Environment Oriented Numerical Modeling*, Nakajima, H., Ed. InTech: Rijeka, 2013; p Ch. 17.
78. Notley, S. M.; Norgren, M., Lignin: Functional Biomaterial with Potential in Surface Chemistry and Nanoscience. In *The Nanoscience and Technology of Renewable Biomaterials*, John Wiley & Sons, Ltd: 2009; pp 173-205.
79. Park, K. C.; Tomiyasu, H., Gasification reaction of organic compounds catalyzed by RuO₂ in supercritical water. *Chem Commun (Camb)* **2003**, (6), 694-5.
80. Cheng, S.; Yuan, Z.; Leitch, M.; Anderson, M.; Xu, C. C., Highly efficient depolymerization of organosolv lignin using a catalytic hydrothermal process and production of phenolic resins/adhesives with the depolymerized lignin as a substitute for phenol at a high substitution ratio. *Industrial crops and products* **2013**, *44*, 315-322.
81. Cheng, S.; Wilks, C.; Yuan, Z.; Leitch, M.; Xu, C., Hydrothermal degradation of alkali lignin to bio-phenolic compounds in sub/supercritical ethanol and water-ethanol co-solvent. *Polymer Degradation and Stability* **2012**, *97* (6), 839-848.

82. Li, C.; Zhao, X.; Wang, A.; Huber, G. W.; Zhang, T., Catalytic Transformation of Lignin for the Production of Chemicals and Fuels. *Chem Rev* **2015**, *115* (21), 11559-624.
83. Kleinert, M.; Barth, T., Towards a Lignin-cellulosic Biorefinery: Direct One-Step Conversion of Lignin to Hydrogen-Enriched Biofuel. *Energy & Fuels* **2008**, *22* (2), 1371-1379.
84. Kleinert, M.; Barth, T., Phenols from Lignin. *Chemical Engineering & Technology* **2008**, *31* (5), 736-745.
85. Kleinert, M.; Gasson, J. R.; Barth, T., Optimizing solvolysis conditions for integrated depolymerisation and hydrodeoxygenation of lignin to produce liquid biofuel. *Journal of Analytical and Applied Pyrolysis* **2009**, *85* (1-2), 108-117.
86. <http://ir.lib.uwo.ca/etd/2323/> (accessed on November 23, 2016).
87. Ang, A.; Ashaari, Z.; Bakar, E. S.; Ibrahim, N. A., Characterisation of sequential solvent fractionation and base-catalysed depolymerisation of treated alkali lignin. *BioResources* **2015**, *10* (3), 4137-4151.
88. Corma, A.; Iborra, S.; Velty, A., Chemical routes for the transformation of biomass into chemicals. *Chem Rev* **2007**, *107* (6), 2411-502.
89. Demirbaş, A., Biomass resource facilities and biomass conversion processing for fuels and chemicals. *Energy Conversion and Management* **2001**, *42* (11), 1357-1378.
90. Ben, H.; Mu, W.; Deng, Y.; Ragauskas, A. J., Production of renewable gasoline from aqueous phase hydrogenation of lignin pyrolysis oil. *Fuel* **2013**, *103*, 1148-1153.
91. Laurichesse, S.; Avérous, L., Chemical modification of lignins: Towards biobased polymers. *Progress in Polymer Science* **2014**, *39* (7), 1266-1290.

92. Klamrassamee, T.; Laosiripojana, N.; Cronin, D.; Moghaddam, L.; Zhang, Z.; Doherty, W. O. S., Effects of mesostructured silica catalysts on the depolymerization of organosolv lignin fractionated from woody eucalyptus. *Bioresour. Technol.* **2015**, *180*, 222-229.
93. Perlack, R. D.; Wright, L. L.; Turhollow, A. F.; Graham, R. L.; Stokes, B. J.; Erbach, D. C. *Biomass as feedstock for a bioenergy and bioproducts industry: the technical feasibility of a billion-ton annual supply*; DTIC Document: 2005.
94. Ma, R.; Hao, W.; Ma, X.; Tian, Y.; Li, Y., Catalytic ethanolysis of Kraft lignin into high-value small-molecular chemicals over nanostructured α -molybdenum carbide catalyst. *Angew. Chem., Int. Ed.* **2014**, *53* (28), 7310-7315.
95. Mai, C.; Milstein, O.; Huttermann, A., Chemoenzymatical grafting of acrylamide onto lignin. *J Biotechnol* **2000**, *79* (2), 173-83.
96. Chakar, F. S.; Ragauskas, A. J., Review of current and future softwood kraft lignin process chemistry. *Industrial Crops and Products* **2004**, *20* (2), 131-141.
97. Zakzeski, J.; Bruijninx, P. C.; Jongerius, A. L.; Weckhuysen, B. M., The catalytic valorization of lignin for the production of renewable chemicals. *Chem Rev* **2010**, *110* (6), 3552-99.
98. Konnerth, H.; Zhang, J.; Ma, D.; Prechtel, M. H. G.; Yan, N., Base promoted hydrogenolysis of lignin model compounds and organosolv lignin over metal catalysts in water. *Chemical Engineering Science* **2015**, *123* (0), 155-163.
99. Pelzer, A. W.; Sturgeon, M. R.; Yanez, A. J.; Chupka, G.; O'Brien, M. H.; Katahira, R.; Cortright, R. D.; Woods, L.; Beckham, G. T.; Broadbelt, L. J., Acidolysis of

α -O-4 Aryl-Ether Bonds in Lignin Model Compounds: A Modeling and Experimental Study. *ACS Sustainable Chemistry & Engineering* **2015**, 3 (7), 1339-1347.

100. Roberts, V.; Fendt, S.; Lemonidou, A. A.; Li, X.; Lercher, J. A., Influence of alkali carbonates on benzyl phenyl ether cleavage pathways in superheated water.

Applied Catalysis B: Environmental **2010**, 95 (1-2), 71-77.

101. Heitner, C.; Dimmel, D.; Schmidt, J., *Lignin and lignans: advances in chemistry*. CRC press: 2016.

102. Younker, J. M.; Beste, A.; Buchanan, A. C., 3rd, Computational study of bond dissociation enthalpies for substituted beta-O-4 lignin model compounds. *Chemphyschem : a European journal of chemical physics and physical chemistry* **2011**, 12 (18), 3556-65.

103. Dorrestijn, E.; Laarhoven, L. J. J.; Arends, I. W. C. E.; Mulder, P., The occurrence and reactivity of phenoxyl linkages in lignin and low rank coal. *Journal of Analytical and Applied Pyrolysis* **2000**, 54 (1-2), 153-192.

104. Parthasarathi, R.; Romero, R. A.; Redondo, A.; Gnanakaran, S., Theoretical Study of the Remarkably Diverse Linkages in Lignin. *The Journal of Physical Chemistry Letters* **2011**, 2 (20), 2660-2666.

105. Derkacheva, O.; Sukhov, D., Investigation of Lignins by FTIR Spectroscopy. *Macromolecular Symposia* **2008**, 265 (1), 61-68.

106. Gao, Y.; Zhang, J.; Chen, X.; Ma, D.; Yan, N., A Metal-Free, Carbon-Based Catalytic System for the Oxidation of Lignin Model Compounds and Lignin.

ChemPlusChem **2014**, 79 (6), 825-834.

107. Deepa, A. K.; Dhepe, P. L., Lignin Depolymerization into Aromatic Monomers over Solid Acid Catalysts. *ACS Catalysis* **2015**, 5 (1), 365-379.

108. Harkin, J. M., Recent Developments in Lignin Chemistry. In *Naturstoffe*, Springer Berlin Heidelberg: Berlin, Heidelberg, 1996; pp 101-158.
109. Amen-Chen, C.; Pakdel, H.; Roy, C., Production of monomeric phenols by thermochemical conversion of biomass: a review. *Bioresour Technol* **2001**, *79* (3), 277-99.
110. Huber, G. W.; Iborra, S.; Corma, A., Synthesis of transportation fuels from biomass: chemistry, catalysts, and engineering. *Chem Rev* **2006**, *106* (9), 4044-98.
111. Wang, H.; Tucker, M.; Ji, Y., Recent Development in Chemical Depolymerization of Lignin: A Review. *Journal of Applied Chemistry* **2013**, *2013*, 1-9.
112. Miller, J. E.; Evans, L.; Littlewolf, A.; Trudell, D. E., Batch microreactor studies of lignin and lignin model compound depolymerization by bases in alcohol solvents. *Fuel* **1999**, *78* (11), 1363-1366.
113. Katahira, R.; Mittal, A.; McKinney, K.; Chen, X.; Tucker, M. P.; Johnson, D. K.; Beckham, G. T., Base-Catalyzed Depolymerization of Biorefinery Lignins. *ACS Sustainable Chemistry & Engineering* **2016**, *4* (3), 1474-1486.
114. Okuda, K.; Ohara, S.; Umetsu, M.; Takami, S.; Adschiri, T., Disassembly of lignin and chemical recovery in supercritical water and p-cresol mixture. Studies on lignin model compounds. *Bioresour Technol* **2008**, *99* (6), 1846-52.
115. Roberts, V. M.; Stein, V.; Reiner, T.; Lemonidou, A.; Li, X.; Lercher, J. A., Towards quantitative catalytic lignin depolymerization. *Chemistry* **2011**, *17* (21), 5939-48.
116. Tymchyshyn, M.; Xu, C. C., Liquefaction of bio-mass in hot-compressed water for the production of phenolic compounds. *Bioresour Technol* **2010**, *101* (7), 2483-90.

117. Fang, Z.; Sato, T.; Smith, R. L., Jr.; Inomata, H.; Arai, K.; Kozinski, J. A., Reaction chemistry and phase behavior of lignin in high-temperature and supercritical water. *Bioresour Technol* **2008**, *99* (9), 3424-30.
118. Wahyudiono; Sasaki, M.; Goto, M., Recovery of phenolic compounds through the decomposition of lignin in near and supercritical water. *Chemical Engineering and Processing: Process Intensification* **2008**, *47* (9-10), 1609-1619.
119. Hepditch, M. M.; Thring, R. W., Degradation of solvolysis lignin using Lewis acid catalysts. *Canadian Journal of Chemical Engineering* **2000**, *78* (1), 226-231.
120. Meier, D.; Berns, J.; Faix, O.; Balfanz, U.; Baldauf, W., Hydrocracking of organocell lignin for phenol production. *Biomass and Bioenergy* **1994**, *7* (1-6), 99-105.
121. Xu, W.; Miller, S. J.; Agrawal, P. K.; Jones, C. W., Depolymerization and hydrodeoxygenation of switchgrass lignin with formic acid. *ChemSusChem* **2012**, *5* (4), 667-75.
122. Song, Q.; Wang, F.; Cai, J.; Wang, Y.; Zhang, J.; Yu, W.; Xu, J., Lignin depolymerization (LDP) in alcohol over nickel-based catalysts via a fragmentation–hydrogenolysis process. *Energy & Environmental Science* **2013**, *6* (3), 994.
123. Pandey, M. P.; Kim, C. S., Lignin Depolymerization and Conversion: A Review of Thermochemical Methods. *Chemical Engineering & Technology* **2011**, *34* (1), 29-41.
124. Guevenatam, B.; Heeres, E. H. J.; Pidko, E. A.; Hensen, E. J. M., Lewis-acid catalyzed depolymerization of Protobind lignin in supercritical water and ethanol. *Catal. Today* **2015**, Ahead of Print.
125. Zhao, C.; Lercher, J. A., Upgrading pyrolysis oil over Ni/HZSM-5 by cascade reactions. *Angewandte Chemie* **2012**, *51* (24), 5935-40.

126. Zhao, C.; Lercher, J. A., Selective Hydrodeoxygenation of Lignin-Derived Phenolic Monomers and Dimers to Cycloalkanes on Pd/C and HZSM-5 Catalysts. *ChemCatChem* **2012**, *4* (1), 64-68.
127. Ghampson, I. T.; Sepúlveda, C.; Garcia, R.; Radovic, L. R.; Fierro, J. L. G.; DeSisto, W. J.; Escalona, N., Hydrodeoxygenation of guaiacol over carbon-supported molybdenum nitride catalysts: Effects of nitriding methods and support properties. *Applied Catalysis A: General* **2012**, *439-440*, 111-124.
128. Adjaye, J. D.; Bakhshi, N. N., Production of hydrocarbons by catalytic upgrading of a fast pyrolysis bio-oil. Part I: Conversion over various catalysts. *Fuel Processing Technology* **1995**, *45* (3), 161-183.
129. Jongorius, A. L.; Jastrzebski, R.; Bruijninx, P. C. A.; Weckhuysen, B. M., CoMo sulfide-catalyzed hydrodeoxygenation of lignin model compounds: An extended reaction network for the conversion of monomeric and dimeric substrates. *Journal of Catalysis* **2012**, *285* (1), 315-323.
130. Ratcliff, M. A.; Johnson, D. K.; Posey, F. L.; Maholland, M. A.; Cowley, S. W.; Chum, H. L., Hydrodeoxygenation of a Lignin Model Compound. In *Research in Thermochemical Biomass Conversion*, Bridgwater, A. V.; Kuester, J. L., Eds. Springer Netherlands: Dordrecht, 1988; pp 941-955.
131. Oasmaa, A.; Johansson, A., Catalytic hydrotreating of lignin with water-soluble molybdenum catalyst. *Energy & Fuels* **1993**, *7* (3), 426-429.
132. Yuan, Z.; Cheng, S.; Leitch, M.; Xu, C. C., Hydrolytic degradation of alkaline lignin in hot-compressed water and ethanol. *Bioresour Technol* **2010**, *101* (23), 9308-13.

133. Huang, S.; Mahmood, N.; Tymchyshyn, M.; Yuan, Z.; Xu, C. C., Reductive depolymerization of kraft lignin for chemicals and fuels using formic acid as an in-situ hydrogen source. *Bioresour Technol* **2014**, *171*, 95-102.
134. Pearl, I. A., Vanillin from lignin materials. *Journal of the American Chemical Society* **1942**, *64* (6), 1429-1431.
135. Mantilla, S. V.; Manrique, A. M.; Gauthier-Maradei, P., Methodology for Extraction of Phenolic Compounds of Bio-oil from Agricultural Biomass Wastes. *Waste and Biomass Valorization* **2015**, *6* (3), 371-383.
136. Haghi, G.; Hatami, A.; Safaei, A.; Mehran, M., Analysis of phenolic compounds in *Matricaria chamomilla* and its extracts by UPLC-UV. *Research in pharmaceutical sciences* **2014**, *9* (1), 31-7.
137. Meier, D.; Oasmaa, A.; Peacocke, G. V. C., Properties of Fast Pyrolysis Liquids: Status of Test Methods. In *Developments in Thermochemical Biomass Conversion: Volume 1 / Volume 2*, Bridgwater, A. V.; Boocock, D. G. B., Eds. Springer Netherlands: Dordrecht, 1997; pp 391-408.
138. Zhao, X.; Wei, L.; Cheng, S.; Kadis, E.; Cao, Y.; Boakye, E.; Gu, Z.; Julson, J., Hydroprocessing of carinata oil for hydrocarbon biofuel over Mo-Zn/Al₂O₃. *Applied Catalysis B: Environmental* **2016**, *196*, 41-49.
139. Zhao, X.; Wei, L.; Cheng, S.; Huang, Y.; Yu, Y.; Julson, J., Catalytic cracking of camelina oil for hydrocarbon biofuel over ZSM-5-Zn catalyst. *Fuel Processing Technology* **2015**, *139*, 117-126.

140. Chen, C.-L., Nitrobenzene and Cupric Oxide Oxidations. In *Methods in Lignin Chemistry*, Lin, S. Y.; Dence, C. W., Eds. Springer Berlin Heidelberg: Berlin, Heidelberg, 1992; pp 301-321.
141. Dzhumanova, Z. K.; Dalimova, G. N., Nitrobenzene oxidation of lignins from several plants of the family Gramineae. *Chemistry of Natural Compounds* **2011**, *47* (3), 419-421.
142. Villar, C. J.; Caperos, A.; García-Ochoa, F., Oxidation of hardwood kraft-lignin to phenolic derivatives with oxygen as oxidant. *Wood Science and Technology* **2001**, *35* (3), 245-255.
143. Sjöström, E., Chapter 4 - LIGNIN. In *Wood Chemistry (Second Edition)*, Academic Press: San Diego, 1993; pp 71-89.
144. Rodrigues, P. C.; Muraro, M.; Garcia, C. M.; Souza, G. P.; Abbate, M.; Schreiner, W. H.; Gomes, M. A. B., Polyaniline/lignin blends: thermal analysis and XPS. *European Polymer Journal* **2001**, *37* (11), 2217-2223.
145. <http://www.sigmaaldrich.com/catalog/product/aldrich/370959?lang=en®ion=US> (accessed on October, 2016).
146. Chu, S.; Subrahmanyam, A. V.; Huber, G. W., The pyrolysis chemistry of a β -O-4 type oligomeric lignin model compound. *Green Chem.* **2013**, *15* (1), 125-136.
147. Lisperguer, J.; Perez, P.; Urizar, S., Structure and thermal properties of lignins: characterization by infrared spectroscopy and differential scanning calorimetry. *Journal of the Chilean Chemical Society* **2009**, *54* (4), 460-463.
148. De Chirico, A.; Audisio, G.; Provasoli, F.; Schieronni, A. G.; Focher, B.; Grossi, B., Differential scanning calorimetry and thermal gravimetric analysis of lignin blended

- with triglycidyl isocyanurate. *Angewandte Makromolekulare Chemie* **1995**, 228 (1), 51-58.
149. Hannah, R. W.; Mayo, D. W., Infrared Spectra of Polymers: Introduction. In *Course Notes on the Interpretation of Infrared and Raman Spectra*, John Wiley & Sons, Inc.: 2004; pp 261-296.
150. Hu, J.; Shen, D.; Wu, S.; Zhang, H.; Xiao, R., Composition Analysis of Organosolv Lignin and Its Catalytic Solvolysis in Supercritical Alcohol. *Energy & Fuels* **2014**, 28 (7), 4260-4266.
151. Silverstein, R. M.; Bassler, G. C., Spectrometric identification of organic compounds. *Journal of Chemical Education* **1962**, 39 (11), 546.
152. Yin, R. Z.; Liu, R. H.; Mei, Y. F.; Fei, W. T.; Sun, X. Q., Characterization of bio-oil and bio-char obtained from sweet sorghum bagasse fast pyrolysis with fractional condensers. *Fuel* **2013**, 112, 96-104.
153. Karunadasa, H. I.; Chang, C. J.; Long, J. R., A molecular molybdenum-oxo catalyst for generating hydrogen from water. *Nature* **2010**, 464 (7293), 1329-33.
154. Yang, H.; Yan, R.; Chen, H.; Lee, D. H.; Zheng, C., Characteristics of hemicellulose, cellulose and lignin pyrolysis. *Fuel* **2007**, 86 (12-13), 1781-1788.
155. Lutzen, N. W.; Nielsen, M. H.; Oxenboell, K. M.; Schulein, M.; Stentebjerg-Olesen, B., Cellulases and their Application in the Conversion of Lignocellulose to Fermentable Sugars. *Philosophical Transactions of the Royal Society of London. Series B, Biological Sciences* **1983**, 300 (1100), 283-291.
156. Goldstein, I., Organic chemicals from biomass. **1981**.

157. Chew, J. J.; Doshi, V., Recent advances in biomass pretreatment – Torrefaction fundamentals and technology. *Renewable and Sustainable Energy Reviews* **2011**, *15* (8), 4212-4222.
158. Lee, J. W.; Kim, Y. H.; Lee, S. M.; Lee, H. W., Optimizing the torrefaction of mixed softwood by response surface methodology for biomass upgrading to high energy density. *Bioresour Technol* **2012**, *116*, 471-6.
159. Claassen, P. A. M.; van Lier, J. B.; Lopez Contreras, A. M.; van Niel, E. W. J.; Sijtsma, L.; Stams, A. J. M.; de Vries, S. S.; Weusthuis, R. A., Utilisation of biomass for the supply of energy carriers. *Applied Microbiology and Biotechnology* **1999**, *52* (6), 741-755.
160. Mohanty, A. K.; Misra, M.; Hinrichsen, G., Biofibres, biodegradable polymers and biocomposites: An overview. *Macromolecular Materials and Engineering* **2000**, *276-277* (1), 1-24.
161. Bhardwaj, R.; Mohanty, A. K., Advances in the properties of polylactides based materials: a review. *Journal of Biobased Materials and Bioenergy* **2007**, *1* (2), 191-209.
162. Tenhaeff, W. E.; Rios, O.; More, K.; McGuire, M. A., Highly Robust Lithium Ion Battery Anodes from Lignin: An Abundant, Renewable, and Low-Cost Material. *Advanced Functional Materials* **2014**, *24* (1), 86-94.
163. Wang, S. X.; Yang, L.; Stubbs, L. P.; Li, X.; He, C., Lignin-derived fused electrospun carbon fibrous mats as high performance anode materials for lithium ion batteries. *ACS Appl Mater Interfaces* **2013**, *5* (23), 12275-82.

164. Kadla, J. F.; Kubo, S.; Venditti, R. A.; Gilbert, R. D.; Compere, A. L.; Griffith, W., Lignin-based carbon fibers for composite fiber applications. *Carbon* **2002**, *40* (15), 2913-2920.
165. Chand, S., Review Carbon fibers for composites. *Journal of Materials Science* **2000**, *35* (6), 1303-1313.
166. Chen, H., Chemical Composition and Structure of Natural Lignocellulose. In *Biotechnology of Lignocellulose: Theory and Practice*, Springer Netherlands: Dordrecht, 2014; pp 25-71.
167. Wang, Z. Q.; Guo, Q. J.; Liu, X. M.; Cao, C. Q., Low temperature pyrolysis characteristics of oil sludge under various heating conditions. *Energy & Fuels* **2007**, *21* (2), 957-962.
168. Abnisa, F.; Arami-Niya, A.; Daud, W. M. A. W.; Sahu, J. N., Characterization of Bio-oil and Bio-char from Pyrolysis of Palm Oil Wastes. *Bioenergy Research* **2013**, *6* (2), 830-840.
169. Hakkou, M.; Pétrissans, M.; Gérardin, P.; Zoulalian, A., Investigations of the reasons for fungal durability of heat-treated beech wood. *Polymer Degradation and Stability* **2006**, *91* (2), 393-397.
170. Tumuluru, J.; Lim, C.; Bi, X.; Kuang, X.; Melin, S.; Yazdanpanah, F.; Sokhansanj, S., Analysis on Storage Off-Gas Emissions from Woody, Herbaceous, and Torrefied Biomass. *Energies* **2015**, *8* (3), 1745.
171. Sarvaramini, A.; Assima, G. P.; Larachi, F., Dry torrefaction of biomass – Torrefied products and torrefaction kinetics using the distributed activation energy model. *Chemical Engineering Journal* **2013**, *229*, 498-507.

172. Arias, B.; Pevida, C.; Feroso, J.; Plaza, M. G.; Rubiera, F.; Pis, J. J., Influence of torrefaction on the grindability and reactivity of woody biomass. *Fuel Processing Technology* **2008**, *89* (2), 169-175.
173. Wei, L.; Gao, Y.; Qu, W.; Zhao, X.; Cheng, S., Torrefaction of raw and blended corn stover, switchgrass, and prairie grass. *Transactions of the Asabe* **2016**, *59* (2), 717-726.
174. Sharma, R. K.; Wooten, J. B.; Baliga, V. L.; Lin, X.; Geoffrey Chan, W.; Hajaligol, M. R., Characterization of chars from pyrolysis of lignin. *Fuel* **2004**, *83* (11-12), 1469-1482.
175. Gandini, A.; Belgacem, M. N., Chapter 11 - Lignins as Components of Macromolecular Materials. In *Monomers, Polymers and Composites from Renewable Resources*, Elsevier: Amsterdam, 2008; pp 243-271.
176. Gellerstedt, G.; Henriksson, G., Chapter 9 - Lignins: Major Sources, Structure and Properties A2 - Belgacem, Mohamed Naceur. In *Monomers, Polymers and Composites from Renewable Resources*, Gandini, A., Ed. Elsevier: Amsterdam, 2008; pp 201-224.
177. Lora, J., Chapter 10 - Industrial Commercial Lignins: Sources, Properties and Applications A2 - Belgacem, Mohamed Naceur. In *Monomers, Polymers and Composites from Renewable Resources*, Gandini, A., Ed. Elsevier: Amsterdam, 2008; pp 225-241.
178. Bridgwater, A., Fast pyrolysis processes for biomass. *Renewable and Sustainable Energy Reviews* **2000**, *4* (1), 1-73.
179. Piskorz, J.; Scott, D. S.; Radlein, D., Composition of Oils Obtained by Fast Pyrolysis of Different Woods. In *Pyrolysis Oils from Biomass*, American Chemical Society: 1988; Vol. 376, pp 167-178.

180. Soltes, E. J.; Milne, T. A., *Pyrolysis Oils from Biomass*. American Chemical Society: 1988; Vol. 376, p 372.
181. Richter, B. E.; Jones, B. A.; Ezzell, J. L.; Porter, N. L.; Avdalovic, N.; Pohl, C., Accelerated Solvent Extraction: A Technique for Sample Preparation. *Analytical Chemistry* **1996**, 68 (6), 1033-1039.
182. Hames, B.; Ruiz, R.; Scarlata, C.; Sluiter, A.; Sluiter, J.; Templeton, D., Preparation of samples for compositional analysis. *Laboratory Analytical Procedure (LAP)*. National Renewable Energy Laboratory **2008**.
183. Sluiter, A., Hames, B., Hyman, D., Payne, C., Ruiz, R., Scarlata, C., Sluiter, J., Templeton, D., and Wolfe, J, Determination of total solids in biomass and total dissolved solids in liquid process samples. **2008**.
184. Sluiter, A.; Ruiz, R.; Scarlata, C.; Sluiter, J.; Templeton, D., Determination of extractives in biomass laboratory analytical procedure. *National Renewable Energy Laboratory* **2005**, 3-8.
185. Sluiter, A.; Hames, B.; Ruiz, R.; Scarlata, C.; Sluiter, J., Determination of structural carbohydrates and lignin in biomass. Laboratory Analytical Procedures (LAP), National Renewable Energy Laboratory (NREL), Golden, CO. Revised version Jul 2011. *There is no corresponding record for this reference* **2012**, 1-15.
186. Hyman, D.; Sluiter, A.; Crocker, D.; Johnson, D.; Sluiter, J.; Black, S.; Scarlata, C., Determination of acid soluble lignin concentration curve by UV-Vis spectroscopy. *Natl Renewable Energy Laboratory (NREL) Analytical Proced* **2008**, 1-13.
187. Bozell, J. J.; Black, S. K.; Myers, M.; Cahill, D.; Miller, W. P.; Park, S., Solvent fractionation of renewable woody feedstocks: Organosolv generation of biorefinery

process streams for the production of biobased chemicals. *Biomass and Bioenergy* **2011**, 35 (10), 4197-4208.

188. Branca, C.; Giudicianni, P.; Di Blasi, C., GC/MS Characterization of Liquids Generated from Low-Temperature Pyrolysis of Wood. *Industrial & Engineering Chemistry Research* **2003**, 42 (14), 3190-3202.

189. Williams, P. T.; Besler, S., The influence of temperature and heating rate on the slow pyrolysis of biomass. *Renewable Energy* **1996**, 7 (3), 233-250.

190. Asadullah, M.; Anisur Rahman, M.; Mohsin Ali, M.; Abdul Motin, M.; Borhanus Sultan, M.; Robiul Alam, M.; Sahedur Rahman, M., Jute stick pyrolysis for bio-oil production in fluidized bed reactor. *Bioresour Technol* **2008**, 99 (1), 44-50.

191. Kirubakaran, V.; Sivaramakrishnan, V.; Nalini, R.; Sekar, T.; Premalatha, M.; Subramanian, P., A review on gasification of biomass. *Renewable and Sustainable Energy Reviews* **2009**, 13 (1), 179-186.

192. Cybulska, I.; Brudecki, G.; Rosentrater, K.; Julson, J. L.; Lei, H., Comparative study of organosolv lignin extracted from prairie cordgrass, switchgrass and corn stover. *Bioresour Technol* **2012**, 118, 30-6.

193. Cheng, S.; Wei, L.; Zhao, X.; Kadis, E.; Cao, Y.; Julson, J.; Gu, Z., Hydrodeoxygenation of prairie cordgrass bio-oil over Ni based activated carbon synergistic catalysts combined with different metals. *N Biotechnol* **2016**, 33 (4), 440-8.

194. Fahmi, R.; Bridgwater, A. V.; Donnison, I.; Yates, N.; Jones, J. M., The effect of lignin and inorganic species in biomass on pyrolysis oil yields, quality and stability. *Fuel* **2008**, 87 (7), 1230-1240.

195. Genel, Y.; Durak, H.; Aysu, T.; Genel, İ., Effect of process parameters on supercritical liquefaction of *Xanthium strumarium* for bio-oil production. *The Journal of Supercritical Fluids* **2016**, *115*, 42-53.
196. Abnisa, F.; Arami-Niya, A.; Wan Daud, W. M. A.; Sahu, J. N.; Noor, I. M., Utilization of oil palm tree residues to produce bio-oil and bio-char via pyrolysis. *Energy Conversion and Management* **2013**, *76*, 1073-1082.
197. del Río, J. C.; Gutiérrez, A.; Romero, J.; Martínez, M. J.; Martínez, A. T., Identification of residual lignin markers in eucalypt kraft pulps by Py-GC/MS. *Journal of Analytical and Applied Pyrolysis* **2001**, *58-59*, 425-439.
198. Faix, O., Classification of lignins from different botanical origins by FT-IR spectroscopy. *Holzforschung-International Journal of the Biology, Chemistry, Physics and Technology of Wood* **1991**, *45* (s1), 21-28.
199. Yang, H.; Yan, R.; Chen, H.; Lee, D. H.; Zheng, C., Characteristics of hemicellulose, cellulose and lignin pyrolysis. *Fuel* **2007**, *86* (12-13), 1781-1788.
200. Oliveira, L.; Cordeiro, N.; Evtuguin, D. V.; Torres, I. C.; Silvestre, A. J. D., Chemical composition of different morphological parts from 'Dwarf Cavendish' banana plant and their potential as a non-wood renewable source of natural products. *Industrial Crops and Products* **2007**, *26* (2), 163-172.
201. Oliveira, L.; Evtuguin, D.; Cordeiro, N.; Silvestre, A. J. D., Structural characterization of stalk lignin from banana plant. *Industrial Crops and Products* **2009**, *29* (1), 86-95.

202. Seca, A. M.; Cavaleiro, J. A.; Domingues, F. M.; Silvestre, A. J.; Evtuguin, D.; Neto, C. P., Structural characterization of the lignin from the nodes and internodes of *Arundo donax* reed. *J Agric Food Chem* **2000**, *48* (3), 817-24.
203. Pepper, J. M.; Casselman, B. W.; Karapally, J. C., Lignin oxidation. Preferential use of cupric oxide. *Canadian Journal of Chemistry* **1967**, *45* (23), 3009-3012.
204. Faix, O., Classification of Lignins from Different Botanical Origins by FT-IR Spectroscopy. In *Holzforschung - International Journal of the Biology, Chemistry, Physics and Technology of Wood*, 1991; Vol. 45, p 21.
205. Xu, F.; Sun, J.-X.; Sun, R.; Fowler, P.; Baird, M. S., Comparative study of organosolv lignins from wheat straw. *Industrial Crops and Products* **2006**, *23* (2), 180-193.
206. Liu, Q.; Wang, S.; Zheng, Y.; Luo, Z.; Cen, K., Mechanism study of wood lignin pyrolysis by using TG-FTIR analysis. *Journal of Analytical and Applied Pyrolysis* **2008**, *82* (1), 170-177.
207. Watkins, D.; Nuruddin, M.; Hosur, M.; Tcherbi-Narteh, A.; Jeelani, S., Extraction and characterization of lignin from different biomass resources. *Journal of Materials Research and Technology* **2015**, *4* (1), 26-32.
208. Murugan, P.; Mahinpey, N.; Johnson, K. E.; Wilson, M., Kinetics of the Pyrolysis of Lignin Using Thermogravimetric and Differential Scanning Calorimetry Methods. *Energy & Fuels* **2008**, *22* (4), 2720-2724.
209. Ehara, K.; Takada, D.; Saka, S., GC-MS and IR spectroscopic analyses of the lignin-derived products from softwood and hardwood treated in supercritical water. *Journal of Wood Science* **2005**, *51* (3), 256-261.

210. Ross, K.; Mazza, G., Characteristics of lignin from flax shives as affected by extraction conditions. *Int J Mol Sci* **2010**, *11* (10), 4035-50.
211. Jin, W.; Singh, K.; Zondlo, J., Pyrolysis Kinetics of Physical Components of Wood and Wood-Polymers Using Isoconversion Method. *Agriculture* **2013**, *3* (1), 12-32.
212. Gnedenkov, S. V.; Sinebryukhov, S. L.; Opra, D. P.; Zemnukhova, L. A.; Tsvetnikov, A. K.; Minaev, A. N.; Sokolov, A. A.; Sergienko, V. I., Electrochemistry of Klason Lignin. *Procedia Chemistry* **2014**, *11*, 96-100.